International Symposium on Recent Observations and Simulations of the Sun–Earth System II

ABSTRACT BOOK

Borovets, Bulgaria, 11–16 September 2011

The Symposium is sponsored by

International Association of Geomagnetism and Aeronomy

International Union of Radio Science

US National Science Foundation

US National Aeronautics and Space Administration

LANL Institute of Geophysics and Planetary Physics

Bt Development Services, Bulgaria

ICT Cluster, Bulgaria

Conveners of ISROSES II:

- Vania Jordanova, Los Alamos National Laboratory, Los Alamos, NM, USA
- Joe Borovsky, Los Alamos National Laboratory, Los Alamos, NM, USA
- Ilia Roussev, University of Hawaii, Honolulu, HI, USA

Scientific Organizing Committee:

- Michael Denton, Lancaster University, Lancaster, UK
- Natalia Ganushkina, Finnish Meteorological Institute, Helsinki, Finland
- Jerry Goldstein, Southwest Research Institute, San Antonio, TX, USA
- Craig Kletzing, University of Iowa, Iowa City, IA, USA
- Benoit Lavraud, CESR/CNRS, Toulouse, France
- William Lotko, Dartmouth College, Hanover, NH, USA
- Yoshizumi Miyoshi, Solar-Terrestrial Environment Laboratory, Nagoya, Japan
- Richard Thorne, UCLA, Los Angeles, CA, USA

Local Organizing Committee:

- Ventzislav Rusanov (Chair), Physics Department, Sofia University
- Valentin Jordanov (Co-Chair), Yantel LLC
- Petko Nedialkov, Physics Department, Sofia University
- Ivanka Stateva, Institute of Astronomy, Bulgarian Academy of Sciences

Including Quasi-linear and Nonlinear Wave-Particle Interactions in Global Rad Belt Models

J. M. Albert[1], J. Bortnik[2], V. K. Jordanova[3], W. Li[2], R. M. Thorne[2]

1 Air Force Research Laboratory, Kirtland AFB, MA 87117, USA, jay.albert@us.af.mil
[2] Department of Atmospheric and Oceanic Sciences, University of California, Los Angeles, California, USA
[3] Los Alamos National Laboratory, Los Alamos, NM 87545, USA

Properly treating wave-particle interactions is crucial to understanding, modeling, and predicting the behavior of radiation belt electrons, and the usual quasi-linear treatment alone cannot capture the specific effects that nonlinear interactions are known to cause. The effects of quasi-linear and nonlinear wave-particle interactions can be described as diffusion and advection respectively, in both energy and pitch angle. It is also necessary to model the ring current accurately, for two reasons: it provides the "seed" electrons which become energized to radiation belt energies, and it generates the chorus waves responsible for much of the energization. We are developing transport (diffusion and advection) coefficients, based on existing analytical treatments of wave-particle interactions, that will be evaluated using realistic, dynamic wave models derived from THEMIS data. These will be used in a modified version of the Ring current-Atmosphere interactions Model (RAM) code to accurately account for chorus waves, energetic electrons which resonate with them, and the resulting interactions. The basic concepts, plans, and recent progress will be reviewed.

Implementing a Global Hybrid Vlasov Magnetospheric Model

S. von Alfthan[1], A. Sandroos[1], I. Honkonen[1,2], M. Palmrooth[1]

[1] *Finnish Meteorological Institute, PO Box 503, Helsinki, FI-00101, Finland, sebastian.von.alfthan@fmi.fi*
[2] *University of Helsinki, Department of physics, Helsinki*

Global simulations of the magnetosphere are currently being done using the magnetohydrodynamic (MHD) model, which FMI has implemented in the GUMICS-4 code. MHD simulations successfully describe phenomena where the important spatial scales are larger than ion gyro radii and the plasma has a well-defined temperature, but the inner magnetosphere is not satisfactorily modeled. This limits the applicability of the simulations for space weather purposes as most of the communication and positioning satellites reside in the inner magnetosphere. Here we describe a new simulation code called Vlasiator that is designed to tackle these challenges.

Vlasiator implements a Vlasov model for the ions, coupled to electrons modeled as a charge-neutralizing fluid. This model can describe multi-component plasmas without noise and in scales unreachable by existing techniques. A large-scale Vlasov-hybrid simulation is highly challenging, as in every grid cell of the ordinary space resides a velocity space, making the simulation six-dimensional. This increases the total number of simulation cells significantly compared to existing three-dimensional MHD simulations, and requires the use of petascale supercomputers in order to simulate a full global model. The time-scales also sets demanding quality criteria for the solver, as the simulation needs to be executed for up to 10^6 time steps.

We describe the algorithms used by the code, with focus on computational challenges that have been solved. The quality of different Vlasov solvers is discussed. The parallelization is implemented through a new finite volume grid library [1], the scalability of which is demonstrated for thousands of processor cores on large-scale supercomputers. As the computational requirement of the code is very large, we have also investigated the use of graphics processing units (GPU). The GPU based approach is described, and the performance and scalability is compared with the CPU based approach. Finally the roadmap towards the fully functional version of Vlasiator is discussed.

The project has received funding from the European Research Council under the European Community's Seventh Framework Programme (FP7/2007-2013) / ERC Starting Grant agreement number 200141-QuESpace. The work of SvA, IH and MP is supported by the Academy of Finland.

References

[1] I. Honkonen, *http://developer.berlios.de/projects/dccrg/*

Cosmic Rays Variation Studies with the BEO-Moussala Muon Telescope for the Period 2006-2011

I. I. Angelov[1,2]

[1] *Institute For Nucler Research and Nuclear Energy – BAS, 72 Tzarigradsko chaussee, Blvd., BG – 1784, Sofia, Bulgaria*

[2] *South West University "Neofit Rilski", Blagoevgrad, Bulgaria, i_angeloff@mail.bg*

The muon telescope at the Basic Environmental Observatory – Moussala (Institute for Nuclear Research and Nuclear Energy – Bulgarian Academy of Sciences) has been operational since August 2006. The telescope is with $1m^2$ effective area and is based on water Cherenkov detectors. The energy threshold for cosmic rays (CR) muons is 0.45 GeV, the count rate is ~150 000 / hour (corresponding to statistical uncertainty ~ 0.27% for 1 h intervals) and the rigidity cut-off for the site is ~ 6.3 GV. The instrument is sensitive to changes in the intensity of the 10-20 GeV range of primary CR spectrum. [1]

Almost full 5 years data set with CR muons intensities recorded every 15 seconds is available. Pressure corrected data are analyzed for periodic and sporadic variations.

The Lomb-Scargle method of spectral analysis was used searching for periodic variations. The peaks corresponding to the known diurnal and 27 – days variations are clearly seen in the periodogram. We used digital filtering (low pass filter for smoothing and high pass filter for trends removing) of the time series data and the method of the superimposed epochs to derive the amplitudes and phases of these periodic variations. The observed diurnal variation is with amplitude ~ 0.15-0.45 % and maximum at ~ 13:45 h local time, the amplitude is variable and for some periods one more maximum is observed. As expected the amplitude and phase of the 27-days variation are highly variable.

Two Forbush decreases (FD) were clearly visible in the data. The first one was in December 2006 [2] and the other in February 2011. The amplitudes and the times for the maximums are in good agreement with the plots from the neutron monitor stations.

References

[1] I. Angelov I., E. Malamova, J. Stamenov, *Sun and Geosphere*, v.3, n.1, 32-37 (2008)

[2] I. Angelov I., E. Malamova, J. Stamenov *Advances in Space Research*, v.43, n.4, 504-508 (2008).

Evidences of Existence of Plasma Ring Around the Earth at Geocentric Distances ~7-10R_E and its Impact on Substorm and Storm Dynamics

E.E.Antonova[1,2], I. P.Kirpichev[2,1], M.V.Stepanova[3], V. V. Vovchenko[2], M.O.Riazantseva[1,2], M.S.Pulinets[1], S.S. Znatkova[1], I.L.Ovchinnikov[1], K.G.Orlova[1]

[1] *Skobeltsyn Institute of Nuclear Physics Moscow State University, Moscow, 119991, Russia, antonova@orearm.msk.ru*
[2] *Space Research Institute (IKI) Russian Academy of Science, Moscow, Russia*
[3] *Physics Department, Science Faculty, Universidad de Santiago de Chile, Chile*

Plasma sheet like particle fluxes have constantly been observed during every satellite crossing of the magnetopause at the subsolar point. This phenonenon is studied in details using the data of Themis mission. This work summaries the evidences of the existence of plasma sheet like plasma population forming the ring around the Earth at the geocentric distances ~7-10RE. Statistical distribution of plasma pressure at geocentric distances 6<R<15RE was obtained using the Themis ESA and SST data from August 2007 till September 2010 (see [1]) and compared with previously obtained results.

It is shown that the distribution of plasma pressure at ~7-10R_E is close to azimuthally symmetric. Nighttime transverse currents in the surrounding the Earth plasma ring are concentrated near equator, daytime transverse currents are spread along compressed by solar wind field lines. However the integral daytime and nighttime transverse currents have nearly the same values at a definite R (see [2,3]), which means the existence of the continuation of the ordinary ring current till geocentric distances of ~10R_E. The high latitude portion of the ring current is supported by directed to the Earth plasma pressure gradient. Plasma sheet like ions with energies ~10 keV produce the main contribution in such pressure.

The existence of the high latitude continuation of the ring current gives the possibility to overcome difficulties related to the suggestion of great contribution of the tail current into the storm time Dst formation. It is shown that the correct values of Dst variation can be obtained from experimentally observed plasma pressure profiles without the contribution of the cross tail current by taking into account the nonlinear distortion of the dipole magnetic field by currents in plasma and that analyzed simple model describes Dst dynamics with comparatively high accuracy

Geomagnetic tail is the region with high velocity and magnetic field fluctuations (see [4,5] and later multiple works). The results of the analysis of the level of plasma sheet velocity fluctuations by INTERBALL, Geotail and THEMIS satellites show the possibility to select definite boundary of the region of high fluctuations at R~10R_E. The amplitudes of plasma bulk velocity fluctuations are greatly decreased at R<10R_E. It is possible to suggest that the internal boundary of turbulent tail current region coincides with the external boundary of the high latitude continuation of the ring current. However, this suggestion requires detailed verification.

Plasma sheet of the magnetosphere of the Earth is traditionally analyzed as the region where the substorm onset takes place. Constantly observed high level of plasma sheet turbulence including BBF presents the real obstacle for the realization of widely discussed “outside-in” model of substorm onset as the development of the instability responsible for substorm onset requires the existence of comparatively stable laminar plasma flow before the onset. Such conditions exist at R<10R_E. This work summarizes the evidences showing location of the isolated substorm onset at geocentric distances <10R_E , i.e. inside of the ring current region. Such feature requires the reanalysis of the existing theories of substorm onset.

The process of first auroral arc brightening during substorm onset is discussed. The process of arc brightening is analyzed taking into account the possibility of acceleration of electrons by preexisting field-aligned potential drop inside the inverted V structure. It is shown that the discussed mechanism is in agreement with the results of experimental observations.

Long-Term Variations of Dst Index and the Solar Wind Parameters in 19-23 Solar Cycles

L.Z. Biktash

Institute of Terrestrial Magnetism, Ionosphere and Radio Wave Propagation, Troitsk, Moscow Region, 142190, Russia, lilia_biktash@mail.ru

We have studied of long-term variations of equatorial Dst index in 19-23 solar cycles to display favorable conditions in interplanetary space which can have an influence on climate change. The Dst index is in common practice in the solar wind-magnetosphere-ionosphere interaction studies as well as in different Sun-Earth relationships up to medicine. Statistical study of the solar wind parameters and evolution of Dst-variations in solar cycles allow us to predict the Dst behavior in future. In this connection the solar wind and interplanetary magnetic field parameters obtained from the OMNI and Ulysses databases. Geomagnetic activity represented by Dst index from beginning 1957 to end 2010 were used in our study. Monthly and 27-day average variations of Dst index and the solar wind parameters were calculated and compared with sunspot numbers for 19-23 solar cycles. Superposed epoch results show Dst variations were the most intensive in 19 and 22 solar cycles. During these unique solar epochs the solar-wind high-speed streams occurred frequently and were the primary contributor to the recurrent Dst variations. It signifies that corotating interaction regions (CIRs) had been responded for high-speed solar wind streams and the resultant geomagnetic storms in Dst had been associated with large, long-lived low latitude solar coronal holes during declining phases of solar cycles. These structures were observed on the Ulysses in the interval of heliocentric distances 1.4–4.2 AU. The maximum in monthly Dst variations was observed in 19th solar cycle in spite of the fact that this solar cycle was the most strong among the latest five cycles. In general, Dst-variations in these solar cycles were going after sunspot numbers and only CIRs had broken this relation. We discuss Climate change in connection with evolution of Dst variations. Since Forbush observed decreases (Forbush decreases-FDs) in the cosmic rays (CR) count rate, scientists tried to understand their origin and influence on the Earth. It was shown good correlation between CR and Dst –index. Many authors have considered the influence of galactic and solar cosmic rays on the Earth's climate and cosmic ray activity as possible mechanism of climate change is the subject of wide speculation now. Recent researches have shown that the Earth's cloud coverage is strongly influenced by cosmic ray intensity. Clouds influence the irradiative properties of the atmosphere by both cooling through reflection of incoming short wave solar radiation, and heating through trapping of outgoing long wave radiation. It was found out that cosmic radiation is the main source of air ionization below 40-35 km. Reexamination made by some authors of the severe Dst events for their relationships with Forbush decreases and interplanetary parameters for SC19-23 shows that the time evolutions of Dst and FDs were very different and negative Dst and FDs had been uncorrelated sometimes. In number of the papers a good correlation between CR and sunspot numbers was shown. For example, a significant time lag near 26 months between the temporal variations of the CR amplitude and the sunspot number (SSN) was used by the authors to obtain the best correlation coefficient. It should be noted that to push ahead on this question the authors try to find good correlation with SSN at any price, whereas we have to use SSN for orientation mostly. Obviously, cosmic rays intensity and its duration will depend on the solar activity as CMIs, CIRs, solar wind and magnetospheric currents intensity and more detail investigations of these relationships are required.

Solar Activity and Equatorial Ionospheric Variations Caused by Different Large Scale Solar Wind Structures

L.Z. Biktash

Institute of Terrestrial Magnetism, Ionosphere and Radio Wave Propagation, Troitsk, Moscow Region, 142190, Russia, lilia_biktash@mail.ru

Intensive ionospheric currents during geomagnetic storms change the quiet ionosphere and short-term variations of the ionospheric characteristics are observed. Under these conditions the critical frequency foF2, virtual height h'F, drift velocities and others ionospheric characteristics are mainly defined by the solar activity and the state of the solar wind flowing around the Earth's magnetosphere. We examined equatorial ionospheric variations during geomagnetic storms of different intensity associated with large scale solar wind structures as coronal mass ejections (CMI) and corotating interaction regions (CIR) for different solar phases and cycles. Virtual ionosphere height and critical frequency foF2 at the equator were analyzed. We show that these variations are defined to a significant degree by the direction of the Bz-component of the interplanetary magnetic field but duration and intensity of these variations depend on origin of the solar wind streams (CMIs or CIRs). The ionospheric heights and foF2 variations at the equator during the northward IMF Bz and the southward IMF Bz (the main phase of the magnetic storm) are very distinguished. Distinction between quiet and disturbance periods in the heights can reach up to100 km and more. The critical frequency foF2 is markedly lower during the southward IMF Bz. It is shown that intensity of the equatorial ionospheric variations is different for the same solar wind conditions and depends on solar activity phases. These phenomena can mainly be explained by the solar wind – magnetosphere – ionosphere coupling.

Radiation-Belt Density Dropouts and Rapid Density Recoveries: Data Analysis and Simulations

J. E. Borovsky[1,2], M. H. Denton[3], D. T. Welling[1], J. Birn[1]

[1] *Los Alamos National Laboratory Los Alamos, New Mexico, 87545 USA, jborovsky@lanl.gov*
[2] *University of Michigan*
[3] *Lancaster University*

In the early phases of high-speed-stream-driven geomagnetic storms, the outer electron radiation belt often undergoes a "dropout" (or more accurately, a "reduction") of the relativistic-electron flux followed a fraction of a day later by a recovery and growth of the flux. It is thought that the dropout represents a loss of electrons from the magnetosphere. Using a density-temperature description of the electron radiation belt, the dropout and recovery is studied. Superposed-epoch analysis of stormtime data indicates that the dropout is temporally associated with a rise of solar-wind ram pressure and the appearance of a superdense plasma sheet. Electron orbits are traced in BATSRUS computer simulations of the dynamic magnetosphere during high-speed-stream-driven storms. Indications from the tracing are that the dropout (reduction) is initially caused by a contraction of the radiation belts to lower L shells caused by a compression of the magnetosphere, rather than a loss of electrons to the magnetopause or atmosphere.

Model of Galactic Cosmic Ray Spectrum during the Solar Cycle

M. Buchvarova, D. Draganov

Space and Solar-Terrestrial Research Institute-BAS, 6 Moskovska Str., Sofia1000, Bulgaria, marusjab@yahoo.com

An analytical model which generalizes the differential galactic cosmic ray spectrum in the heliosphere is proposed. The model parameterizes the spectrum at different physical conditions, including the most important effects controlling the CR intensity like diffusion - convection and energy losses. By a suitable choice of fitted parameter proposed model turns into two approximations: solution close to “force - field" model (describing the energy losses of CR in the in the inner heliosphere) and “convection-diffusion" equation (giving the reduction of CR intensity in the outer heliosphere). A mathematical relation between parameters in the proposed model and the modulation potential φ is derived. It is shown the model is more flexible to the data fitting than force - field approximation. The dependence of the model parameters on the solar activity parameters is discussed.

The Magnetospheric Multiscale Mission

J. L. Burch

Southwest Research Institute, P. O. Drawer 28510, San Antonio, TX, 78228-0510, USA, jburch@swri.edu

Magnetic reconnection is responsible for many energetic phenomena observed throughout the universe and in laboratory plasmas. Imaging of the solar corona with ever higher resolution shows conclusively that the explosive energy release and magnetic interconnection produced by reconnection are responsible for solar flares and coronal mass ejections as well as many smaller-scale phenomena in the solar transition region. Measurements of magnetic fields and plasma temperatures and densities within magnetic containment fusion devices show that reconnection is responsible for electron-temperature limiting phenomena such as sawtooth crashes. While comprehensive in situ plasma and field measurements are not possible in the solar atmosphere (too hot) or Tokamaks (reconnection scale sizes too small), the boundary regions of the Earth's magnetosphere provide an accessible laboratory for definitive magnetic reconnection experiments. Spacecraft missions such as ISEE, Polar, and Cluster have conducted such experiments and have verified the predictions of reconnection theory at the MHD and ion scales.

The next step in experimental magnetic reconnection research is the definitive exploration of the electron-scale phenomena because it is at this scale that the fundamental processes leading to the conversion of magnetic energy to particle energy and the interconnection of magnetic field lines occur. In addition to the challenges of making measurements at the spatial scales where electron inertia and the divergence of the electron pressure tensor become important is the fact that the reconnection regions are in constant rapid motion, either inward and outward at the magnetopause or down the magnetic tail in the neutral sheet. The NASA Magnetospheric Multiscale mission has been carefully designed, based on the results of the previous missions and the latest reconnection theories and numerical models, to answer the basic questions about reconnection, including the identification of its fundamental cause at the electron scales, the trigger mechanism that causes it to occur explosively, and the rate at which it proceeds in the different plasma boundaries in geospace.

Instrument Capabilities	
Instrument	**Parameters/Time Resolution**
DC B	*3D **B**/10 ms*
DC E	*3D **E**/~1 ms*
AC B	*Waveform, spectra to 6 kHz*
AC E	*Waveform, spectra to 100 kHz*
Plasma Electrons	*3D $f_e(v)$ 10 eV – 30 keV/30 ms*
Plasma Ions	*3D $f_i(v)$ 10 eV – 30 keV/150 ms*
Plasma Composition	*3D ion composition (H^+,He^{++},He^+,O^+) 1 eV – 30 keV/10 s*
Energetic Electrons	*3D $f_e(v)$ 10 keV – 500 keV/10 s*
Energetic Ions	*3D $f_i(v)$ 20 keV – 500 keV/10 s*
Energetic Ion Composition	*3D ion composition (H^+,He^{++},He^+,O^+) 20 keV – 500 keV/20 s*

The measurement requirements for MMS are based on data and modeling results on the size, motion and particle and field populations expected in the ion and electron diffusion regions. The most stringent requirement, based on rapid motion of the magnetopause past the spacecraft, is for full 3D plasma electron distribution functions every 30 ms. As on Cluster, an ASPOC plasma neutralizer will maintain spacecraft potentials to less than +4V.

The four MMS spacecraft cluster will maintain a tetrahedral shape when near the magnetopause and neutral sheet with separations between 10 and 160 km (magnetopause) and 30 and 400 km (neutral sheet).

On-Board Burst Triggers	
Physical Signature	**Trigger Parameter**
Reconnection Jets	*Ion Flow Reversals*
Magnetopause/Neutral Sheet Detection	*Large **B** variations or Large Electron Currents*
Large Flows Surrounding Reconnection Sites	*Large **E***
Particle Acceleration	*Electron and Ion Beams*
Electron Diffusion Region	***E** Parallel to **B***

In the regions of interest, (> 9 R_E day side, >15 R_E night side) all instruments will acquire data at the maximum (burst) rate with about two orbits stored on board. On-board burst triggers will be used to select burst data intervals. Prior to the burst downlink a scientist-in-the-loop on the ground will use lower-rate fast survey data to select other (either additional or replacement) burst intervals for downlink on the next data pass.

Ring Current Modeling and ENA Data Analysis

N. Buzulukova[1]

[1] *NASA Goddars Space Flight Center/University of Maryland, Greenbelt, Maryland, 20771, USA, nbuzulukova@gmail.com*

A geomagnetic storm is identified through the global deviation of the H-component of the geomagnetic field at low latitudes (i.e., the Dst index). The main source of substantial negative deviations in the Dst index is the ring current. It is formed by plasma with energies ~1-100 keV surrounding the Earth (3-10 R_E in the geomagnetic equatorial plane). We describe state-of-the-art approaches to model the ring current plasma. Observationally, we study the ring current temporal and spatial evolutions from Energetic Neutral Atom (ENA) images. ENAs are formed as a result of charge-exchange process between ring current plasma and geocorona. We show ENA emissions from ring current acquired by IMAGE and TWINS missions. ENA emissions reflect particle injection, formation of asymmetric ring current and the subsequent symmetrization. Based on ring current model results, we calculate synthetic ENA images. By comparing real images with synthetic ones we have developed a powerful tool to investigate the physical processes that control the ring current variability during geomagnetic storms. Additionally we show an analysis of ENA emissions arriving from low altitudes. We show different dynamics of low altitude emissions and ring current emissions during geomagnetic storm. We discuss the relationship between low altitude emissions, ring current trapped population and precipitating particles.

Study of Deep See Fe-Mn Sediments and the Possibility to use these Formations as Paleoclimatic Indicator

K. Chakarova[1], V. Rusanov[2], A. X. Trautwein[3]

[1] *American College of Sofia, P. B. 873, 1000 Sofia, Bulgaria, chakarova@acs.bg*
[2] *Faculty of Physics, University of Sofia, 5 James Bourchier Blvd., 1164 Sofia, Bulgaria*
[3] *Institut für Physik, Universität zu Lübeck, Ratzeburger Allee 160, D-23538 Lübeck, Germany*

The iron-bearing compounds in Fe-Mn deep see sediments (nodules and slabs) are studied by Mössbauer spectroscopy at 77, 4.2 and 0.3 K. The Mössbauer parameters and the concentration of the two main components detected, α-FeOOH (Goethite) and $Fe_5HO_8.4H_2O$ (Ferrihydrite), are measured in 1 mm steps. The mineral Goethite exhibits defect crystal structure and at 77 K a Mössbauer sextet with broad and asymmetric lines, at room temperature partially a doublet due to superparamagnetic state. Ferrihydrite has a very low blocking temperature (< 20 K) and, according to our measurements at 0.3 K, shows a Mössbauer sextet with broad lines.

X-ray topography pictures of Fe-Mn nodules and slabs show specific layer structure related to two long-period variations (1.9 million years (Ma) of the eccentricity *e* and 1.2 Ma of obliquity ε of Earth′s axis) which according to the Milankovitch-astronomical-theory can enforce drastic changes of climate [1]. The hydrogenetic Fe-Mn crusts have a very low growth rate of 3-6 mm/Ma, while the diagenetic nodules grow faster, i.e. 10-20 mm/Ma [2], so we could cover time intervals up to 20 Ma by our investigation. One example of our study with five sublayers is presented in Fig. 1. The layer structure probably correlates to the astronomical data of the variations of Earth's axis obliquity. Another example related to specific changes of the eccentricity is presented in Fig. 2. The global geological events as the initiation of Northern Hemisphere glaciations (about 3 Ma BP), the rise of the Isthmus of Panama and beginning of the modern bottom water circulation (about 6.4 Ma BP) will be also discussed.

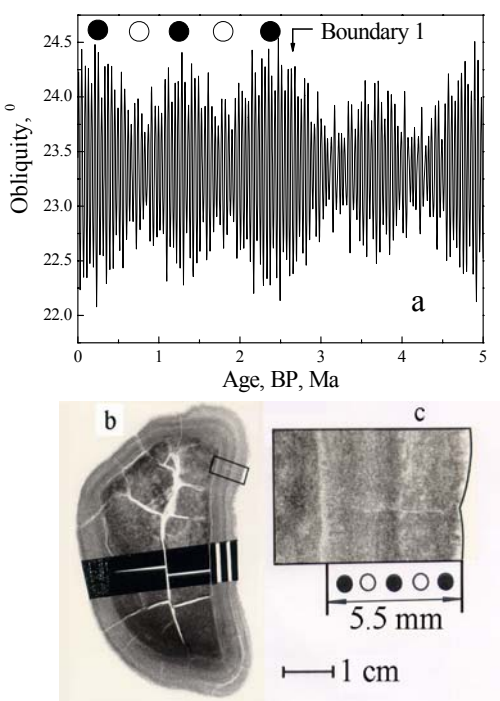

Figure 1. a) Data of the obliquity of Earth's axis variations for the last 5 Ma BP after [3]; b) X-ray picture (positive) of Indian Ocean nodule slab, about 3 mm thick. Five thin layers postdate boundary 1 are marked; c) selected part shows these five layers at larges magnification. The colder intervals are marked by open circles, the warmer by solid circles.

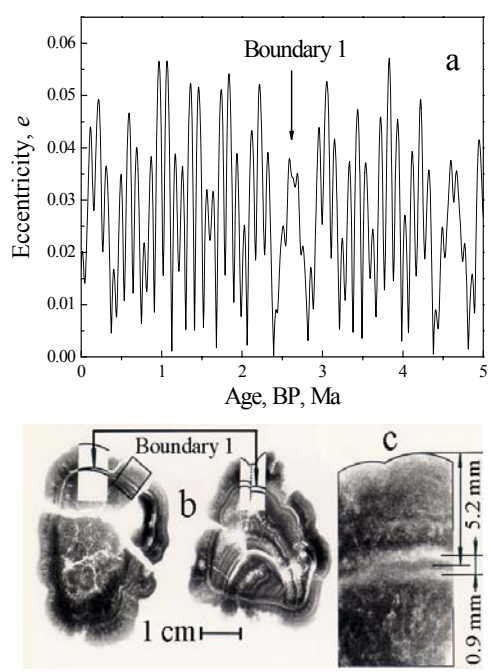

Figure 2. a) Data of the Earth's eccentricity variations for the last 5 Ma BP after [3]. The arrow marks the age which may be associated with boundary 1 of the nodules; b) X-ray picture (positive) of Indian Ocean nodule slabs, about 3 mm thick. A sharp double boundary 1 in the nodule structure is marked; c) selected profile of boundary 1 at larges magnification.

V. Rusanov and A. X. Trautwein acknowledge the continuous support by the Alexander von Humboldt-Foundation.

References

[1] V. Rusanov, V. Angelov, K. Chakarova and G. Ajdanlijsky, *Naturwissenschaften* **80**, 170 (1993).
[2] M. Segl et al., *Nature* **309**, 540 (1984).
[3] A. L. Berger and M. F. Loutre, *Quat. Sci. Rev.* **10**, 297 (1991).

Cross Scale Coupling and Particle Energization Through the 'Gap' Region

C. C. Chaston[1], T. Sakanoi[2], K. Seki[3], K. Asamura[4], M. Hirahara[3]

[1] *Space Sciences Laboratory, 7 Gauss Way, Berkeley, CA, 94720, USA, ccc@ssl.berkeley.edu*
[2] *Planetary and Atmopheric Research Center, University of Tohoku, Sendai, Japan*
[3] *Solar Terrestrial Environment Laboratory, University of Nagoya, Nagoya, Japan*
[4] *Institute of Space and Astronautical Science, Japan Aerospace Exploration Agency, Kanagawa, Japan.*

Through the combined use of observations from the FAST and Reimei spacecraft we discuss the nature of energy transport and particle acceleration through the auroral acceleration region sometimes referred to as the 'Gap' region in global modeling efforts. Recent high resolution imager and conjugate particle measurements now provide an unprecedented opportunity to examine the processes through which energy is transported across scales through auroral arcs that can lead to filamentary structures and intense localized regions of ion outflow. Through the implementation of image analysis techniques and 3-D simulations of auroral current sheets we suggest physical mechanisms which facilitate the energy transport across scales through auroral arcs which may lead to the acceleration observed. We present statistics from the FAST mission to show that these processes drive large fluxes of energized ionospheric ions outward from high latitudes to populate the plasma sheet and to perhaps provide a source for ring current ions during storm times.

Global MHD Simulations of Field Line Resonances and Waveguide Modes

S. G. Claudepierre[1], M. K. Hudson[2], W. Lotko[3], J. G. Lyon[2], R. E. Denton[2]

[1] *The Aerospace Corporation, 2350 E El Segundo Blvd., M2-260, El Segundo, CA 90245, USA*
seth.g.claudepierre@aero.org
[2] *Dartmouth College, Department of Physics and Astronomy, 6127 Wilder Laboratory, Hanover, NH 03755*
[3] *Dartmouth College, Thayer School of Engineering, 8000 Cummings Hall, Hanover, NH 03755*

Solar wind driving of the Earth's magnetosphere is investigated with the Lyon-Fedder-Mobarry global, 3D, single-fluid MHD simulation code. We explore the role that solar wind dynamic pressure fluctuations play in the generation of magnetospheric ULF waves, using idealized solar wind configurations to drive the MHD simulations. In this numerical experiment, we impose both monochromatic and quasi-broadband dynamic pressure fluctuations in the Pc3-5 ULF range on the magnetosphere. We find both toroidal mode field line resonances (FLRs) and waveguide modes in the magnetospheric response, consistent with well-established mode coupling theory [e.g. *Chen and Hasegawa,* 1974; *Kivelson and Southwood,* 1985]. The overall features of the simulated resonances are in agreement with commonly observed ULF wave characteristics. To the best of our knowledge, these results are the first to explicitly and unambiguously reproduce inner magnetospheric resonances using a global MHD simulation of the solar wind magnetosphere interaction. When compared with previous ULF modeling studies [e.g. *Lee and Lysak*, 1989], the realistic geometry of the LFM magnetosphere and its interaction with the solar wind provides a more accurate, global representation of ULF waves in the coupled solar wind magnetosphere-ionosphere system. In particular, we demonstrate how global MHD simulations can be used as a powerful tool to track the flow of energy through the entire coupled system.

References

[1] M. G. Kivelson and D. J. Southwood, *Geophys. Res. Lett.*, **12**, 49 (1985).
[2] L. Chen and A. Hasegawa, *J. Geophys. Res.*, **79**, 1024 (1974).
[3] D.-H Lee and R. Lysak, *J. Geophys. Res*., **94**, 17097 (1989).

Relativistic Electron Fluxes and Dose Rate Variations Observed on ISS

Ts.P. Dachev[1], B.T. Tomov[1], Y.N. Matviichuk[1], P.G. Dimitrov[1], N.G. Bankov[1]
G. Reitz[2], G. Horneck[2], D.-P. Häder[3]

[1]*Space and Solar-Terrestrial Research Institute,Bulgarian Academy of Sciences,Sofia,Bulgaria, tdachev@bas.bg*
[2]*DLR, Institute of Aerospace Medicine, Köln, Germany*
[3]*Neue Str. 9, 91096 Möhrendorf, Germany*

Understanding the dynamics of relativistic electrons in the inner magnetosphere is of significant importance from both a practical and space physics point of view.

The paper presents observation of relativistic electrons on the International Space Station. Never the less that their presence and important role for the formation of the dose records of the astronauts during Extra Vehicular Activity (EVA) was predicted many years ago [1] our observations are one of the first experimentally proved and reported [2].

Data for this paper are collected by the Radiation Risk Radiometer-Dosimeter R3DE during the flight of the instrument at the European Technology Exposure Facility (EuTEF) on the Columbus External Payload Adaptor at the ISS inside of the ESA EXPOSE-E facility in the period February 20, 2008– June 26, 2009 and during the flight of the R3DR instrument inside of the ESA EXPOSE-R facility on the external pallet of the Russian Zvezda module during the period of outer radiation belt enhancement in April 2010. The construction of the R3DE/R instruments shows that the total external and internal shielding before the Si detector (0.3 mm thick, 2 cm^2 area) is 0.41 g cm^{-2}. The calculated stopping energy of normally incident particles to the detector is 0.78 MeV for electrons and 15.8 MeV for protons.

Statistical analysis of R3DE data shows gradually decrease of the daily observed relativistic electrons from values of 200-250 μGy day^{-1} in February 2008 down to values of few μGy day^{-1} at the end of period in June 2009. The decrease is connected with the extremely low solar activity in the end of the 23rd solar cycle.

Figure 1 presents data between 1st of April and 6th of May 2010 with dose to flux ratio less than 1 nGy cm^{-2} $part^{-1}$ and dose rates above 15 μGy h^{-1}, which guarantee population by electrons with energy above 0.78 MeV only [3]. On the X axes is plotted the UT time. The panel (a) in figure presents the Dst index, which gives information about the strength of the ring current around earth http://cdaweb.gsfc.nasa.gov/ (King and Papatashvilli, 2011). The axes presents Dst in reverse than usual way of presentation to be underlined the correlations between the negative Dst index and the values in Figure 1b, where 3 variable are plotted: the doses as measured by the instrument, the calculated daily dose and the accumulated from the beginning dose in μGy.

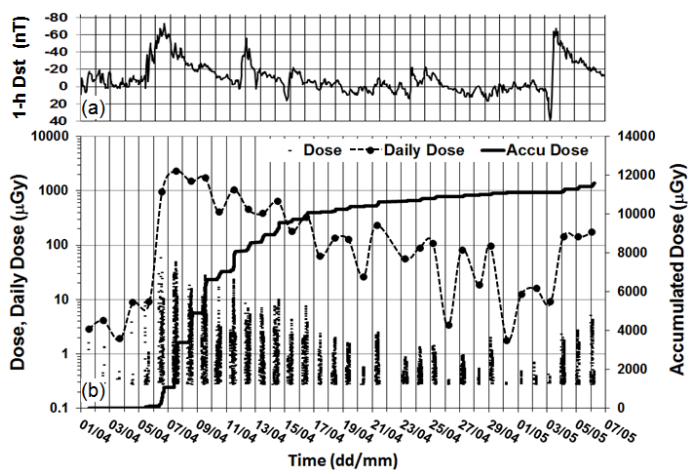

After the Coronal Mass Ejection (CME) on 3 of April (09:54 UTC) on 5 of April a shock was observed at the ACE spacecraft at 07:56 UTC, which led to a sudden impulse at Earth at 08:26 UTC and creation of moderate magnetic storm shown with Dst index in upper panel. Our high resolution study of the dose rate dynamics on 5th of April shows that the first crossing of high latitude region in Southern hemisphere, reaching L=5.12 we observe highest per day dose rate of 3,302 μGy h^{-1} at 11:06:53 UTC, which is well seen on Figure 1b. Unfortunately all other crossings of high latitudes on 5th of April show smaller values. So we may conclude that the outer radiation belt enhancement is not happen "at once" but time is needed to be filled up first lower altitude field lines next highest. This process continues on 6th of April and takes its final highest value in the dose and daily dose on the recovery phase of the magnetic storm on 7th of April. Also decrease of equatorwards boundary is observed.

The accumulated dose (look right axes and heavy black line) increase up to value of 11700 μGy for the whole period. According to the TEPC data http://cdaweb.gsfc.nasa.gov/ (Zapp, 2011) on the ISS the astronauts collect during the docking with ISS between 7:44 hour on 7th of April and 12:52 at 17th of April 2010 totally 2766 μGy or 6663 μSv. For the same period R3DR behind smaller shielding (0.41 g cm^{-2}) collect 14523 μGy or 18187 μSv. The additional dose according to R3DR data for the NASA astronauts Rick Mastracchio and Clayton Anderson collected during the 3 EVA is 1067 μGy or enhancement with 38.6% in comparison with other astronauts not being on EVA. The equivalent additional dose according to R3DR data is 1170 μSv or enhancement with 17.6%.

Never the less that the accumulated by the astronauts from relativistic electrons skin doses are relatively small and do not pose real danger for their health the R3DE/R measurements gives important experimental information, which confirms the necessity of permanent active monitoring of the radiation doses of astronauts during EVA [1].

References

[1] Committee on Solar and Space Physics, NRC, *ISBN: 0-309-51536-X,* p. 37, (2000).
[2] T. Dachev et al., *J. Adv. Space Res.* 44, 1433-1440, (2009).
[3] T. Dachev, *J. Adv. Space Res., **44**, 1441-1449,* (2009).

Overview of the Results Obtained with Bulgarian Build Instruments for the Ionizing Radiation Distribution from the Earth Surface to the Moon Orbit

Ts.P. Dachev

Space and Solar-Terrestrial Research Institute, Bulgarian Academy of Sciences, Sofia Bulgaria, tdachev@bas.bg

Since 2000 scientists from Space and Solar-Terrestrial Research Institute at the Bulgarian Academy of Sciences contributed with Bulgarian build instruments in number of experiments for measurements of the incoming Space radiation from Earth Surface to the Moon Orbit. This paper summarizes the results carried out by different Liulin type instruments: (1) Mobile Dosimetry Unit (MDU) MDU-2 was used on French balloon flight up to 32 km on 14th of June 2000; (2) MDU-5 was used for more than 8000 h between 2001 and 2009 on aircraft of Czech Airlines (CSA) at different routes. Most significant results were the measurements at about 10.7 km altitude during the SPE and Ground level event (GLE-15) on 15th of April 2001 [1] and the use of the instrument to proof the results for the individual monitoring of the aircrew [2]. Similar and more sophisticated instruments (see Figure 1.) were used for aircraft radiation monitoring by colleagues from Canada [3], Germany [4], Australia [5], Spain [6] and others; (3) Mobile Radiation Exposure Control System – Liulin-E094 containing four active battery-powered dosimeters worked successfully between May and August 2001 on the board of US Laboratory module of the International Space Station (ISS) [7]. Very important results are the validation of HZETRN model [8,9] and the time serial analysis of the induced LEO environment [10]; (4) R3D-B2 Radiometer-Dosimeter with 256 channels ionizing radiation spectrometer and four UV channels spectrometer was flown 31 May–16 June 2005 inside of the ESA Biopan 5 facilities on Foton M2 satellite [11]; (5) Liulin-ISS contains four MDU with displays and Control and interface unit and will be used for 15 years in the Service Radiation Monitoring System of the Russian segment of ISS; (6) 3 battery-powered MDUs were operated during the 8 June 2005 certification flight of the NASA Deep Space Test Bed (DSTB) balloon at Ft. Sumner, New Mexico, USA [12]; (7) R3D-B3 and Liulin-Photo instruments were used 14–29 September 2007 inside of the ESA Biopan 6 facilities on Foton M3 satellite. Good agreement with GEANT4 Monte-Carlo code and experimental observations was obtained [13]; (8) Liulin-R was launched successfully on HotPay2 rocket January 31, 2008 up to 380 km altitude from Andoya Rocket Range (ARR) in Norway; (9) R3DE instrument worked on EuTEF platform outside of the European Columbus module of ISS between February 20th 2008 and September 1st 2009. Major results of the experiment are: the proof of the Liulin ability to characterize the near Earth radiation environment [14], the observed for first time fluxes and dose rates by relativistic electrons on ISS [15] and the observed drops down of the ISS radiation environment during the Space Shuttle dockings [16]; (9) on 22nd of October 2008 RADOM instrument [17] was launched successfully on Indian Chandrayaan-1 satellite and worked inside of the Earth radiation belts and on 100/200 km circular lunar orbit [18]; (10) R3DR instrument worked on EXPOSE-R platform outside of the Russian Zvezda module of ISS between March 2009 and January 2011; (11) Liulin-6I, Liulin-6R and Liulin-6MB are internet based instruments, which generate web pages. They work online at Jungfrau (Switzerland) http://130.92.231.184/), Moussala (Bulgaria) http://beo-db.inrne.bas.bg/moussala/ and Lomnicky Stit (Slovakia) http://147.213.218.13/ peaks. Main advantage of the Liulin type spectrometers are their low weight (~100 g), low power consumption (~100 mW) and low cost (~10,000 Euro). The high scientific and application value of the obtained data is coming mainly from the extensive calibrations [19] at different accelerators and from well-developed data analysis procedures. Data from all mentioned above experiments are analysed, compared and plotted to reveal harmonized picture how the different ionizing radiation sources contribute and build the distribution from the earth surface to the moon orbit.

References

[1] F. Spurny, F. and T. Dachev, *Radiation Protection Dosimetry, **95**, 273-275*, 2001.
[2] O. Ploc et al., *Radiation Protection Dosimetry,**144**, 611-614,* (2011).
[3] B. Lewis et al., *Radiation Protection Dosimetry, **116**, 320-326, (*2005).
[4] F. Wissmann et al., *Radiation Protection Dosimetry, **140**, 319-325,* (2010).
[5] I. Getley et al., *Advances in Geosciences**, 2, ST),** 303-310*, (2007).
[6] J. Sáez Vergara and R. Dominguez-Mompell Román, *Radiation Protection Dosimetry, **136**, 291-296,* (2009).
[7] G. Reitz et al., *Radiation Protection Dosimetry, **116**, 374-379,* (2005).
[8] J. Nealy et al., *J. Adv. Space Res. **40**, 1593-1610, (2007).*
[9] T. Slaba et al., *J. Adv. Space Res., **47**, 600-610, (*2011).
[10] J. Wilson et al., *J. Adv. Space Res., **47**, 1562-1570,* (2007).
[11] D. Häder et al., *J Adv. Space Res., **43**, 1200-1211,* (2009).
[12] J. Adams et al., *Nuclear Instruments and Methods in Physics Research A*, ***579,** 522–525,* (2007).
[13] M. Damasso et al., *Radiation Measurements, **44**, 263-272,* (2009).
[14] T. Dachev, *J. Adv. Space Res., **44**, 1441-1449,* (2009).
[15] T. Dachev et al., *J. Adv. Space Res. **44**, 1433-1440, (2009).*
[16] T. Dachev et al., *J. Adv. Space Res. **47**, 2030-2038, (2011).*
[17] T. Dachev et al., *Current science, **96**, 544-546,* (2009).
[18] T. Dachev et al., *J. Adv. Space Res. (2011).* (accepted article) doi:10.1016/j.asr.2011.05.009
[19] Y. Uchihori et al, *J. Radiation Measurements **35,** 127 – 134, (2002)*

The Dynamics of the Plasmasphere

F. Darrouzet[1], J. De Keyser[1], V. Pierrard[1], H. Matsui[2], N. Ganushkina[3]

[1] *Belgian Institute for Space Aeronomy (IASB-BIRA), 3 Avenue Circulaire 1180 Brussels, Belgium, Fabien.Darrouzet@oma.be*

[2] *Space Science Center, University New Hampshire, Durham, NH, USA*

[3] *Finnish Meteorological Institute, Helsinki, Finland*

The plasmasphere is a very dynamic region. This dynamics is mainly determined by the convection electric field combined with the corotation electric field. The plasmasphere is disturbed during geomagnetic storms and substorms, with formation of a sharp plasmapause closer to the Earth and generation of a plume in the afternoon MLT sector.

We review here the characteristics of plasmaspheric plumes determined from recent missions (Cluster and IMAGE), and shown by a three dimensional physical dynamic model. In particular, we present a statistical analysis of plasmaspheric plumes observed by WHISPER during 6 years of the Cluster mission.

Small-scale density fluctuations appear to exist inside plasmaspheric plumes. They are accompanied by corresponding fluctuations in the magnetic and electric fields. Those fluctuations are examined in an event study with data from the Cluster and IMAGE missions.

Knowing the field-aligned density distribution in the plasmasphere is of fundamental importance for understanding processes such as plasmaspheric refilling. We discuss here a new technique to infer field-aligned density profiles from the densities sampled by the individual spacecraft as they traverse the plasmasphere. The method is applied to a few Cluster data sets to show its potential.

The plasmaspheric region has direct influence on other regions of the magnetosphere. For instance, radiation belt energetic particle populations are very sensitive to the core plasmasphere distribution and specifically to the position of the plasmapause. The relationship between the position of the plasmapause and the inner edge of the outer radiation belt is studied on basis of recent Cluster observations.

The Density and Temperature of the Outer Electron Radiation Belt: Temporal and Spatial Changes during Different Types of Solar-Wind Driving

M. H. Denton[1] and J. E. Borovsky[2]

[1] *Department of Physics, Lancaster University, Lancaster, LA1 4YB, UK. m.denton@lancaster.ac.uk*

[2] *ISR-1, Los Alamos National Laboratory, Los Alamos, NM 87545, USA. jborovsky@lanl.gov*

The Earth's outer electron radiation belt is a highly dynamic region in which sources and losses have yet to be firmly constrained. We present results whereby bi-Maxwellian fits are made to the electron fluxes measured by the SOPA instrument at geosynchronous orbit. This leads to a density-temperature description of the outer electron radiation belt.. We describe the spatial and temporal changes which can be observed in the density and temperature of the outer belt during different types of solar-wind driver. We also describe how the density-temperature description differs from a more traditional flux description.

Auroral Disturbances Associated with the Fronts of High-Speed Streams in the Solar Wind

I.V. Despirak[1], A.A. Lubchich[1], R. Koleva[2]

[1] *Polar Geophysical Institute, Akademgorodok 26a, Apatity, 184209, Russia, despirak@gmail.com*
[2] *Space and Solar-Terrestrial Research Institute, BAS, Sofia, Bulgaria*

Unusually large auroral expansions occur during solar wind structures called Sheaths and CIR. The Sheaths and CIRs, characterized by high solar wind plasma density and intense and variable IMF Bz, are the regions of interaction of the undisturbed solar wind with the recurrent streams and magnetic clouds. The Sheaths and CIRs also relate to magnetic storms. Although the auroral disturbances during Sheaths and CIRs have signatures of auroral substorm development (localized onset and formation of the auroral bulge), a question arises if the disturbances are substorms. To answer this question we considered data from the Geotail spacecraft in the magnetotail. Solar wind parameters were taken from the Wind spacecraft observations; the auroral bulge parameters were obtained by the Ultra Violet Imager onboard Polar. Some ten events are selected when Geotail was in the plasma sheet during the auroral bulge formation related to Sheath and CIR. We noted that some signatures of a typical substorm were observed in the magnetotail, namely: tailward-to-Earthward plasma flow reversals associated with the reconnection process, as well as a sharp decrease of the total pressure following the interval of pressure increase. This enables us to consider the auroral disturbances during Sheath and CIR as substorm.

Solar and Geomagnetic Activity Effects on Heart Rate Variability

S. Dimitrova[1], I. Angelov[2,3], E. Petrova[4]

[1]*Space and Solar-Terrestrial Research Institute, Bulgarian Academy of Sciences, Acad. G. Bonchev Str., Bl. 3, Sofia 1113, Bulgaria, svetla_stil@abv.bg*

[2]*South West University, Blagoevgrad, Bulgaria*

[3]*Institute for Nuclear Research and Nuclear Energy, Bulgarian Academy of Sciences, Sofia, Bulgaria*

[4]*Institute of Experimental Morphology, Pathology and Anthropology with Museum at the Bulgarian Academy of Sciences, Sofia, Bulgaria*

Numerous scientific studies indicate possible influence of physical environmental factors such as solar activity, geomagnetic storms, cosmic rays and climate changes on human physiology and psychophysiology and different diseases, especially on cardiovascular and nervous system.

Heart rate variability (HRV) is determined based on the length of successive RR intervals in electrocardiogram (ECG). It is an important indicator of the activity of the autonomous (vegetative) nervous system. Reduced HRV is a negative prognostic factor, often preceding and/or accompanying various cardiovascular diseases, including fatal diseases as well as cases of sudden cardiac death (1). There are investigations which have shown that space weather changes are associated with reduced HRV (2, 3, 4).

Two healthy volunteers recorded their ECG for a period of 1 year (April 2008 – April 2009). The first person was 35-years old female and the second one 39-years old male. The volunteers recorded two 5 minutes ECG every day – in the morning after awakening and in the evening before falling asleep.

Additionally a group of 14 healthy persons with an average age of 47.2 years was also examined from 23.03.2009 to 30.04.2009. Data about their ECG, arterial blood pressure (BP) and subjective psycho-physiological complaints (SPPC) were gathered.

ECGs were processed by custom software and HRV parameters in time domain (RRmin, RRmax, RRavg, SDNN, RMSSD, pNN50) and frequency domain (LF, HF, LF/HF) were derived.

Physiological parameters were analyzed regarding geomagnetic activity (GMA), estimated by daily planetary Ap-index. Gradation of GMA levels was described in (5).

The statistical method of the *ANalysis Of VAriance* (ANOVA) was applied to establish a statistical significance of the influence of GMA levels on HRV parameters, BP and SPPC. The effect of geomagnetic activity up to three days before and after the respective events on the examined parameters was also investigated by the help of ANOVA and superimposed epoch method.

The period of examinations was characterized by minimal solar and GMA. Results revealed strong variations of HRV parameters of the group from the day before (-1st day) till three days after (+3rd day) the weak storms, which were registered during the time of investigation. Unfortunately there were no geomagnetic storms with higher intensity from 23.03.2009 to 30.04.2009. BP and SPPC increased statistically significantly from 0 day till +2nd day. There was a trend for decrease in heart rate on 0 day.

Personal everyday measurements of the two volunteers for a period of 1 year revealed that morning measurements were more sensitive to space weather variations in comparison to evening measurements. It is probably due to accumulation of other social factors during the course of everyday activities.

It is interesting that both persons reacted in different way to geomagnetic storms with different intensities. They decreased heart rate during moderate storms but increased this parameter during weak and major storms and on the days before and after the respective storms. HRV parameters varied significantly also on these days.

The strong increase as the decrease of the HRV indices is related to raised risk of incidences like arrhythmia, infarctions, other cardio-vascular diseases and also sudden cardiac death. These results show that further investigations should be performed in this direction. The determination of the impact degree of the solar activity factors on the cardio-vascular parameters will make it possible to recommend under which changes of the respective factors it will be desirable to undertake preventive measures.

References

[1] Task Force. Heart rate variability: Standards of measurement, physiological interpretation and clinical use. Task Force of the European Society of Cardiology and the North American Society of Pacing and Electrophysiology, *European Heart Journal*, **17**, pp. 354–381, (1996).

[2] R.M. Baevsky, V.M. Petrov, A.G. Chemikova 1998. Regulation of autonomic nervous system in space and magnetic storms, *Adv. Space Res.,* **22(2)**, pp. 227-234, (1998).

[3] G. Cornelissen, G., F. Halberg, Breus, T., Syutkina, E., Baevsky, R., Weydahl, A., Watanabe, Y., Otsuka, K., Siegelova, J., Fiser, B., E. Bakken. Non-photic solar associations of heart rate variability and myocardial infarction. *JASTP* **64**, pp. 707-720 (2002).

[4] S. Oinuma, Y. Kubo, K. Otsuka, T. Yamanakata, S. Murakami, O. Matsuoka, S. Ohkawa, G. Cornelissen, A. Weydahl, B. Holmeslet, C. Hall, F. Halberg. Graded response of heart rate variability, associated with an alteration of geomagnetic activity in a subarctic area. *Biomedicine & pharmacotherapy,* **56** (sup 2), pp. 284-288 (2002).

[5] S. Dimitrova. Different geomagnetic indices as an indicator for geo-effective solar storms and human physiological state, *JASTP* **70**, pp. 420-427, (2008).

Modeling the Magnetosheath Response to the Passage of the Interplanetary Magnetic Cloud

P. S. Dobreva[1], G. N. Zastenker[2], N. L. Borodkova[2], M. D. Kartalev[1]

[1] *Institute of Mechanics, Bulgarian Academy of Sciences, Acad G. Bontchev Str. Block 4, Sofia, 1113, Bulgaria, polya2006@yahoo.com*

[2] *Space Research Institute, RAN, Profsousnaya 84/32, Moscow, 117811, Russia*

We utilize a new numerical model of the solar wind interaction with the system magnetosphere-magnetosheath in modeling this system interaction with interplanetary magnetic clouds. The used model integrates self-consistently a 3D numerical magnetosheath model and a modified Tsyganenko magnetosphere model with numerically computed shielding field, providing in particular 3D magnetosheath and shock wave geometries and positions. It is demonstrated that the relatively simplified model predicts adequately the magnetosheath structure, and especially – the magnetopause behavior, following by the magnetic cloud's parameters variation. A special attention is paid on the magnetic cloud event on 6-11 January when the Interball-1 was around the Earth's magnetosheath, detecting multiple crossings, supposed to be caused by the magnetic cloud passing.

Simulation of Altitude Variation of Aerosol Production during Solar Cycle

D. Draganov[1], M. Buchvarova[2]

[1] *Space and Solar-Terrestrial Reseach Institute, BAS, 6 Moskovska St,. Sofia 1000, Bulgaria*
[2] *Space and Solar-Terrestrial Reseach Institute, BAS, 6 Moskovska St., Sofia 1000, Bulgaria*

To further evaluate GCR-cloud link it is proposed a computational simulation of altitude variation of stratospheric and tropospheric ultra fine aerosol production during the 11-year solar cycle on the base of ion-nucleation mechanism. The computational simulations in the troposphere are based on ion-mediated nucleation (IMN) theory [1],[2]. The stratospheric ultra fine aerosol particles are calculated with Hofman and Rosen'equation [3]. To the parameters controlling the particle formation (ambient conditions and altitude) ion-nucleation theory adds ion concentration (or ion production rate - Q). In the proposed computer model the ionization is estimated with Corsika Code Simulations.

References

[1] Yu, F., and R. P. Turco, From molecular clusters to nanoparticles: The role of ambient ionization in tropospheric aerosol formation, J. Geophys. Res., 106, 4797– 4814, 2001.
[2] Yu, F., and R. P. Turco, Ultrafine aerosol formation via ion-mediated nucleation, Geophys. Res. Lett., 27, 883– 886, 2000.
[3] Hofmann, D. J. and Rosen, J. M.: 1983a, Sulfuric acid droplets formation and growth in the stratosphere after the 1982 eruption of El Chichon, Science 222, 325-327.

Numerical Investigation of Surfatron Acceleration Efficiency of the Charged Particles by Wave Packets in Space Plasma

N. S. Erokhin[1], L.A. Mikhailovskaya[1], N. N. Zolnikova[1], R. Shkevov[2]

[1] *Space Research Institute - Russian Academy of Sciences, 117997, 84/32 Profsoyuznaya Str, Moscow, Russia, nerokhin@mx.iki.rssi.ru*

[2] *Space and Solar-Terrestrial Research Institute - Bulgarian Academy of Sciences, 6 Moskovska Str., Sofia 1000, Bulgaria, shkevov@space.bas.bg – corresponding autor*

A theoretical studying of charged particles relativistic acceleration efficiency by a finite amplitude electromagnetic wave packet in space plasma is presented. The effect of surfatron mechanism particle acceleration is investigated by thenumerical analysis of second order nonstationary, nonlinear equation for the wave packet phase at the particle trajectory. The influence of the phase and group velocities of the wave packet at the wave packet carrying frequency on acceleration efficiency is studied. The optimal conditions for particles capture by electromagnetic wave packet with the following highly relativistic charges acceleration are determined. The particle acceleration rate for the regime of surfatron relativistic acceleration is estimated. The temporal dynamics of particles acceleration is investigated. The conclusion about possibilities of ultralrelativistic surfatron acceleration of charges by a wave packet with smooth envelope of its amplitude was done.

Some *work* plots from the future paper:

Based on the numerical analysis of the equation (1):

$$\frac{d^2}{d\tau^2}\Psi(\tau) - \frac{\left[1-\beta^2\cdot\left(1-\frac{d}{d\tau}\Psi(\tau)\right)^2\right]^{1.5}}{\beta\cdot\sqrt{1+h^2+[J+\beta\cdot u\cdot(\tau-\Psi(\tau))]^2}}\cdot\frac{\sigma\cdot\cos(\Psi(\tau))}{1+\left(\frac{\tau-\Psi(\tau)}{\rho}\right)^2} - \frac{u\cdot[J+\beta\cdot u\cdot(\tau-\Psi(\tau))]}{\beta\cdot\left[1+h^2+[J+\beta\cdot u\cdot(\tau-\Psi(\tau))]^2\right]}\cdot\left[1-\beta^2\cdot\left(1-\frac{d}{d\tau}\Psi(\tau)\right)^2\right] = 0 \qquad (1)$$

Can be received graphs for dynamical parameters of the accelerated particle by wave packet in space plasma:

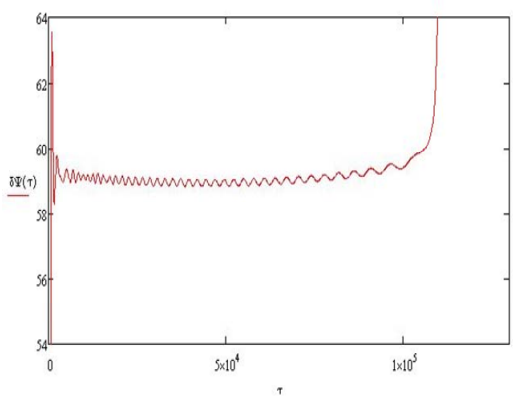

Fig.1. Phase temporal dynamics δΨ(τ).

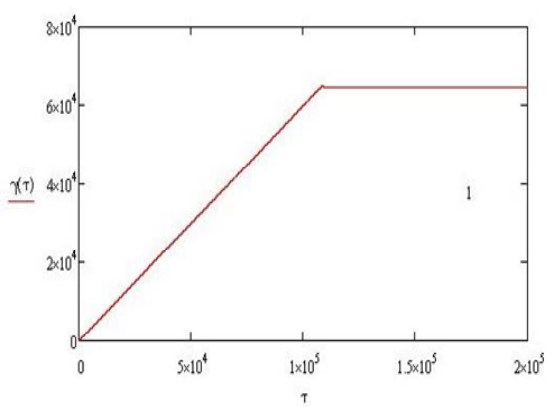

Fig.2. Particle relativistic factor γ(τ).

References

[1] Katsouleas N., J.Dawson. Physical Review Letters, v.**51**, № 5, 392. (1983)

[2] Erokhin N.S., Moiseev S.S., Sagdeev R.Z. Astronomical Journal Letters, **15**, No. **1**, 3. (1989)

[3] Kichigin G.N. JETP, **119**, No. **6**, 1038. (2001)

[4] N. Erokhin, N. Zolnikova, R. Shkevov, L.A. Mikhailovskaya, P. Trenchev. Proceedings of the Bulgarian Academy of Sciences (Comptes rendus) - Tome **60**, No.**9**, p.967. (2007)

[5] Erokhin N.S., N.N. Zolnikova, P.P. Grinevich, L.A. Mikhailovskaya. Problems of Atomic Science and Technology, series "Plasma electronics", No. **5**, p.152. (2006)

[6] Ptuskin V.S. UFN, т.**177**, № **5**, 558. (2007)

[7] Loznikov V.M., Erokhin N.S., Problems of Atomic Science and Technology, series "Plasma electronics", № **4 (68)**, 121. (2010)

Solar Activity and Tropical Cyclogenesis Correlations Variability

N. S. Erokhin[1], L.A. Mikhailovskaya[1], N. N. Zolnikova[1], R. Shkevov[2]

[1] *Space Research Institute - Russian Academy of Sciences, 117997, 84/32 Profsoyuznaya Str, Moscow, Russia, nerokhin@mx.iki.rssi.ru*

[2] *Space and Solar-Terrestrial Research Institute - Bulgarian Academy of Sciences, 6 Moskovska Str., Sofia 1000, Bulgaria, shkevov@space.bas.bg – corresponding autor*

The possible correlations between intensity of the solar activity with the large-scale vortical perturbations like typhoons in tropical cyclogenesis regions are considered. The variability of the correlation functions of solar activity and tropical cyclogenesis are analyzed and their spectra are compared. A mathematical oscillator model under influence of external force applied to tropical cyclogenesis intensity based on differentiable functions is proposed. Model allows to describe the tropical cyclogenesis intensity phase space and to improve our understanding of possible correlation relationships between large-scale vortical processes in the Earth atmosphere and solar activity variations. The possible areas of these results applications are the seasonal behavior of regional tropical cyclogenesis and the analysis of solar-terrestrial interactions influence on dynamics of large-scale atmospheric processes.

Some results from the paper:

The mutual correlation function Crf(n) of W (Wolf's number) and T (Tropical disturbances number) fluctuations near these trends $\delta V_j = V_j - X_j$, $\delta T_j = T_j - Y_j$ is presented in **Fig.2b**. It is clear that relationship of LVP (Large Vortical Processes) with SA (Solar Activities) has a complicated nature. So the consecutive mathematical model of relationship between the solar activity and large-scale vortical processes in the Earth atmosphere must take into account a number factors of principle like large-scale instability triggering, the large vortices generation, nonlinear stabilization of instabilities, perturbations dissipative decay, the ration between typical periods of subsystems variability (SA and LVP). According to this we develop the oscillator x(t) model allowing to explain the observable features of T(t)-W(t) correlations.

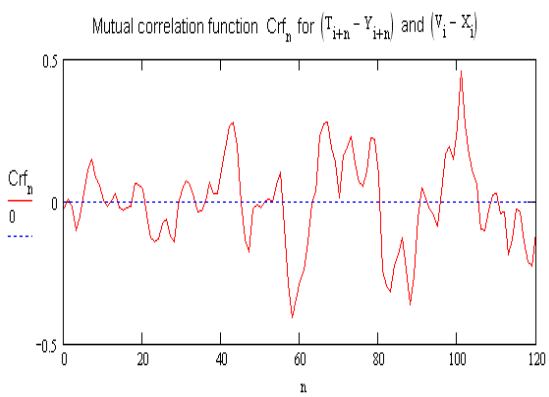

Fig.2b.

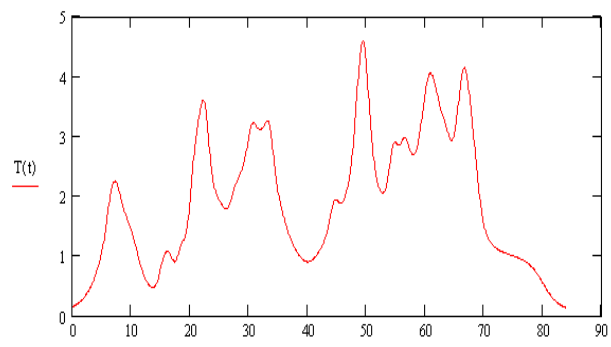

Fig.5b.

Therefore, the life cycle of single LVP with number k is described by the function $f_k(t) = p_k(t) \cdot q_k(t)$, shown in Fig.5a. Now the cyclogenesis intensity may be determined like this $T(t) = \sum_k f_k(t)$, where $1 \le k \le 53$. The plot of intensity T(t) for the chosen season is given in Fig.5b. It is important that we have the analytical formula for LVP-intensity in the form of differentiable functions. This allows us to study the phase plane (T, Q), where $Q(t) = dT / dt$ or in the discrete form we obtain now $Q_j = (T_{j+1} - T_j) / \Delta t$, where Δt - is the temporal step so $t_{j+1} = t_j + \Delta t$. The phase plane (T_j , Q_j) of the system considered is shown in the Fig.6 for the entire season considered and in some time intervals. These figures indicate the complicated structure of phase plane studied.

References

[1] Yaroshevich M.I. and Ingel L.Kh. Academy of Sciences Reports,v.**399**, № **3**, p.397, (2004).

[2] Erokhin N.S., Mikhailovskaya L.A. and Erokhin N.N. Scientific Session MEPHI-2007, Proceedings, MEPHI, Moscow, v.**5**, p.72. (2007).

[3] Yaroshevich M.I. and Ingel L.Kh. Physics of Atmosphere and Ocean, v.**42**, № 6, p.1. (2006).

[4] Pankov V., Gusev A., Pugacheva G., Voitskovsky M., Prokhin V., Martin I. COSPAR-2006-A-01016, Session C2.1-0049-06. (2006).

[5] Tinsley B.A. Space Science Reviews, v.**94**, p.231. (2000).

[6] Tsiropoul S. Journal of Atmospheric and Solar-Terrestrial Physics, v.**65**, p.469. (2003).

[7] Astafieva N.M., Raev M.D. Modern problems of the Earth remote sensing from space. v.**7**, No 1, p.61. (2010).

[8] N.S. Erokhin, N.N. Zolnikova, L.A. Mikhailovskaya, R. Shkevov, Sun and Geosphere **4(1)**, p.13. (2009).

Aspects of the Interaction of Magnetic Clouds / Interplanetary Coronal Mass Ejections with the Earth's Magnetosphere

C. J. Farrugia[1], M. P. Freeman[2], P. E. Sandholt[3], V. K. Jordanova[4], S. Muehlbachler[5], R. B. Torbert[1]

[1] *Space Science Center, University of New Hampshire, Durham, NH 03824, USA, charlie.farrugia@unh.edu*
[2] *British Antarctic Survey, Cambridge, UK*
[3] *Department of Physics, University of Oslo, Oslo, Norway*
[4] *Los Alamos National Laboratory, Los Alamos, NM*
[5] *Austrian Academy of Sciences, Vienna, Austria*

The interaction of magnetic clouds with the magnetosphere exhibits various interesting features due principally to interplanetary parameters which change slowly and go to extreme values of long duration. These, in turn, allow us to explore aspects of geomagnetic response to continued and extreme forcing of the magnetosphere. In this presentation we shall attempt to discuss elements of the following: (i) recurrent substorm activity; (ii) ionospheric convection; (iii) temporal-spatial structure of polar cap convection in relation to magnetopause reconnection and magnetospheric substorms; (v) changes in geoeffectiveness brought about by the coalescence of ICMEs on their way to Earth; and (vi) cross-polar cap saturation phenomena.

Recent Developments on the LANL DREAM project

R.H.W Friedel[1], G. D. Reeves[2] , C. A. Jefferey[3]

[1] *Los Alamos National Laboratory, MS D466, Los Alamos, NM 87545, United States, friedel@lanl.gov*
[2] *Los Alamos National Laboratory, MS D466, Los Alamos, NM 87545, United States, reeves@lanl.gov*
[3] *Los Alamos National Laboratory, MS D466, Los Alamos, NM 87545, United States, reeves@lanl.gov*

The Los Alamos DREAM project (Dynamic Radiation Environment Assimilative Model) project is now in its 4th year and has lead to a number of developments in Radiation Belt modeling work. We will report here on the current state of this modeling effort, covering several variants of the DREAM model – the data assimilative version (both real-time and historical), and the physics-based end to end version with some of its application to HANE (High Altitude Nuclear Explosions) belt modeling.

Here we will also present the first results from recent parameterizations of the Summers et al., 2005 [1] pitch angle diffusion coefficients formulation. One of the obstacles in running realistic real-time radiation belt models is the ability to quickly and continuously calculate realistic pitch angle diffusion coefficients as conditions change. We show here how in the case of plasmaspheric hiss a simple parameterization of pitch angle diffusion as a function of center hiss frequency, hiss wave magnitude, energy, L and a plasmaspheric background density profile parameter can be found.

References

[1] Summers, D, Quasi-linear diffusion coefficients for field-aligned electromagnetic waves with applications to the magnetosphere, *J. Geophys. Res. (Aug 27 2005) Vol.110*, iss.A8 A08213

Magnetic Reconnection at the Dayside Magnetopause

S. A. Fuselier[1], K. J. Trattner[1], S. M. Petrinec[1]

[1] *Lockheed Martin Advanced Technology Center, Dept A022S, Bldg 255, 3251 Hanover St, Palo Alto, CA, 94304, USA, stephen.a.fuselier@lmco.com*

The understanding of reconnection at the magnetopause has grown significantly since the launches of Cluster, Double-Star, and THEMIS. On the macro-scale, an empirical model for the location and type of reconnection that has been tested successfully using independent observations at the magnetopause. On the micro-scale, single and multi-spacecraft have explored the ion diffusion region and confirmed theoretical predictions of many of its properties. While these spacecraft have not had sufficient time resolution to investigate the electron diffusion region, several electron-scale features of the electron and ion diffusion regions have been identified. Finally, basic properties such as the reconnection rate have been measured for a reasonable number of events and, in general, they agree with theory.

Fundamental questions about reconnection remain and, at the same time, significant progress from the observational side has generated many new questions. Many of these fundamental questions require plasma and field observations in the electron diffusion region with sufficient time resolution. However, using existing and new data in statistical and individual case studies, many of the new questions about the process may be answered. In particular, in the near future, it may be possible to determine the prevalence of magnetic islands in magnetopause reconnection, both on a macro- and a micro-scale. Reconnection variability may be better understood both on a short and a long time-scale. Finally, it may be possible to determine if boundary conditions at the magnetopause current layer are adjusted by the solar wind-magnetosphere interaction so that reconnection always occurs somewhere on the magnetopause.

Storm-Time Ring Current: Model-Dependent Results

N. Yu. Ganushkina[1,2], M. W. Liemohn[1]

[1] *University of Michigan, Ann Arbor, USA, ganuna@umich.edu*

[2] *Finnish Meteorological Institute, Helsinki, Finland*

The main point of this study is to investigate how much the modeled ring current depends on the models used in simulations. Two storm events, one moderate (Dst minimum of -120 nT) on November 6-7, 1997 and one intense (Dst minimum of -230 nT) on October 21-22, 1999, are modeled. A rather simple ring current model is employed, namely, the Inner Magnetosphere Particle Transport and Acceleration model (IMPTAM), in order to make the model-dependency of the results most evident. Four different magnetic field models, two electric field models and four boundary conditions are used. We find that different combinations of the magnetic and electric field models and boundary conditions result in very different modeled ring current, and, therefore, the physical conclusions based on simulation results can differ significantly. A time-dependent model boundary outside of 6.6 RE gives a possibility to take into account the particles in the transition region (between dipole and stretched field lines) forming partial ring current and near-Earth tail current in that region. Calculating the model Dst* by Biot-Savart's law instead of the widely used Dessler-Parker-Sckopke (DPS) relation gives larger and more realistic values, since the currents are larger due to the smaller magnetic field. Therefore, the model boundary location and the method of Dst* calculation are of key importance for ring current data-model comparisons to be correctly interpreted.

Ultra Violet C Radiation on the Earth Surface and Wildfires Early Detection

G. S. Georgiev, R. H. Kancheva

Space and Solar-Terrestrial Research Institute, Bulgarian Academy of Sciences, Acad. G.Bonchev st., bl.3, 1113 Sofia, Bulgaria, rumik@abv.bg

Forests fires which are especially severe and wide-spread during the last years are not only dangerous for human life, property and industrial infrastructure, but also may strongly damage our environment. Indeed, forests are the most important air cleaning factory: they act as carbon sinks and as physical air filter. The analysis of the preconditions, reasons and factors leads to the conclusion that Bulgaria is joining the Mediterranean region with traditionally high risk of forest fires according to the parameters of the risk of fires on its territory. The consequences of the fires in the Sakar Mountain, for instance, had the dimensions of a local ecological catastrophe, but the ones that followed during the next years led those to the scale of a national natural disaster. The damages were not only economical ones but on a much bigger scale – inestimable damage on the conditions for the plants, led to erosion and destruction of the soils, to disturbing of the warmth and moisture balance of the ecosystems, to changes of the basic tree species, to the flora composition and the phytocenological structure, to change on the water flow character, to worsening of the sanitary condition of the neighboring unburnt stands, to sudden decrease of the CO2 absorbing capacity of nature – all in all to total or partial destruction of the existing biogenocenosis.

Recently the UV-C spectral band begins to find a wide application in various scientific and technology fields. This interest is justified by the relatively low level of background noise in this spectral band and the new possibilities that it provides. In this paper the characteristics of different types of fire detectors working in the Ultra Violet C spectral range are discussed, namely: spectral response, sensitivity, power consumption, easy to driven, etc. Early forest fires detection is neeed because of the fact that a wildfire doubles its area every few minutes. In this context the main idea of the paper is the development of fire warning network which will cover a large forest area and will be no man working during a few years. Each node of the network will work over an area of one square kilometer and will detect the fire by an optical method just when the fire flames. The spectral (wavelength selective) attenuation by the atmosphere of the coming from the sun and from forest fires UV-C radiation is also discussed in terms of maximum area to be covered by one node of the fire warning network.

Latitudinal Anisotropy in Ring Current Energetic Neutral Atoms

J. Goldstein[1,2], P. Valek[1,2], D. J. McComas[1,2], J. Redfern[1]

[1] *Southwest Research Institute (SwRI), San Antonio, Texas, United States, JGoldstein@SwRI.edu*

[2] *University of Texas San Antonio (UTSA), San Antonio, Texas, United States*

Stereo energetic neutral atom (ENA) images obtained by Two Wide-angle Imaging Neutral-atom Spectrometers (TWINS) are analyzed to quantify the latitudinal anisotropy of ring current ENAs, and by implication, the system-level pitch-angle response during a moderate geomagnetic storm on 6 April 2010. During a 15-min interval just after midday, TWINS 1 and 2 were at similar local times but different latitudes, and thus were able to simultaneously sample two different pitch angles from selected locations. The observations show a global dawn-dusk asymmetry in the ring current ENA latitudinal anisotropy, the dusk side being one to three orders of magnitude more anisotropic than the dawn side. The latitudinal dependence of the ENAs implies a duskside ion distribution that is more equatorial than isotropic; this anisotropy becomes less pronounced with increasing energy. The observed duskside ENA distribution is consistent with a source proton population that has experienced strong scattering by electromagnetic ion cyclotron waves.

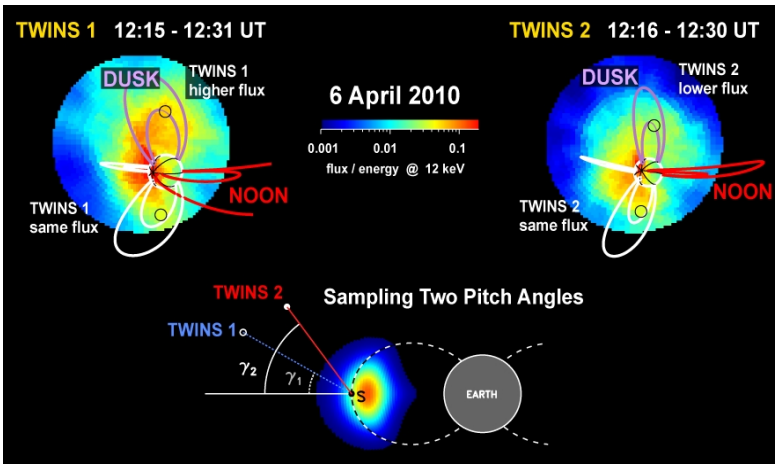

Figure 1. TWINS 1 and 2 images from just after midday on 6 April 2010 (Top), showing stereo ENA flux maps taken from similar local times but different latitudes. This viewing geometry provides samples of two different pitch angles, simultaneously (Bottom). A dawn-dusk asymmetry in pitch angle anisotropy is evident in the TWINS images. Whereas at dawn, both TWINS 1 and 2 see the same flux, on the duskside TWINS 2 (viewing from higher pitch angle) sees less than half the flux measured by TWINS 1 (viewing from lower pitch angle).

Superposed Epoch Analysis of Plasmaspheric Electron Density

J. Goldstein[1,2], C. R. Chappell[3], R. E. Denton[4], R. R. Anderson[5]

[1] *Southwest Research Institute (SwRI), San Antonio, Texas, United States, JGoldstein@SwRI.edu*
[2] *University of Texas San Antonio (UTSA), San Antonio, Texas, United States*
[3] *Vanderbilt University, Nashville, Tennessee, United States*
[4] *Dartmouth College, Hanover, New Hampshire, United States*
[5] *University of Iowa, Iowa City, Iowa, United States*

We perform statistical superposed epoch analysis of multiple years of electron density data and obtain the first global empirical characterization of plasmaspheric density that explicitly includes plumes produced during stormtime erosion. It is well established that the plasmaspheric density distribution evolves in phases (analogous to storm phases), in which the formation and subsequent development of plumes follow epochs divided by changes in the relative strength of convection. Plasmaspheric (plume) phases are an obvious and consistent feature in single-event case studies. Statistical analysis requires a superposed epoch analysis to reveal phases, but this approach requires a very large amount of data to provide anything but a very crude empirical characterization of global density structure versus epoch and geomagnetic activity. Density data are derived from plasma wave measurements from four missions: (1) Imager for Magnetopause-to-Aurora Global Exploration (IMAGE), years 2001 through 2005; (2) Polar, years 1996 and 1997; (3) International Sun-Earth Explorer 1 (ISEE-1), years 1977 through 1987; and (4) Combined Release and Radiation Effects Satellite (CRRES), years 1990 and 1991. Superposed epoch analysis reveals clear evidence of plume phases, and yields a global model for plume density versus epoch time, something not achieved by previous empirical global density (and plasmapause location) models that have employed ranges of values of geomagnetic indices (Kp, Dst, and AE) to organize plasmaspheric data. Quantitative analysis of sub-global density structure will also be presented, showing the evolution versus epoch of density structure at various sub-global spatial scales, and its empirical (epoch-based) characterization.

The Effect of Ionospheric Conductivity in the Electric Fields at Intermediate and Small Scales Observed by the FAST Satellite

I.V. Golovchanskaya [1], B.V. Kozelov[1], I.V. Despirak[1]

[1] *Polar Geophysical Institute, Akademgorodok 26a, Apatity, 184209, Russia, despirak@gmail.com*

Physical mechanisms of magnetosphere-ionosphere coupling at intermediate (1-100 km) and small (< 1 km) scales are not fully understood as yet. The prevailing viewpoint is that this coupling is implemented by dispersive Alfvén waves which include the non-uniformity of perturbations in the transverse to the background magnetic field plane on scales the order of the electron inertia length (or ion gyroradius). Such interpretation in terms of waves (either freely propagating or standing) seems to be inconsistent with the seasonal variation in the small-scale electric fields observed in the topside ionosphere, which, on the contrary, can be readily explained in the model of static current circuits. Previously, this effect was addressed in a detailed study by *Heppner et al.*, [1993], where low-resolution data of the *Dynamics Explorer 2* satellite (altitudes from 300 km to 900 km) were employed. In the present study we investigate this effect by highly resolved FAST observations of the electric fields at altitudes near FAST apogee (h = 4000 km) and clarify if it can be reasonably understood within the frameworks earlier proposed by *Lysak* [1998] and *Golovchanskaya* [2007].

Contribution of Magnetotail Reconnection to the Cross-Polar Cap Potential Drop

E. Gordeev[1], V. A. Sergeev[2], T. I. Pulkkinen[3], M. Palmroth[4]

[1] *Saint-Petersburg State University, 1 Ulyanovskaya st., St. Petersburg, 198504, Russia, evgeniy_gordeev@yahoo.com*
[2] *Saint-Petersburg State University, Russia*
[3] *School of Electrical Engineering, Aalto University, Espoo, Finland*
[4] *Finnish Meteorological Institute, Helsinki, Finland*

Since the work of Dungey [1961], the global circulation pattern with two (dayside and nightside) reconnection regions has become a classic concept. However, the contributions of dayside and nightside sources to the cross-polar cap potential (PCP) are not fully understood, particularly, the relative role and specifics of the nightside source are poorly investigated both in quantitative and qualitative terms. To fill this gap, we address the contributions of dayside and nightside sources to the PCP by conducting global MHD simulations with both idealized solar wind input and an observed event input. The dayside source was parameterized by solar wind-based 'dayside merging potential' (Φ_d or DPD) $\Phi_d = L_{eff}VB_t \sin^4(\theta/2)$, whereas to characterize the nightside source we integrated across the tail the dawn-dusk electric field in the plasma sheet to obtain the 'cross-tail potential' (Φ_n or NPD). For the idealized run we performed simulations using four MHD codes available at Community Coordinated Modelling Center (CCMC) to show that contribution of the nightside source is a code-independent feature (although there are many differences in the outputs provided by different codes). Particularly, we show that adding a nightside source to the linear fit function for the ionospheric potential (i.e., using the fit function $\Phi_{fit} = K_d\Phi_d + K_n\Phi_n + \Phi_0$) considerably improves the fitting results both in the idealized events as well as in the simulation of an observed event. According to these simulations the nightside source contribution to the PCP has a fast response time (< 5min) and a modest efficiency (potential transmission factor from tail to the ionosphere is small, K_n<0.2), which is closely linked to the primarily inductive character of strong electric field generated in the plasma sheet. The latter time intervals are marked by strongly enhanced nightside (lobe) reconnection and can be associated with substorm expansion phases. This association is further strengthened by the simulated patterns of precipitation, the R1-type field-aligned substorm current wedge currents and Hall electrojet currents, which are consistent with the known substorm signatures.

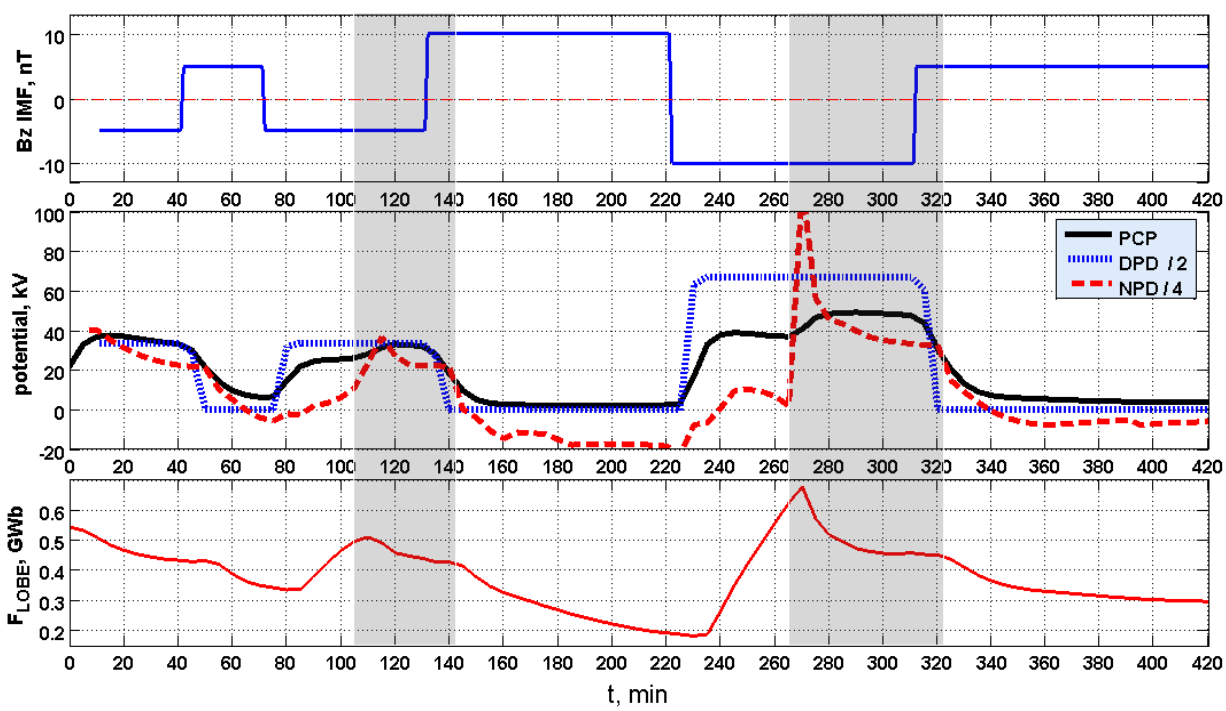

Figure 1. In the top panel: interplanetary magnetic field Bz–component time-shifted to the X_{GSM} = 10 Re. Middle panel qualitatively demonstrates the strong link of ionospheric electric potential drop (PCP, solid line) to 'solar wind potential' (DPD, dotted line) and 'cross-tail potential' (NPD, dashed line). The rapid enhancement of PCP simultaneously with DPD (at t = 75 and 225 min) demonstrates the strong solar wind control of ionospheric potential. However, the additional PCP increase (at t = 105 and 265 min) is observed during the tail magnetic flux unloading periods (see bottom panel), that corresponds to the substorm expansion phases (shaded areas). Such periods are associated with primarily inductive strong electric fields in the tail plasma sheet which are not directly mapped to ionosphere.

Ground-Based Observations of the Auroral Emissions during Substorms

V. H. Guineva[1], I. V. Despirak[2], R. H. Werner[1], E. Trøndsen[3]

[1] *Space and Solar-Terrestrial Research Institute (SSTRI), BAS, Stara Zagora Department, P.O.Box 73, 6000 Stara Zagora, Bulgaria, v_guineva@yahoo.com*

[2] *Polar Geophysical Institute (PGI), RAS, 14 Fersman str., Apatity 184200, Russia*

[3] *University of Oslo (UiO), Department of Physics, Boks 1072 Blindern NO-0316 Oslo, Norway*

Aurora is closely connected with the solar wind-magnetosphere-ionosphere interaction. The magnetic substorms are clearly expressed in auroral displays. Therefore auroral observations are important for the understanding of these phenomena. We present some results of auroral emissions behaviour during substorms. The 5577 Å and 6300 Å intensities have been studied. The I_{6300}/I_{5577} ratio that is widely used as a characteristic of the precipitating electrons energy distribution has been examined. The emissions intensities in front of the polar edge of the auroral bulge, in the polar edge and inside it have been compared and estimations about the nature of the particle precipitation spectra in these regions have been made.

Data from two All-Sky Imagers: at Andenes, Norway (69.3°N, 16.03°E) and at Longyearbyen, Svalbard (78.20°N, 15.83°E) from 2005-2006 observations have been used. The interplanetary conditions have been determined by WIND satellite data. The substorm development has been followed up by the magnetic field components data from the IMAGE magnetometer network.

It is found out that the intensity emissions ratio is lower at the polar edge of the auroral bulge than inside it, which bespeaks the most energetic particles precipitation at the polar edge of the substorm bulge. The I_{6300}/I_{5577} ratio in the arcs inside the auroral bulge is about 1.25 times higher than the one at its polar edge. In some cases, in front of the polar edge of the auroral bulge a region of enhanced red emission is observed, which may result from a downward current in these regions (proton precipitation) or to an upward field-aligned current (softer electron precipitation – a pulse of increased electron number flux of average energy < 100eV) depending on the MLT zone.

High Resolution Measurements and Modeling of (0,0) and (1,0) Bands of the O_2 Atmospheric System

V. H. Guineva[1], R. H. Werner[1], I. Vince[2], A. Kirilov[3]

[1] *Space and Solar-Terrestrial Research Institute (SSTRI), BAS, Stara Zagora Department, P.O.Box 73, 6000 Stara Zagora, Bulgaria, v_guineva@yahoo.com*

[2] *Astronomical Observatory Belgrade (AOB),7 Volgina str., Belgrade 11060, Serbia*

[3] *Polar Geophysical Institute (PGI), RAS, 14 Fersman str., Apatity 184200, Russia*

Ground based spectroscopic observations have been used for the effective temperature evaluation. High resolution measurements of rotational absorption lines from the P branches of the (0,0) and (1,0) bands of the molecular oxygen atmospheric system have been performed by the solar telescope of Belgrade Astronomical Observatory and by the spectroscopic system in Stara Zagora. Synthetic spectra of the above bands have been created based on line-by-line calculations, in the case of direct measurements and indirect measurements, single scattering assumed. The theoretical equivalent widths have been computed. The theoretical and measured line profiles and their equivalent widths have been compared. The dependence of the equivalent widths on the rotational quantum number has been worked out assuming strong absorption. It allows the evaluation of the effective atmosphere temperature. The possible contaminations as water vapour lines in some cases are discussed. The theoretical estimates and the measurement results have been examined. The possibility to use high resolution measurements and theoretical estimation to evaluate the low troposphere temperature profile is considered.

Ionospheric Response to Changes in the Solar Wind at Solar Minimum and Solar Maximum

R.A. Heelis[1]

[1] *University of Texas at Dallas, Hanson Center for Space Sciences, PO Box 830688, Richardson, TX 75083, heelis@utdallas.edu*

During solar minimum the influences of drivers originating in the solar wind on the ionosphere appear as recurrent inputs that are easy to identify due to the absence of the larger, but more sporadic inputs that prevail at solar maximum. While the solar wind drivers are much weaker than those typically seen in at solar maximum they result in frictional heating in the polar cap ionosphere and a global elevation of the neutral temperature. The high latitude electric fields, while smaller than those seen at solar maximum, penetrate to low and middle latitudes with equal, or perhaps greater efficiency at solar minimum.

Observations from the DMSP satellite at a fixed local time are used to investigate the response of the topside ionosphere to recurrent high-speed streams at solar minimum and to the passage of CME's at solar maximum. The similarities and differences in the ionospheric response will be discussed in terms of changes in the ionospheric temperature and composition and in terms of magnetosphere-ionosphere interactions that determine the extent to which the dynamics of the plasmasphere is influenced by external drivers in the solar wind.

Towards a Global Hybrid Vlasov Magnetospheric Model: A Test Particle Simulation

I. Honkonen[1,2], A. Sandroos[1], M. Palmroth[1]

[1] *Finnish Meteorological Institute, P.O. BOX 503, Helsinki, FI-00101, Finland, ilja.honkonen@fmi.fi*

[2] *University of Helsinki, Department of Physics, Helsinki, Finland*

We are developing a global hybrid Vlasov model and as a first step towards that goal we use our parallel six-dimensional Vlasov solver to drive a global test particle simulation using the electric and magnetic fields from the state-of-the-art three-dimensional global MHD simulation GUMICS-4. In this test a Maxwellian distribution of protons with the average properties of the measured solar wind is constantly inserted into the sunward edge of the test particle simulation located at 16 Re upstream from the Earth. The protons are propagated by a six-dimensional (three space + three velocity dimensions) Vlasov solver using the method of Kurganov and Tadmor (2000) for solving advection equations. We present our approach to developing a new massively parallel hybrid Vlasov simulation, including a scalable and easy-to-use C++ finite volume grid library. We compare the results from the global test particle simulation to the results from the global MHD simulation and discuss the capabilities of the final fully coupled model.

The project has received funding from the European Research Council under the European Community's Seventh Framework Programme (FP7/2007-2013) / ERC Starting Grant agreement number 200141-QuESpace. The work of IH and MP is supported by the Academy of Finland.

Parallel GUMICS

I. Honkonen[1,2], P. Janhunen[1], M. Palmroth[1]

[1] *Finnish Meteorological Institute, P.O. BOX 503, Helsinki, FI-00101, Finland, ilja.honkonen@fmi.fi*

[2] *University of Helsinki, Department of Physics, Helsinki, Finland*

GUMICS-4 is a state-of-the-art global three-dimensional magnetohydrodynamic model that has been tested extensively against observations. In order to use GUMICS for real-time simulations (e.g. space weather prediction) or simulations with cell sizes below 1/4 Earth radii it must be paralellized. We will present the challenges involved in paralellizing a global MHD code that uses a cell-by-cell refined grid and temporal subcycling. In order to make the parallel code modular (and hence easier to develop and debug) a separate finite volume grid library was written in C++. The library supports using any C++ class or structure as cell data and automatically handles the MPI communication required for updating cell data between processes during time-stepping. We will describe the programming techniques used in the grid library and its features. We will also show the results of weak and strong scaling tests of the parallel version of GUMICS and how the physical results compare to those of GUMICS-4. In a weak scaling test the computational size of the problem is increased with the number of processors used, while in a strong scaling test the problem size remains constant. GUMICS uses modern C++ programming techniques such as a modular object-oriented design for program readability, ease of development and debugging and template programming for performance. These will also be discussed.

The project has received funding from the European Research Council under the European Community's Seventh Framework Programme (FP7/2007-2013) / ERC Starting Grant agreement number 200141-QuESpace. The work of IH and MP is supported by the Academy of Finland.

A Radiation Belt Electron Response to CME- and CIR-Driven Geomagnetic Storms

M. Hudson[1], T. Brito[1], S. Elkington[2], B. Kress[1], Z. Li[1], M. Wiltberger[3]

[1]*Physics and Astronomy Department, Dartmouth College, Hanover, NH 03755, USA, mary.hudson@dartmouth.edu*
[2]*LASP, University of Colorado, Boulder, CO 80303*
[3]*NCAR HAO, Boulder CO 80307*

CME-shock driven geomagnetic storms are characterized by prompt change in outer zone electron fluxes including radial loss as well as loss to the atmosphere, at times faster than convective buildup of the ring current, which produces radial losses when combined with inward motion of the magnetopause[1]. Particularly strong CME shocks also produce radial transport of multi-MeV electrons on a drift time scale which can produce a 'new belt', less common than drift time scale loss. Two CME-shock driven storms during 2004-2005 have been examined using the LFM-MHD code to compute internal magnetospheric E and B fields from upstream solar wind parameters, combined with 2D and 3D guiding center test particle codes to examine: 1) radial transport and 2) enhanced precipitation loss to the atmosphere. Inward radial transport increases flux at a given energy and L value, while outward radial transport to the inward moving magnetopause produces loss, along with enhanced loss to the atmosphere. On the longer time scale of a storm, including buildup of the ring current, additional radial loss results from fully adiabatic and diffusive transport. Enhanced ULF wave activity can produce both coherent and diffusive transport and energy exchange with electrons in drift resonance with azimuthally propagating ULF waves. Coherent interaction with ULF waves can occur at a rate which exceeds nominal radial diffusion estimates but is slower than prompt injection on a drift time scale. Precipitation losses for the January 21, 2005 storm occur on the time scale of magnetosonic impulse propagation through the magnetosphere, following arrival of a CME-shock, much faster than the time scale for build up of the ring current and enhanced EMIC wave precipitation losses. The balance between enhanced and decreased phase space density when losses are included will be examined, along with CIR-driven storm comparisons from the Whole Heliosphere Interval in 2008, during the declining phase of solar activity approaching the recent minimum. The latter can produce sustained electron flux increases exceeding those of CME-driven storms.

Reference:

Mary K. Hudson, Brian T. Kress, Hans-R. Mueller, Jordan A. Zastrow and J. Bernard Blake, Relationship of the Van Allen radiation belts to solar wind drivers, *J. Atmos. and Solar. Terr. Phys*., Vol 70/5 pp 708-729, 10.1016/j.jastp.2007.11.003, 2008.

The Influence of the Geocoronal Hydrogen Distribution on the Modeling of the Ring Current

R. Ilie[1], R. Skoug[1], H. Funsten[1], M. Liemohn[2], J. Bailey[3], M. Gruntman[3]

[1]*Los Alamos National Laboratory, MS D466, Los Alamos, NM, 87545, USA, rilie@lanl.gov*
[2] *University of Michigan, Ann Arbor, MI*
[3]*University of Southern California, Los Angeles, CA*

The ring current decay during the recovery phase of a magnetic storm leads to the restoration of the surface geomagnetic field and the return of the magnetosphere to a less disturbed state. The long-term ring current decay is mainly due to collisions of ring current particles with neutral atoms from the upper atmosphere. Since neutralized ring current particles are able to escape the inner magnetosphere-trapping region, charge exchange processes act as a major loss mechanism for the ring current. Therefore, knowing the density distribution of these cold and tenuous neutral hydrogen atoms will enable us to better understand the ring current formation and decay.

Several models of the neutral geocoronal density distribution have been developed. The *Rairden et al.* [1986] model is based on the spherically symmetric isothermal *Chamberlain* [1963] model of the exospheric hydrogen density where the density distribution was fitted to observations from the Dynamic Explorer 1. *Hodges* [1994] developed a mathematical model for the exospheric hydrogen density, which provides the means for a 3 dimensional hydrogen density distribution. Based on observations from the Imager for Magnetopause-to-Aurora Global Exploration (IMAGE) mission, *Ostgaard et al.* [2003] developed a model of the hydrogen distribution that has only radial dependence; however, the H-density also changes as a function of solar zenith angle. More recently, *Bailey et al.* [2010] modified the *Hodges* [1994] model and fit the expansion parameters to observations from the Two Wide-angle Imaging Neutral-atom Spectrometers (TWINS) mission. Their model reveals day/night asymmetries as well as the existence of a geotail-like H-density structure.

Since all geocoronal hydrogen density models predict different distributions for the exospheric hydrogen, we investigate the influence of these distributions when modeling the ring current. For this study, we employ the Hot Ion Drift Integrator (HEIDI) model (*Liemohn et al*. [2004]) to simulate several storm intervals that occurred during the TWINS era. All 4 models of H-density are implemented in the HEIDI model. Synthetic Energetic Neutral Atom (ENA) images are constructed from the modeled ion fluxes and compared to the observed TWINS images. It is noted that the ring current topology depends greatly on the hydrogen model used, therefore knowing the H-distribution is very important in understanding how the ring current recovers following a magnetic storm.

References

[1] Rairden, R. L., L. A. Frank, and J. D. Craven**,** *J. Geophys. Res.* **91**, (1986).
[2] Hodges, R. R., *J. Geophys. Res.* **99**, (1994).
[3] Ostgaard, N., Mende, S. B., Frey, H. U., Gladstone, G. R., Lauche, H., *J. Geophys. Res* **108**, (2003).
[4] Bailey, J. et al., *J. Geophys. Res.*, (2010), submitted
[5] Liemohn, M. W, Ridley, A. J., Gallagher, D. L., Ober, D. M., Kozyra, J. U., *J. Geophys. Res* **109**, (2004).

Using the AMDA Web-Based Tool for Solar Wind-Magnetosphere Interaction Studies: Magnetotail Dynamics

C. Jacquey[1], L. Palin[1], V. Génot[1], E. Budnik[2], R. Hitier[3], M. Bouchemit[1], M. Gangloff[1], A. Fedorov[1], B. Cecconi[4], N. André[1], B. Lavraud[1], F. Pitout[1], C. Briand[4], N. Dufourg[5], B. Besson[5], E. Pallier[1], and E. Penou[1]

[1] *CDPP/IRAP, CNRS/Université Paul Sabatier, 9, avenue du colonel Roche, 31028 Toulouse, France.*
[2] *NOVELTIS, 2, Avenue Europe, 31520 Ramonville Saint Agne, France*
[3] *Co-Libri, Cremefer 11290 Montréal, France*
[4] *LESIA, Observatoire de Paris-Meudon, 5, place Janssen, 92195 Meudon*
[5] *CNES, Centre spatial de Toulouse, 18 avenue E. Belin, 31401 Toulouse*

AMDA is a web-based facility for on line analysis of space physics data coming from either its local database or distant ones. This tool allows the user to perform on line classical manipulations such as data visualization, parameter computation or data extraction. AMDA also offers innovative functionalities such as event search on the content of the data in either visual or automated way. These functionalities extendable for automated recognition of specific signatures can be used for performing classification of events and for generating time-tables and catalogues. These time-tables/catalogues can be seen as a brick of up-coming virtual observatories in space physics. In this presentation, we will show examples of statistical studies using AMDA of the SW/magnetosphere interaction focusing on the magnetotail multi-scale dynamics.

Modeling Ring Current Electron and Ion Dynamics and Plasma Wave Excitation

V. K. Jordanova[1], J. M. Albert[2], Y. Chen[1], R. H. Friedel[1], R. B. Horne[3], N. Meredith[3], Y. Miyoshi[4]

[1] *Los Alamos National Laboratory, Los Alamos, NM 87545, USA, vania@lanl.gov*
[2] *Kirtland Air Force Base, Albuquerque, NM 87117, USA*
[3] *British Antarctic Survey, Cambridge, UK*
[4] *Solar-Terrestrial Environment Laboratory, Nagoya University, Japan*

Self-consistent simulations of plasma wave dynamics and their effects on energetic particles in near-Earth space is a long-standing challenge. We present global studies of the excitation of two dominant magnetospheric plasma waves, whistler mode chorus emissions and electromagnetic ion cyclotron (EMIC) waves during geomagnetic storms after the fresh injection of plasma sheet particles into the inner magnetosphere. We use our four-dimensional (4-D) ring current-atmosphere interactions model (RAM), which solves the kinetic equation for H^+, O^+, and He^+ ions and electrons and is coupled with a dynamic 2-D plasmasphere model. RAM includes time-dependent convective transport, radial diffusion, and all major loss processes; the model was recently updated to incorporate pitch angle scattering by plasmaspheric hiss and chorus waves. The boundary conditions are specified by a plasma sheet source population at geosynchronous orbit that varies both in space and time as the solar wind driving changes. We calculate the pitch angle anisotropy of ring current ions and electrons and identify equatorial regions for potential growth of EMIC and/or whistler mode chorus waves. We find that the linear growth rate of chorus waves maximizes outside the plasmasphere in the dawn local time sector, while EMIC waves are most intense within plasmaspheric drainage plumes in the afternoon sector. The modeling results are compared with plasma wave observations from CRRES satellite.

Vegetation Reflectance of Solar Radiation and Fluorescence Emittance as Spectral Indicators of Environmental Conditions

R. H. Kancheva, G. S. Georgiev

Space and Solar-Terrestrial Research Institute, Bulgarian Academy of Sciences, Acad. G.Bonchev st., bl.3, 1113 Sofia, Bulgaria, rumik@abv.bg

During the last years destructive processes caused by natural disasters or human activity are in the focus of the scientific research and occupy the concern of social communities and government authorities. A great variety of projects has been developed aimed at environmental monitoring and control. Recent developments in environmental studies are greatly connected with worldwide ecological problems related to anthropogenic impacts on the biosphere and first of all on vegetation. Advanced monitoring and alerting techniques, on-time information extraction, modeling and forecasting technologies are a preposition for successful data application and decision support in environmental studies. The interrelated nature of many environmental problems has imposed the need of multipurpose programs, data integration and information sharing between different databases. Remote sensing technologies are widely used for natural resources management, farmland and crop assessment, land covers change detection, ecosystems preservation and many other world significant problems.

Ecological problems relevant to natural and anthropogenic impacts on the environment are of global importance. They have drawn the multidisciplinary attention of various scientists imposing the development of efficient means for assessing the affects of different factors specifically on vegetation land covers. Soil, water and air pollution is one of the most severe problems concerning natural vegetation resources as well as agricultural crops. Among other methods used for plant phytodiagnostics, an increasing role becomes to play the analysis of land covers radiation behavior. Visible and near infrared remote sensing measurements have proved abilities in vegetation monitoring for the assessment of plant biophysical parameter. These parameters are associated with plant development and are closely related to vegetation physiological state. In this study multispectral reflectance and fluorescence data of various agricultiral species have been used to demonstrate the detection of plant physiological state as a function of the environmental conditions. The stress effects caused by the soil properties, nitrogen deficiency and heavy metal pollution are associated with plant growth variables and chlorophyll variations derived from reflectance and fluorescent data.

Solar Wind Interaction with Planetospheresand Cometary Exospheres

M. D. Kartalev

Geospace Modeling and Forecasting Center, Institute of Mechanics, Bulgarian Academy of Sciences; Acad. G. Bontchev Str., Block 4, 1113 Sofia, Bulgaria

Some advantages of the "modular" approach in modeling of the solar wind interaction with planetospheres (magnetospheres or ionospheres) and cometary exospheres are discussed. This method provides the possibility to describe, if necessary, different regions of the interaction in different model approaches.

In the presented example of the solar wind interaction with the Earth's magnetosphere, the magnetosheath is modeled in 3D gasdynamic approach, while a modification Tsyganenko model is utilized for the magnetosphere. The shock wave and magnetopause geometries are obtained self-consistently as a part of the solution. Many comparisons with CLUSTER and Interball measurements confirm the coincidence with predicted (under certain solar wind conditions) geometries of the magnetosheath boundaries even in such details as magnetopause cusp indentations. Besides the realistic 3D magnetosheath, the approach provides a modified Tsyganenko model with realistic magnetopause and numerically obtained shielding magnetic field.

The gasdynamic module of the models in the case of the SW interaction with nonmagnetic planets and comets, where the mass-loading process becomes very essential, requires inclusion the terms, describing source and sink photo-chemical processes in the equations. The contribution of these processes could be different in separated region of interaction. It is demonstrated on the example of the SW – Venus interaction that the creation of the planetosphere (ionosphere) ionized gas is only due to the ionization in the planetary neutral exosphere. A self-consistent numerical modeling of the planetosphere and planetosheath (ionosheath) with mass-loading process included in both regions provides the parameters' distribution (dynamics) there along with the self-consistent boundary (planetopause).

The utilized "grid –characteristic" explicit first – order non-conservative finite difference scheme ensures in the simulation of the SW – comet Halley interaction better than in other approaches coincidence with the Giotto measurements in the inner comet coma. A new interpretation of the so called diamagnetic cavity boundary is proposed, proving that this is rather the inner shock wave. The latter statement is based on the introduction (discovering) of a new kind of magnetic field diffusion caused by the specifics of the mass-loading process and directed against the neutral particles flow.

References

[1] M. Kartalev, P. Dobreva, E. Amata, M. Dryer, and S. Savin, J.Atmos. Solar-Terr. Phys**. 70,** 627–636 (2008)
[2] M. Kartalev, M. Dryer, K. Grigorov, and E. Stoimenova, J. Geophys. Res., **111**, doi: 10.1029/2006JA011760 (2006).
[3] P. Dobreva , M. Kartalev, N. Shevyrev, G. Zastenker.. Planet. Space Sci**, 53**, p. 117-125 (2005).
[4] V. Keremidarska, and M. Kartalev, J. Theor. Appl. Mech., XXIX, **No 1**,(1999)
[5] M. Kartalev, Geophys. Astrophys. Fluid Dynamics, **88**, 131-164, (1998)
[6] M. Kartalev, and V. I. Nikolova, Geophys. Astrophys. Fluid Dynamics, **89,** 145-168, (1998)
[7] M. Kartalev, V. Nikolova, V. Kamenetsky and I. Mastikov, Planet. Space Sci., **44**,, 1195-1208, (1996)
[8] M. Kartalev, M. Kaschiev, and D. Koitchev. J. Comput. Physics, **119,** 220-230, (1995)
.

What We Don't Know about the Solar Influence on Climate?

N.A. Kilifarska

National Institute of Geophysics, Geodesy and Geography, E-mai: nkilifarska@geophys.bas.bg

One of the main unresolved problems in Solar-Earth relations is a missing mechanism for the solar influence on Climate. The total solar irradiance directly influences the surface temperature, but its variability is very small to account for the observed amplitude of climate changes (current and historical). The amplitude of the spectral solar irradiance is higher, but it is absorbed in the upper stratosphere by the ozone and thus the short-wave solar signal do not reach the ground. Galactic cosmic rays (GCR) – the intensity of which is modulated by heliomagnetic field – looks more promising, because the most energetic of them penetrate to the Earth surface. So the hypothesis of Svensmark and Friis-Christensen [1] – relating the GCR with cloud cover and correspondingly the Earth radiation balance – is exciting the climate community for more than 10 years. However, recent studies based on satellite and ground-based measurements of microphysical parameters of clouds and aerosols [i.e. 2,3] do not support this hypothesis.

On the other hand, for more than 30 years modelers have noticed the strong climate sensitivity to variations in lower stratospheric ozone [4÷7]. Thus O_3 depletion in the lower stratosphere exerts a strong negative forcing, i.e. cooling of the surface temperature [4÷6]. At the same time the tropospheric ozone has increased (supposedly by increased emission of gases from NO_x family and other ozone pre-cursors), which have a positive impact on the Earth radiation budget [8-9]. These result have small effect on scientific community, because the radiative effect of stratospheric and tropospheric ozone treated separately eliminate each other in a great extent.

In this study we show that linear methods are absolutely non-applicable for estimation of climate response to different forcing - at time scales of climate change (i.e. more than 30 years). We have created a non-linear model of land air temperature, driven by multi-decadal and interannual variation of total ozone, which is able to describe ~ 75% of land air temperature variability (see Fig.1).

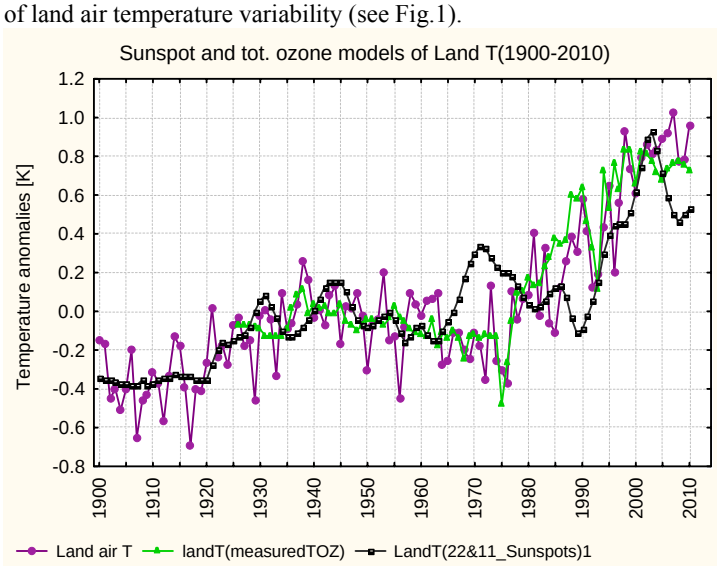

Figure 1. Comparison of measured land air temperature anomalies (filled dots curve) and modeled one by nonlinear models driven by measured Arosa total ozone – TOZ (filled triangles curve) and sunspot numbers (open squires curve).

Non-linear analysis of the longest in the world ozone time series, from Arosa, Switzerland, reveals that GCR are the most important driver of the lower stratospheric ozone variations during the last 85 years. This result indicates that *lower stratospheric ozone is the main mediator* of the solar influence on climate (through a modulation of GCR). However, for more than 30 years the ozone continuously has depleted, while the global surface temperature have increased with ~0.7K. Climate models estimate a negative forcing on climate by the reduced lower stratospheric ozone [4÷6].

We resolved this paradox taking into account that lower level O_3 depends on its optical depth aloft – an effect known as *ozone self-healing*. This means that reduction of stratospheric ozone leads to its enhancement at tropospheric levels. Analytical model of the ozone self-healing - we have created - shows that the effectiveness of the ozone creation in the lower atmosphere depends on the wavelength of solar UV and the altitude of its reduction aloft.

Finally, synthesizing the great amount of studies on solar-terrestrial relations, a quantitatively new arrangement of the solar - climate puzzle will be shown.

References

[1] H. Svensmark and E. Friis-Christensen, J. Amosph. Solar-Terr. Phys., **59**(11), 1225 (1997).
[2] M. Kulmala et al., Atmos. Chem. Phys., **10**, 1885 (2010)
[3] J. E. Kristj´ansson et al., Atmos. Chem. Phys., **8**, 7373 (2008)
[4] V. Ramanatan, L.B. Callis and R.E. Boucher, J. Atmos. Sci., **33**, 1092 (1976)
[5] W-Ch. Wang, J.P. Pinto and Y.L. Yunk, I. Atmos. Sci., **37**, 333 (1980)
[6] P.M. deF. Foster and K. Shine, J. Geophys. Res., **102** (D9), 10841 (1997)
[7] N. Stuber, R. Sausen, and M. Ponater, Theor. Appl. Climatol. **68**, 125 (2001)
[8] W-Ch. Wang, Y-Ch. Zhuang and R. Bojkov, Geophys. Res. Lett., **20**(15), 1567 (1993)
[9] M. Gauss et al., Atmos. Chem. Phys., **6**, 575 (2006)

Stormy (Space) Weather: The Radiation Belt Storm Probes Mission

C. A. Kletzing[1]

[1]*Department of Physics and Astronomy, The University of Iowa, Iowa City, IA, 52242, USA, e-mail: craig-kletzing@uiowa.edu*

The two-satellite NASA Radiation Belt Storm Probes (RBSP) mission will be launched in 2012 to investigate the dynamic environment of the Earth's radiation belt. The two satellite NASA mission will fly through the Van Allen belts more than 50 years after their discovery with the most comprehensive set of instruments ever deployed in this region of space. Thought for many years to be an essentially solved problem in space science, measurements and theory over the past 15 years have found that, quite to the contrary, the radiation belts are a highly variable part of space that still holds many questions for active research. In particular, a wide variety of physical processes including several wave-particle interactions drive radiation belt acceleration, transport, and loss. Among the wave types invoked for these processes are EMIC waves, whistler mode chorus, VLF hiss, and magnetosonic waves. The field and particle measurements to be made on RBSP are presented , some of the current theory on radiation belt processes are discussed, and the current status of the mission is given.

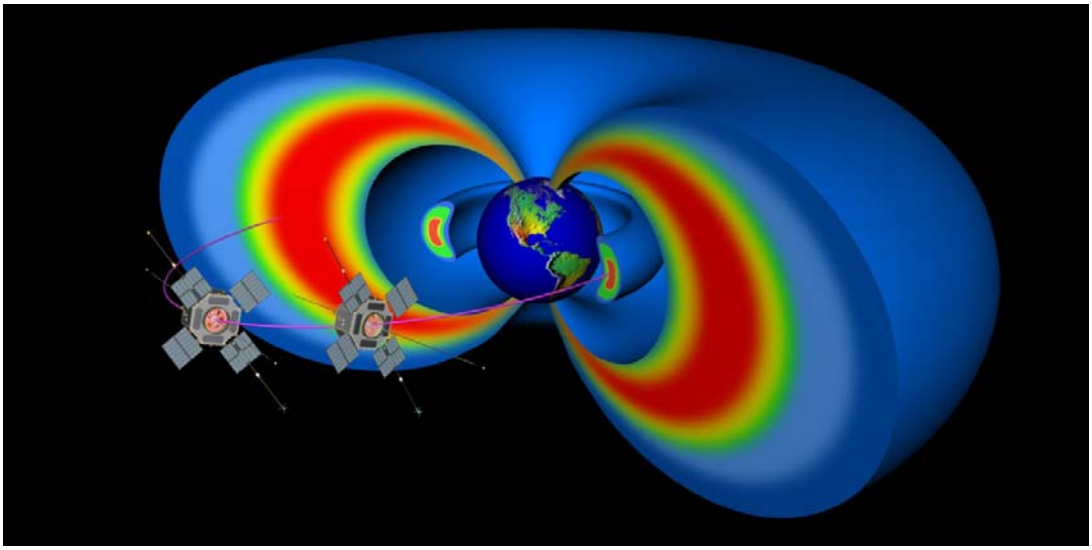

PSBL Plasma Structures during Different Periods of Geomagnetic Activity and Their Possible Ground Manifestations

R. Koleva[1], E. E. Grigorenko[2], L. M. Zelenyi[2], J.-A. Sauvaud[3]

[1] *Space and Solar-Terrestrial Research Institute of BAS, Sofia 1000, Bulgaria, rkoleva@stil.bas.bg*
[2] *Space Research Institute of RAS, elenagrigorenko2003@yahoo.com*
[3] *IRAP, University of Toulouse, CNRS*

Field-aligned high-velocity ion beams are frequently observed in the plasma sheet boundary layer (PSBL) and it is naturally to expect the associated field-aligned currents (FAC) streaming in the lobe-plasma sheet interface. Our analysis of 200 PSBL crossings by CLUSTER spacecraft revealed two different types of ion beams related with two different regimes of current sheet acceleration. 1) Energy collimated and spatially localized ion beams (beamlets) having a rather long duration (up to 20 min) and energies less than 20 keV, observed during quiet geomagnetic periods, together with isotropic electrons. These features indicate on ion acceleration in spatially localized resonant sources located in the distant current sheet in the region of closed magnetic field lines and rather far from the distant X-line [1]. No FACs or FACs of very small current density, carried mainly by beamlet ions, are registered in these cases. During such events CLUSTER trajectory is projected on POLAR UV images in the region of weak (diffuse) aurora light. Magnetograms of appropriate ground stations do not exhibit variations in the magnetic field. 2) In active periods, powerful (up to 140 keV) field-aligned ion beams with large parallel temperatures are observed along with anisotropic electron fluxes, formed out of an accelerated electron beam streaming from the acceleration source and of cold electrons moving towards the source. This feature implies that the acceleration of ion beam takes place near the X-line located in near CS regions ($X \geq -50$ R_E) [1]. Strong FACs with current densities ~ 10 nA/m^2 and more, carried by electrons, are registered. During such PSBL crossings a change of FACs' sign is always observed: near the lobeward edge of PSBL earthward FAC is observed while inside PSBL FAC is directed towards the acceleration source, i.e. tailward. The projection of the corresponding part of CLUSTER orbit on POLAR UV images is located just adjacent to the brightest auroral spot. For several events multipoint Cluster measurements allow to estimate spatial and temporal scales of the current structures. The spatial size of the earthward FAC is less than 2000 km, i.e. it is comparable with the ion inertial length. The spatial size of the tailward FAC is more difficult to estimate. The upper limit of this estimation is ~1 R_E. The observed durations of the current structures may reach several minutes but they are shorter than the durations of the corresponding accelerated ion beam. This may imply that the ion non-adiabatic acceleration in the magnetotail current sheet is more steady process than the process maintaining Hall current system.

References

[1] Grigorenko, E.E., Hoshino, M., Hirai, M., Mukai, T., and Zelenyi, L.M., J. Geophys. Res. 114, A03203 (2009).

Instrument ELMAVAN for the RESONANCE Mission

I. Kolmasova[1], O. Santolik[1,2], L. Uhlir[1], J. Chum[1], J. Base[1], F. Hruska[1]

[1] *Institute of Atmospheric Physics, Academy of Sciences of the Czech Republic, Bocni II/1401, 14131 Praha 4, Czech Republic, Phone: +420267103081, E-mail: iko@ufa.cas.cz*

[2] *Charles University, Faculty of Mathematics and Physics, V Holesovickach 2, 18000 Praha 8, Czech Republic*

The instrument ELMAVAN is being prepared at the Institute of Atmospheric Physics, Prague for the Russian RESONANCE project with international participation, currently scheduled to be launched in 2015. The aim of this four-spacecraft mission is to investigate wave-particle interactions and plasma dynamics in the inner magnetosphere of the Earth with the focus on phenomena occurring along the same field line and within the very same flux tube of the Earth's magnetic field.

The electromagnetic wave analyzer ELMAVAN will measure intensity, polarization, coherence, and propagation properties of waves in magnetospheric plasmas. 3 orthogonal magnetic search coil antennas and 4 electric monopoles will be used for the measurements. The instrument will measure 3D set of components of the electric and magnetic field fluctuations in the frequency range 10 Hz - 20 kHz. The scientific motivation is to investigate properties of whistler-mode chorus emissions, nonlinear wave-particle interactions, properties of equatorial emissions, and auroral hiss. These emissions attract increasing attention because of their potential influence on the dynamics of the Earth's radiation belts [1,2].

The instrument ELMAVAN will use the state of art electronics and mechanical design taking into account specific requirements for the orbit inside the radiation belts. From this point of view this instrument will also be important as a technological experiment.

The input signals of ELMAVAN will consist of

- 3 analog signals from orthogonal magnetic search coil antennas (sensitivity at f>1kHz: 10^{-5} nT /√Hz, max. amplitude 10 nT at f>100 Hz)
- 4 analog signals from electric monopoles (sensitivity 0.1 μV/m /√Hz, max. amplitude 300 mV/m at f>100 Hz)

Two types of output data will be generated:

- Burst mode data will use the telemetry volume of 280 kbit/s for a 5% coverage of digital 16-bit waveforms from 3 orthogonal magnetic search coil antennas and 4 electric monopoles, or a higher coverage rate for a limited number of components.
- Continuous survey mode data at a rate of 16 kbit/s will consist of averaged spectral matrices or propagation and polarization parameters. Onboard data processing will be implemented into an Actel FPGA and will include calculations of wave intensity, polarization, coherence and propagation properties as a function of frequency and time.
- Direct telemetry is under discussion

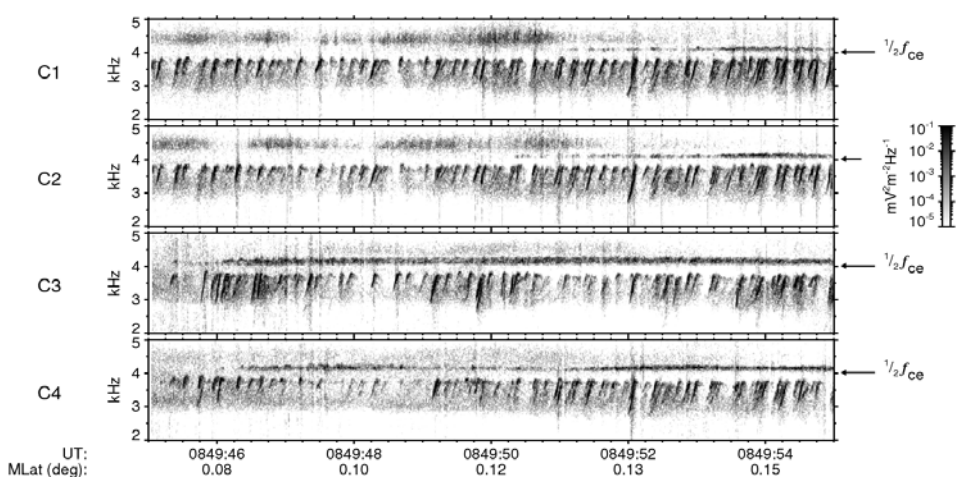

Figure 1. Time-frequency power spectrogram of whistler-mode chorus recorded by the four Cluster spacecrafts on 18 April 2002 (from Santolik and Gurnett, 2003)

The RESONANCE project represents an excellent opportunity for the magnetospheric research, and together with similar missions which are currently under preparation (for example, the two-spacecraft US mission Radiation belts Storm Probes), it will contribute to our understanding of Earth's Van Allen radiation belts and inner magnetosphere.

Operator-Splitting Kalman Filter as Efficient Data Assimilation Method for Radiation Belts

D. Kondrashov[1], Y. Shprits[2], D. Subbotin[3] and M. Ghil[4]

[1] *Department of Atmospheric and Oceanic Sciences and Institute of Geophysics and Planetary Physics, University of California, Los Angeles, CA, 90095, USA, dkondras@atmos.ucla.edu*

[2] *Department of Atmospheric and Oceanic Sciences and Institute of Geophysics and Planetary Physics, University of Califronia, Los Angeles, CA, 90095, USA*

[3] *Department of Atmospheric and Oceanic Sciences and Institute of Geophysics and Planetary Physics, University of Califronia, Los Angeles, CA, 90095, USA*

[4] *Department of Atmospheric and Oceanic Sciences and Institute of Geophysics and Planetary Physics, University of Califronia, Los Angeles, CA, 90095, USA and Geosciences Department and Laboratoire de Meteorologie Dynamique (CNRS and IPSL), Ecole Normale Superieure, F-75231 Paris Cedex 05, FRANCE*

The Van Allen radiation belts were discovered in 1958, but their dynamics is still poorly described, since satellite observations are often restricted to single-point measurements and thus have only limited spatial coverage. Therefore, to fill the spatio-temporal gaps in their description and thus lead to a better understanding of the dominant dynamical processes in the radiation belts, physics-based models should be combined with data in an optimal way. Data assimilation aims to smoothly blend incomplete and inaccurate observational data with dynamical information from a physical model. With more observational data coming from new and existing spacecraft, and radiation belts models becoming more sophisticated, it becomes possible to analyze dynamics in the radiation belts by relying on advanced data assimilation techniques, such as Kalman Filter.

The Kalman filter allows one to follow not only the evolution of the radiation belts state given by the phase-space density (PSD) of relativistic electrons, but it also propagates forward in time error estimates of state variables, thus naturally accounting for the system's evolving spatio-temporal uncertainties. In the Kalman filter formulation, this information is readily provided by the dynamical evolution of time-dependent error covariance matrices. The use of a dynamical model is of fundamental importance in the Kalman filter, and sets it aside from other assimilation schemes and ad-hoc data analysis techniques.

In this study, we rely on operator splitting to make Kalman filter computationally efficient for assimilating PSD into UCLA Versatile Electron Radiation Belt (VERB) model, which solves 3-D time-dependent Fokker-Plank diffusion equation in energy, particle pitch angle, and radial location. The primary computational difficulty in implementing a straightforward Kalman filter formulation for realistic 3-D VERB simulation is that the numerically discretized PSD solution has a very large number $N = O(10^6–10^7)$ of components. Consequently, corresponding model's state error covariance matrix has over a million squared elements, that needs to be evaluated, stored and evolved in time. We compare the straightforward Kalman filter, on the one hand, and the operator-splitting modification developed in this study, on the other, by assimilating synthetic PSD data, as well as actual satellite observations, into 3-D VERB code.

Operator-splitting Kalman filter relies on sequential data assimilation for each diffusion operator in the Fokker-Plank equation for PSD, that allows evolve error covariance matrices much smaller in size. The operator-splitting Kalman filter is considerably faster compared to the standard Kalman filter implementation, while yielding similar analysis errors.

References

[1] Kondrashov, D., Y. Sprits, R. Thorne and M. Ghil, A Kalman Filter Technique to Estimate Relativistic Electron Lifetimes in the Outer Radiation Belt, *J. Geophys. Res*., **112**, A10227, (2007).

[2] Y.Shprits, D.Kondrashov, Y.Chen, R.Thorne, M.Ghil, R.Friedel, and G.Reeves, Reanalysis of Relativistic Radiation Belt Electron Fluxes using CRRES Satellite Data, a Radial Diffusion Model, and a Kalman Filter, *J. Geophys. Res*., **112**, A12216, (2007).

[3] Subbotin, D. A., and Y. Y. Shprits, Three-dimensional modeling of the radiation belts using the Versatile Electron Radiation Belt (VERB) code, *Space Weather*, **7**, S10001, doi:10.1029/2008SW000452, (2009)

Space Radiation Environment in Low Earth Orbit Measured by Daichi Satellite during Solar-Activity Minimum Period from 2006 through 2011

H. Koshiishi

Japan Aerospace Exploration Agency, 2-1-1 Sengen, Tsukuba, Ibaraki, 3058505, Japan, koshiishi.hideki@jaxa.jp

The Technical Data Acquisition Equipment (TEDA) on board the Daichi satellite (Advanced Land Observing Satellite: ALOS) was launched on 24 January 2006, and had been operated in low earth orbit at 700 km altitude with 98 degree inclination until 21 April 2011. The TEDA consists of the Light Particle Telescope (LPT) for measurements of energetic electrons, protons, and alpha-particles, as well as the Heavy Ion Telescope (HIT) for observations of energetic ions from helium to iron. The LPT has a capability to measure electrons in the energy range from 0.1 MeV - 4 MeV in 14 bins, protons from 2 MeV to 34 MeV in 22 bins, and alpha-particles from 11 MeV to 137 MeV in 16 bins with 1-second temporal resolution. The LPT can also distinguish nuclei of hydrogen and helium isotopes, namely, nucleus of hydrogen/deuterium/tritium and 3He/4He.

In low earth orbit, the proton radiation environment is composed of the SAA (South Atlantic Anomaly) region that is settled by the combination of the distribution of geomagnetic field and trapped protons in the inner radiation belt, and the proton components in galactic cosmic rays that distribute along with the geomagnetic cut-off rigidity distribution. The electron radiation environment has also the horn region that corresponds to the foot points of the outer radiation belt as well as those two components.

The operation period of the Daichi satellite was through the solar-activity minimum period. The space radiation environment around the Daichi satellite had been almost stable. However, large solar flares followed by CMEs occurred in December 2006, and disturbed the space radiation environment in the orbit of the Daichi satellite. The enhancements of proton and electron flux due to the solar event were measured in this period both in the polar and the horn regions. In addition, high speed solar wind often flowed during the operation period of the Daichi satellite. The modulation of electron flux due to the solar wind variations was measured in the horn region all through the operation period. On the other hand, a little variation was seen in the SAA region.

In this paper, the space radiation environment in low earth orbit measured by the Daichi satellite during solar-activity minimum period from 2006 through 2011 in comparison with the calculation result obtained from the usual space radiation models is reported.

Investigations of the Impact of the Environmental Changes on Plants Using Hyperspectral Remote Sensing Techniques

D. Krezhova

Space and Solar-Terrestrial Research Institute, Bulgarian Academy of Sciences, Acad. G. Bonchev str. Bl.3, Sofia 1113, Bulgaria, dkrezhova@stil.bas.bg

Knowledge about variations in vegetation species and community distribution patterns, alterations in vegetation phenological cycles, and modifications in the plant physiology and morphology provide valuable insight into the climatic, edaphic, geologic, and geophysical characteristics of earth areas. Plant growth can have a considerable effect on the climate. Through the process of photosynthesis, plants use energy from the sun to draw down carbon dioxide from the atmosphere and then use it to create the carbohydrates that are needed to their growth. Carbon dioxide is one of the most abundant greenhouse gases and its removal from the atmosphere may moderate the warming of our planet as a whole. Another influence of plants on the particular landscape is its direct cooling through the process known as transpiration. When the surrounding atmosphere heats up, plants will often release excess water into the air from their leaves. By releasing evaporated water, plants cool themselves and the surrounding environment. Owing to these processes, it is generally believed that plants may have a considerable impact on global climate in the future.

During the past decade remote sensing techniques have been used to monitor plants throughout their growing period to help in making decisions for sustained development of the natural resources. The spectral remote sensing methods provide the possibility for early, efficient and objective assessment of plant responses to different stress factors. Hyperspectral remote sensing data have been widely used to assess changes in various biophysical and biochemical properties of plants and ecosystems in response to the changes in the environment. When combined with remarkable advances in Global Positioning System (GPS) receivers, microcomputers, geographic information systems (GIS), and enhanced crop simulation models, remote sensing technology has the potential to transform the ways that people manage the environment.

The objective of this paper is to show some aspects of the progress that has been made in remote sensing applications for crop management and, in particular, the applicability of the remote sensing techniques hyperspectral leaf reflectance and chlorophyll fluorescence for assessment of the effects of some environmental stresses (salinity, enhanced UV-B radiation, viral infections) in young plants (tomato, pepper, tobacco).

Hyperspectral data for leaf reflectance and fluorescence were collected in visible (VIS) and near infrared (NIR) ranges (450-850 nm and 600-850 nm, respectively) using a portable fiber-optics spectrometer. The reflectance measurements were carried out on an experimental setup in laboratory. As a light source a halogen lamp providing homogeneous illumination of measured leaf surfaces was used. For fluorescence measurements as a source of actinic light, a LED diode with light output maximum at 470 nm was used. The tested leaves were dark adapted before the measurements. The control of the spectrometer and the acquisition and processing of data were carried out by means of specialized software.

The results indicated that stress detection and discrimination by means of changes of reflectance and fluorescence data are realized in specific spectral regions as follows: green, red and red-edge (520-580 nm; 640-680 nm; 690-720 nm) due to chlorophyll degradation (necrotic or chlorotic lesions); as fluorescence (690-740 nm) due to photosynthesis disturbance, in the VIS and NIR (680-800 nm) due to senescence revealed by browning. The statistically significant differences were assessed by means of the Student's t-criterion. It is shown that using hyperspectral data in the field of remote sensing has greatly enhanced our ability to detect and quantify physical and biological stresses that affect the health and growth of the plants.

Influence of Flight Parameters on the Dosimetric Characteristics Measured with Liulin Semiconductor Detector on Board ISS during Solar Maximum and Minimum

J. Kubancak[1], Z. Mrázová[1], T. Dachev[2], O. Ploc[3]

[1] *Institute of Nuclear Physics of the ASCR, Department of Radiation Dosimetry, Prague, Czech Republic & Czech Technical University in Prague, Faculty of Nuclear Sciences and Physical Engineering, Prague, Czech Republic kubancak@ujf.cas.cz*

[2] *Space and Solar-Terestrial Reserch Institute of BAS, Sofia, Bulgaria ,dachev@bas.bg*

[3] *National Institute of Radiological Sciences, Chiba, Japan & Institute of Nuclear Physics of the ASCR, Department of Radiation Dosimetry, Prague, Czech Republic, ploc@ujf.cas.cz*

Cosmic radiation measurements at low Earth orbit are essential for evaluation of spacecraft crew exposure. The total absorbed dose and dose equivalent of members of a given mission depend on many details of the mission itself; one can state the orbit parameters of the spacecraft, solar cycle phase, thickness and material of the shielding as examples. Our research was aimed on the influence of flight parameters such as altitude, position against the South Atlantic anomaly (SAA), and solar cycle phase. Preliminary calculations show influence of the altitude on absorbed dose inside the ISS, 10 km change in altitude causes about 10% change. This effect is more important inside of SAA.
The work deals with evaluation and comparison of data measured with Liulin-type semiconductor spectrometers on-board the International Space Station. We will present the energy deposition spectra and dose equivalent rates measured with two types of Liulins: R3DE and E094. The R3DE device was placed on-board EuTEF platform during the period from 22nd of February 2008 to 2nd September 2009 (solar minimum). The Liuin-E094 system was placed on US Laboratory module between May and August 2001 (solar maximum). In particular, attention is paid on examination of changes of energy deposition spectra with respect to perigee and apogee and altitude changes inside and outside of the SAA. Further the work deals with comparisons of measured data at low Earth's orbit during the solar minimum and maximum.

References

[1] Dachev, T. (2009) Characterization of the near Earth radiation environment by Liulin type spectrometers. *Advances in Space Research.* Vol. 44, s. 1441-1449

[2] Spurný F., Ploc O., Dachev Ts (2007) On the neutron contribution to the exposure level onboard International Space Station. Radiat. Prot. Dosim., 125(1-4), p. 519-523

Advanced Topside Ionosphere and Plasmasphere Electron Density Profiling Technique

I. Kutiev

National Institute of Geophysics, Geodesy and Geography, BAS, Acad. G. Bonchev str., bl. 3, Sofia 1113, Bulgaria, ivankutiev@yahoo.com

The safety and security of space operations requires that spacecraft operators know and understand the environment around their spacecraft. A measure of the ionospheric element of that environment is given by the precise values of the partial total electron content (TEC), i.e. the integral of the electron density between the spacecraft and some location on the surface of the Earth - and in some cases between two spacecrafts. Therefore knowledge of the analytical presentation of the electron density up to GNSS orbit heights is highly required. While the bottomside part of the ionospheric electron density can be determined, at least over specific locations, from ionogram inversion, in the topside ionosphere direct observations of electron density are sparse. Electron density models of high accuracy are required to fill in the gap.

A number of empirical models, like IRI, PIM (Parameterized Ionospheric Model), NeQuick and others provide electron density (Ne) profiles in topside ionosphere and plasmasphere in a global scale. Recently, new models are being developed, involving more physics in describing the Ne profiles above the ionospheric maximum. One of these new models, named TaD (TSM-assisted Digisonde) reconstruction model, is designed to improve the accuracy of Ne profiles produced by Digisonde software, as a complement to the measured bottomside profile. TaD [1] uses the TSM Profiler (TSMP), developed on the base of TSM (Topside Sounder Model) [2]. TSM model obtains topside scale height (H_T), transition height (h_T), and their ratio (R_T), as functions of the day-of-the- year, geomagnetic latitude, local time, solar flux ($F_{10.7}$), and Kp. TSMP [3] expresses the shape of the Ne profile above the F layer peak as a sum of O^+ and H^+ profiles, as the O^+ scale height and O^+- H^+ transition height are taken from TSM, while the H^+ scale height is statistically determined from ISIS-1 topside sounder profiles. When electron density NmF2 and height hmF2 are specified at the lower boundary, TSMP provides Ne profile up to GPS orbit heights. To reconstruct the topside Ne profile, TaD uses the actual (measured) NmF2 and hmF2 from Digisonde, as well as the scale height Hm determined by fitting the around maximum profile with α-Chapman formula. TaD multiplies Hm with a predefined factor (approximately 2.5) and uses the modified scale height (2.5Hm) to run TSMP. In this way, the measured F peak parameters and the modified scale height represent the actual (instant) state of ionosphere, comparing to the average TSM parameters. In TaD profiler, transition height h_T and the plasmasphere scale height Hp are statistically connected to the O^+ (topside) scale height H_T. A special procedure is developed which changes the Ne integral by varying the scale height factor in order to equalize it with the corresponding measured GPS-TEC value. It is demonstrated that this procedure, which improve significantly the reconstructed Ne profile, can be implemented in the operational Global Navigation Satellite System (GNSS) practice.

References

[1] Kutiev I., P. Marinov, A. Belehaki, B. Reinisch, N. Jakowski, *Advances and Space Research*, **43**, 1683 (2009).
[2] Kutiev, I., and P. Marinov, *Adv. Space Res*., **39**, 759 (2007).
[3] Kutiev, I., P. Marinov, A. Belehaki, N. Jakowski, B. Reinisch, C. Mayer, and I. Tsagouri, *Acta Geophysica*, **58**, (2009).

Geometric Effects of the Solar Wind–Magnetosphere Interaction in Planetary Geomagnetic Activity

T.V. Kuznetsova and A.I. Laptukhov

Pushkov Institute of Terrestrial Magnetism, Ionosphere and Radio Wave Propagation, Russian Acad. of Science (IZMIRAN), Moscow region, Troitsk 142190, Russia; E-mail addresses: tvkuz@izmiran.ru, laptuhov@izmiran.ru

We put as one of our main aims to explain such long-standing problem of solar-terrestrial physics as observed semiannual (with peaks at equinoxes) and UT variation of geomagnetic activity. Two main mechanisms which have both semiannual and UT variation of geomagnetic activity have been proposed. The equinoctial hypothesis (Bartels, 1925) has key angle between the solar wind flow direction and the Earth's dipole axis Ψ; activity maximizes (for as yet unknown reasons) at the equinoxes when $\Psi=90^0$. In the Russell-McPherron (RM) mechanism (Russell and McPherron, 1973), magnetic fields in the solar equatorial plane have a peak southward component at the Earth in GSM coordinates in early April or October, depending on their polarity. Influence of the angles (geometric parameters) of these two hypothesises are subject of our study. We attract also a reconnection model elaborated by us made allowance for changes of geometry of the solar wind–magnetosphere interaction during annual and diurnal motions of the Earth. Key angle of our model is angle between the solar wind electric field (E) and geomagnetic moment (M), which determines reconnection rate [1-3 and references therein].

We present here results of our study of dependence of geomagnetic activity (Kp, Ap, Dst, Am indeces) from orientation of the solar wind velocity (V), the Interplanetary Magnetic Field (IMF), electric field E with respect to the Earth's moment direction M. Geometric parameters determining mutual orientation of each from these vectors and the M vector are calculated on basis of measurements of V and IMF near the Earth's orbit for the period 1963-2005 and computation of orientation of M at GSE. We did not make any assumption concerning interaction mechanism when angles between the vectors were calculating; evaluation of geoeffectness of each from them was carried out on basis of reaction of Kp, Ap, Dst, Am to changes of these angles. It follows from our study that in themselves changes of orientation of the IMF with respect to the dayside geomagnetic field can explain about 35% of observed variations of K_p We demonstrate that variation of orientations of vectors V and M explains less than 15% of the Kp variation. The variation of orientation of vectors E and M explains 50% of Kp changes (and 75% Dst, Ap). So we concluded that our reconnection mechanism based on determining role of direction of the solar wind electric field (angle between vectors E and M) is the most effective compared with equinoctial mechanism (angle between vectors of V and M) and reconnection one based on main role of the southward IMF (angle between vectors of the IMF and M, that is close to RM mechanism). Taken as a whole geoeffective parameter Emv suggested by us explains 95% of observed statistical variations of the indices. Moreover, we detected clear increasing of Kp, Ap with increasing of value of the northward IMF (relative to vector M) and suggested our interpretation of this effect [2,3]. We discuss applications of our results for explanation geomagnetic storm during northward IMF and geoefficiency of CMEs (MCs).

Based on our results we suggest a new explanation of semiannual and UT variation of GA. In particular, phase of statistical annual variation of geomagnetic activity is determined by annual variation of the geomagnetic moment component My caused by oscillations of the Earth's magnetic dipole at the yz plane of GSE coordinate system during its annual motion: maximal value at equinoxes and minimal value at solstices. Amplitude of the annual variation is modulated by the solar wind electric field component Ez perpendicular to the ecliptic plane. By the other words, annual variation of My at the yz plane makes extrema of My at equinoxes that produces maxima of the dawn–dusk component of electric field Emv at the yz plane at spring equinox for toward polarity and at fall equinox for away polarity of the IMF. [3]

References

[1] Kuznetsova, T.V., Laptukhov, A.I. A study of magnetopause dynamics and magnetospheric state in case of reconnection between the Earth's magnetic field and an IMF of arbitrary orientation, in: Shroeder, W. (Ed.), New and Old Problems in Physics and Geophysics. Science Publishing, Germany, pp. 10–26, (2002).

[2] Kuznetsova, T.V., Laptukhov, A.I., Kuznetsov, V.D. Allowance for the geometry of solar wind interaction with the Earth's magnetic field in geoeffective parameters and in the prediction of geomagnetic activity. *Solar System Research* **40**, 513–520, (2006)

[3] Kuznetsova T.V., Laptukhov A.I. Contribution of geometry of interaction between interplanetary and terrestrial magnetic fields into global magnetospheric state and geomagnetic activity. *Adv. Space Res.* **47** p. 978–990, (2011) doi:10.1016/j.asr.2010.11.022

Steadiness of the Semiannual and UT Variations of Geomagnetic Activity for Different Levels of Disturbances

T.V. Kuznetsova and A.I. Laptukhov

Pushkov Institute of Terrestrial Magnetism, Ionosphere and Radio Wave Propagation, Russian Acad. of Science (IZMIRAN), Moscow region, Troitsk 142190, Russia; E-mail addresses: tvkuz@izmiran.ru, laptuhov@izmiran.ru

The report presents results of our study of semiannual and UT variation of geomagnetic activity for different levels of disturbances. The cause of the semiannual variation of geomagnetic activity, characterized by stronger and more frequent storms in equinoxes compared in soltices, is a long-standing question of solar-terrestrial question. We suggested a new explanation of statistical semiannual and UT variation of geomagnetic activity [1-3]. Because our explanation was based on conclusions from a reconnection model elaborated by us made allowance for changes of geometry of the solar wind–magnetosphere interaction during annual and diurnal motions of the Earth [1], it was important to verify the conclusions for large geomagnetic disturbances. Moreover, explanation of semiannual and UT variation of large geomagnetic activity is a good test for any model of the solar wind–magnetosphere interaction. We made our first study of the semiannual and UT variation of large disturbances in [4].

We used here for our study geomagnetic indices Kp (1932-2005), aa (1868-2005) and Dst (1957-2005).

We obtained (for all geomagnetic indices) that as the level of intensity increases, the classical season variation with peaks in vicinity of equinoxes is well preserved. Even for strong disturbances in range of Kp=8-9 we obtained the same profile of the semiannual variation. Additional peaks in July and November are imposed upon the classical season variation. We see the same positions of peaks and their intensity for level aa>200 nT. So, the semiannual variation of great disturbance is remarkably pronounced. This implies that the semiannual variation for large disturbances is not random storm occurrence but primarily the effect of storm themselves. Based on our results we suggest a possible explanation of additional peaks in July and November. We discuss also the UT variation of all discussed indices for the high levels of geomagnetic activity. At last we discuss applications of our results for explanation of geoefficiency of CMEs (MCs).

References

[1] Kuznetsova, T.V., Laptukhov, A.I. A study of magnetopause dynamics and magnetospheric state in case of reconnection betweenthe Earth's magnetic field and an IMF of arbitrary orientation, in: Shroeder, W. (Ed.), New and Old Problems in Physics and Geophysics. Science Publishing, Germany, pp. 10–26, (2002).

[2] Kuznetsova, T.V., Laptukhov, A.I., Kuznetsov, V.D. Allowance for the geometry of solar wind interaction with the Earth'smagnetic field in geoeffective parameters and in the prediction of geomagnetic activity. *Solar System Research* **40**, 513–520, (2006)

[3] Kuznetsova T.V., Laptukhov A.I. Contribution of geometry of interaction between interplanetary and terrestrial magnetic fields into global magnetospheric state and geomagnetic activity. *Adv. Space Res.* **47** p. 978–990, (2011) doi:10.1016/j.asr.2010.11.022

[4] Kuznetsova T.V., Laptukhov A.I. Semiannual and UT variation of geomagnetic activity for different level of disturbances. Proceedings of conference "Experemental and theoretical studies of forecasting heliophysical activity. IZMIRAN, 10-15 October, 2005, p. 217-222, 2006 (in Russian)

Properties and Processes that Influence CME Geo-Effectiveness

B. Lavraud

[1] *IRAP/ CNRS/Université de Toulouse, France*

This presentation will provide a review of CMEs (1) intrinsic properties (e.g., magnetic field structure, velocity, Mach number, etc.) and (2) processes that may occur during propagation (e.g., compressions, merging, erosion, etc.) or in the magnetosphere (e.g., preconditioning mechanisms) that can have a significant influence on their geo-effectiveness. Their relative importance will be discussed.

Recent Progress in Modeling the Dynamics of Magnetic Storms at The Aerospace Corporation

C. L. Lemon[1], M. W. Chen[1], T. B. Guild[2]

[1] *The Aerospace Corporation, P.O. Box 92957, Los Angeles, CA, 90009-2957, USA, colby@aero.org*

[2] *The Aerospace Corporation, 15049 Conference Center Drive, CH3/330, Chantilly, VA, 20151, USA*

The enhancement of the Earth's ring current during the main phase of magnetic storms is a dynamic process that is not yet thoroughly understood. In order to clarify those dynamics, we present simulations of both idealized and observed magnetic storm events. Recent progress in ring current modeling has shown the importance of a self-consistent treatment of particle transport and magnetic and electric fields in the inner magnetosphere. Models with and without self-consistency lead to different magnitudes and spatial distributions of plasma pressure and magnetic field during disturbed times. Furthermore, the plasma sheet properties (including density, temperature, and composition) and the convection strength are crucial inputs for determining both the overall strength of the ring current and the detailed dynamics that unfold during storms. Importantly, the feedback inherent in self-consistent models leads to a complex interplay between these drivers of the ring current dynamics that will be demonstrated through our simulations. Our simulation model is the Rice Convection Model with an Equilibrium magnetic field solver (RCM-E), which includes feedback between the Birkeland currents and the electric field, and between the plasma pressure and the magnetic field. We also include a time-varying magnetopause driven by upstream solar wind and interplanetary magnetic (IMF) conditions. Results from idealized parametric simulation studies will be shown to contrast the outcome of 1) simulations with and without magnetic and electric self-consistency and 2) different plasma sheet source parameters. In addition, detailed comparisons will be made between our simulated storm events and observed in-situ magnetic fields (from GOES, Polar/MPA, and THEMIS), proton flux spectra (LANL/MPA and SOPA, Polar/CAMMICE, and THEMIS), and energetic neutral atom fluxes (TWINS). Such comparisons test the accuracy of our model for characterizing the ring current environment and storm-time inner magnetospheric magnetic field, and give confidence in our ability to assess the roles of different physical processes in the observed storm-time dynamics.

Quantifying Field-Aligned Current Loops in the Inner Magnetosphere

M. Liemohn[1], D. L. De Zeeuw, R. Ilie[2], N. Y. Ganushkina[1]

[1]*University of Michigan, Ann Arbor, MI, 48109, USA, liemohn@umich.edu*
[2]*Los Alamos National Laboratory, MS D466, Los Alamos, NM, 87545, USA*

A single near-tail magnetic field line can be part of a variety of cross-field current systems, making the interpretation of such currents difficult. The identification of the current systems is important, though, because closure through the ionosphere (along field-aligned currents) alters the electric potential pattern of the inner magnetosphere. Therefore, the feedback on the hot ions carrying the current is very different depending on the eventual closure of the current they are carrying. It is shown that global, coupled-model simulation results from the 22 October 1999 storm (using the Space Weather Modeling Framework [1]) reveal this complicated and dynamic structure of current flow through the near-Earth nightside magnetosphere. For example, a field line crossing at 8 R_E downtail during the main phase was found to contain streamtraces of partial ring current, symmetric ring current, and tail current simultaneously (at different latitudes. Such field lines with multiple currents are common in the near-Earth tail. At other times, current systems are distinctly separated from each other, yet exist on adjacent magnetic field lines. An initial study [2] of the equatorial plane innermost extent of the tail current revealed that this current system boundary moves systematically with the phases of the storm, pushing all the way out to ~11 R_E downtail at the peak of the storm. In these simulation results for this storm interval, most of the cross-field current is carried by the symmetric and partial ring currents rather than the tail current.

Here, a systematic analysis of cross-field currents during this storm is presented and discussed. In particular, the separation of partial ring current, defined here as that part of the cross-field current closing through the ionosphere via field-aligned currents (i.e., region 2 currents), is quantified and compared against the intensity and location of the symmetric ring current and tail current. During the first part of the main phase, the partial ring current dominates over the other current systems, yielding large region 2 FACs that result in strong distortions of the near-Earth electric potential distribution. As the storm develops and strengthens, the other current systems become comparable and eventually dominate the cross-field current intensity.

References

[1] Toth, G., et al., *J. Geophys. Res.,* **110**, A12226 (2005).
[2] Liemohn, M. W., et al., *Geophys. Res. Lett.,* submitted, (2011).

A Review of the Saturation of the Cross-Polar Cap Potential

R. E. Lopez[1]

[1] *Department of Physics, University of Texas at Arlington Arlington Tx, 76019, USA, relopez@uta.edu*

The interaction between the solar wind and the magnetosphere produces a potential difference across the polar cap that is a measure of the overall convection in the magnetosphere driven by the forces exerted by the solar wind. The cross-polar cap potential (CPCP) is driven primarily by reconnection, which is the primary mechanism by which solar wind energy and momentum is delivered to the magnetosphere. For relatively low levels of driving the response of the CPCP is roughly linear with respect to the merging field, but for large values of driving the CPCP becomes insensitive to the value of the merging field. This is referred to as the saturation of the CPCP, and while the initial identification of saturation was during periods of strongly southward IMF, the same behavior is seen for other periods in which there is a large, transverse IMF. In this paper I will review the observational evidence for the saturation of the CPCP, as well as the fact that the ring current injection rate does not saturate while the CPCP and the amount of open magnetic flux does. I will also review the models that have been presented to explain the saturation of the CPCP. While there are still a number of issues around saturation that are not yet resolved, I will argue that that the basic problem of saturation has in fact been solved.

What Causes Sawtooth Oscillations of the Magnetosphere-Ionosphere System?

W. Lotko[1], O. J. Brambles[1], B. Zhang[1], M. Wiltberger[2], J. G. Lyon[3], R. J. Strangeway[4]

[1] *Thayer School of Engineering, Dartmouth College, Hanover, Hew Hampshire, USA*
[2] *High Altitude Observatory, National Center for Atmospheric Research, Boulder, Colorado, USA*
[3] *Department of Physics and Astronomy, Dartmouth College, Hanover, New Hampshire, USA*
[4] *Institute for Geophysics and Planetary Physics, University of California, Los Angeles, California, USA*

The 2-5 hour planetary-scale oscillation in geospace known as the sawtooth mode was discovered in geostationary satellite data twenty years ago, yet its origins remain unknown. We show that ionospheric O^+ outflows can induce sawtooth oscillations in multifluid simulations of the solar wind-magnetosphere-ionosphere (SW-M-I) interaction for steady SW driving. When the simulated, mean hemispheric fluence of the outflow exceeds $\approx 10^{26}$ ion/s, accumulation of O^+ in the plasma sheet exceeds reconnection mass loss. The O^+ pressure eventually overcomes the confining tension of the geomagnetic field, a plasmoid is ejected, and the field dipolarizes. The strength of SW-M-I driving controls the outflow fluence and the period of repetition. Below $\approx 10^{26}$ ion/s, mass loss and outflow are in balance, and quasi-steady convection ensues. The threshold for oscillation depends on the bulk properties and spatial distribution of the outflow.

The simulated outflows are causally regulated using an empirical relation derived from FAST data, specifying the local flux F_{O+} of outflowing O^+ in ions/cm^2-s given the local downward flowing Alfvénic Poynting flux $S_{\|}$ in mW/m^2:

$$F_{O+} = 2.97\times 10^{10}(\alpha S_{\|})^{1.2}. \quad (1)$$

The scaling parameter α is varied to study the effects of variance in the FAST data regression and of subgrid, non-MHD processes contributing to the observed $S_{\|}$ but missing in the simulations.

The Poynting flux flowing downward at the simulation boundary,

$$S_{\|} = \pm\delta\mathbf{E}\times\delta\mathbf{B}\cdot\mathbf{B}_m/B_m\mu_0, \quad (2)$$

is calculated using a 180-s running average $\boldsymbol{B}_m$ of the simulated B-field, and 6-180 s bandpass filtered electric $\delta\mathbf{E}$ and magnetic $\delta\mathbf{B}$ perturbations. The choice $\pm$ corresponds to Poynting flux in the northern/southern ionosphere.

The system response was examined for various solar wind velocities V_{sw} and IMF B_z while fixing SW density ρ_{SW} at 5m$_p$/cm^3, temperature at 10 eV and $B_{x,y} = 0$. For fixed α (= 3.8 in the table), the simulated, 20-hour mean of the hemispheric outflow fluence $\langle F_{TOT}\rangle$ in 10^{26} ions/s is found to increase linearly with strength $\varepsilon = V_{SW}B_{IMF}\sin^2(\theta/2)(\rho_{SW}V_{SW}^2)^{1/6}$ of SW driving:

$$\langle F_{TOT}\rangle = 0.6\varepsilon + 0.2. \quad (3)$$

ε is given in (mV/m) (nPa)$^{1/6}$. The IMF clock angle $\theta = 180°$ for all runs.

SIMULATION RESULTS. Shaded rows: quasi-steady convection; unshaded: sawtooth modes.

V_{SW} km/s	B_z nT	α	ε	$\langle F_{TOT}\rangle$ 10^{26}/s	Period hrs
400	-10	0	3.7	0	SC
400	-10	1	3.7	0.5	SC
400	-10	2.1	3.7	1.2	8.9
400	-10	3.8	3.7	2.4	4.4
400	-10	5.3	3.7	3.6	2.8
400	-10	6.8	3.7	4.8	2.6
400	-10	12	3.7	9.6	1.7
200	-10	3.8	1.5	1.1	SC
600	-10	3.8	6.4	4.0	2.0
400	-5	3.8	1.9	1.4	5.3
400	-2.5	3.8	0.9	0.8	SC

The sawtooth mode is distinguished from isolated substorms by the broad extent in magnetic local time of signatures such as field line stretching and dipolarization. We examined this feature by comparing a superposed epoch analysis of magnetic inclination angle near geostationary orbit for observed sawtooth events with a superposed epoch of simulated sawtooth events with periods of 1.75 to 5 hours (Fig. 1).

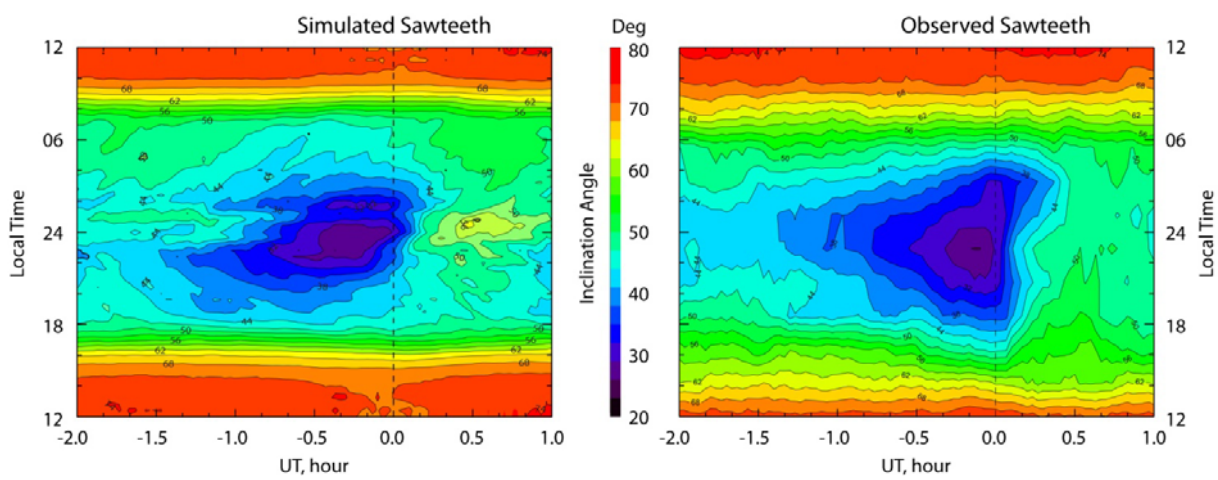

Figure 1. Superposed epoch of magnetic inclination angle near geostationary orbit from simulations [1] and observations [2].

References

[1] O. J. Brambles, W. Lotko, B. Zhang, M. Wiltberger, J. G. Lyon and R. J. Strangeway, *Science*, 3 June 2011.
[2] X. Cai, M. G. Henderson and C. R. Clauer, *Ann. Geophys. 24*, 3481–3490, 2006.

Effects of High-Speed Solar Wind Streams on the Magnetosphere and Ionosphere/Thermosphere: Similarities and Differences

G. Lu[1]

[1] *High Altitude Observatory, National Center for Atmospheric Research, 3080 Center Green Drive, Boulder, CO 80301, USA; ganglu@ucar.edu*

High-speed solar wind stream (HSS) has been well recognized as one of the leading causes of geomagnetic disturbances. There is ample observational evidence showing the effects of HSS on thermospheric density and composition as well as on magnetospheric energetic particles. However, it is yet to be understood how exactly energies are being transferred from the solar wind and dissipated into the magnetosphere and ionosphere/thermosphere during HSS events. The main emphasis of the paper is on the similarities and differences between the magnetosphere and the ionosphere in response to HSSs. It will also address the important issue concerning the energy coupling efficiency between the solar wind and magnetosphere/ionosphere during HSSs, which will be compared to those CME-driven events to shed new lights on the coupling processes between the solar wind and magnetosphere-ionosphere under the different solar wind conditions.

Numerical Simulations of ICME Structure

N. Lugaz[1] and I. I. Roussev[1]

[1] *Institute for Astronomy, University of Hawaii, 2680 Woodlawn Dr., Honolulu, HI, 96822, USA*

Interplanetary coronal mass ejections (ICMEs) have complex magnetic and density structures, which are the result of their interaction with the structured solar wind and with previous eruptions. ICMEs are revealed by in situ measurements and in the past five years, through remote-sensing observations by heliospheric imagers. However, to understand and analyze these observations often requires the use of numerical modeling. It is because no instrument can yet provide a simple view of ICMEs in two or three dimensions. Numerical simulations can be used to determine the origin of complex ejects observed near Earth, or to analyze the origin, speed and extent of density structures observed remotely. Here, we review and discuss recent efforts to use numerical simulations of ICMEs to investigate the magnetic topology, density structure, energetics and kinematics of ICMEs in the interplanetary space. 3-D simulations can also help determining the origins of the fronts observed by SECCHI and SMEI, especially for complex events. We also discuss instances, when an ICME expected geo-effectiveness is significantly modified during its propagation. Our focus is on the propagation and interaction of successive ICMEs from the Sun to the Earth and the understanding of the mechanisms which may result in larger and more geo-effective structures.

Solar Cycle Changes in Solar Wind-Magnetosphere Coupling Efficiency

R.L. McPherron[1], T-S. Hsu[1], J.Kissinger[1], X. Chu[1]

[1] *Department of Earth and Space Sciences, Univ. Calif., Los Angeles, 90095-1567, rmcpherron@igpp.ucla.edu*

Geomagnetic activity depends on a variety of factors including solar ultraviolet radiation, strength of the interplanetary magnetic field, speed and density of the solar wind, orientation of the Earth's dipole, the distance of the Earth from the Sun, occurrence of CMEs and CIRs, and possibly other parameters as well. We have investigated a number of these factors using state-dependant linear prediction filters. For a given state the prediction filter transforms a coupling function such as VBs to an output like the AL index. The area of this filter calculated from the sum of the filter coefficients is a measure of the efficiency of the coupling. In situations where the input and output are steady for a time longer than the duration of the filter the ratio of output to input is equal to the area of the filter. We find that the coupling efficiency defined in this way for VBs to AL (and AU) is weakest at solar maximum and strongest at solar minimum. AL coupling displays a semiannual variation being weakest at the solstices and strongest at the equinoxes. AU coupling in contrast has an annual variation being weakest at winter solstice and strongest at summer solstice. AL and AU coupling also vary with time relative to a stream interface. Coupling is stronger after the interface than it is before. The change is efficiency with the solar cycle can be explained as an effect of the strength of the driver. Strong driving at solar maximum causes saturation of the polar cap potential and a weaker ratio of AL to solar wind electric field. Stronger AL coupling at the equinoxes indicates the existence of some process that makes magnetic reconnection more efficient when the dipole axis is orthogonal to the Earth-Sun line than when it is tilted towards or away from the Sun. Strong AU coupling at summer solstice is a result of high conductivity in northern summer. The increase in coupling after a stream interface is correlated with the presence of strong wave activity in ground and satellite measurements.

Ozone Dynamics over Bulgaria

B. D. Mendeva[1], D. G. Krastev [1], Ts. N. Gogosheva

[1] *Space and Solar-Terrestrial Research Institute –BAS, Stara Zagora Department, P.O.Box 73, Stara Zagora 6000, Bulgaria, bmendeva@abv.bg*

The aim of this paper is to present the investigation of the total ozone content (TOC) over Bulgaria in the time period 1997-2008. Data from ground-based measurements as well as from satellite experiments are used.

The ground-based measurements are performed in Stara Zagora, (42°25‘N, 25°37’E), Bulgaria by the scanning spectrophotometer Photon. This instrument is used to measure and examine the temporal variations of the ultraviolet radiation, reaching the Earth’s surface and the total ozone content in the atmosphere. The spectrophotometer measures the direct solar light in the range 255-400 nm, with 1 nm resolution. TOC is determined from direct solar spectra by applying the Bouguer-Lambert’s law for radiation attenuation during transition through the Earth’s atmosphere and different absorption of the separate wavelengths by the ozone molecules.

The total ozone dynamics is analyzed using data from the spectrophotometer Photon, as well as these by the satellite instruments GOME, TOMS-EP and SCIAMACHY. The course of the daily and monthly mean ozone values is presented. The seasonal TOC variations are clearly marked. These variations are expressed by an abrupt maximum in the spring and a gently sloping decrease in the autumn. Quasi-biennial periodicity in the amplitude of the ozone maxima can be seen. The experimental data show that there is no any trend in the ozone course during the period 1997-2008. Despite the absence of a trend in the whole period the calculations give different trend values in the various seasons.

Solar Wind-Radiation Belt Coupling via Wave Particle Interactions

Y. Miyoshi[1], R. Kataoka[2], Y. Kasahara[3], and A. Kumamoto[4]

[1] *Solar-Terrestrial Environment Laboratory, Nagoya University, Nagoya 464-8601, Japan, miyoshi@stelab.nagoya-u.ac.jp*
[2] *Tokyo Institute of Technology, Tokyo 152-8550, Japan*
[3] *Kanazawa University, Kanazawa 920-1192, Japan*
[4] *Tohoku University, Sendai 980-8578, Japan*

We investigate the solar wind-radiation belt coupling process, focusing on the large flux enhancements of outer belt electrons associated with high speed coronal hole streams. Flux enhancements of the outer belt tend to occur during the high-speed streams with the predominantly southward interplanetary magnetic field (IMF). Considering the internal acceleration model of relativistic electrons by wave-particle interactions, this IMF dependence of the enhancements can be understood as follows. The internal acceleration by wave-particle interactions is especially effective when a continuous source of hot electrons and a shrink of the plasmapause can be maintained to produce chorus waves for several day periods because the hot electrons provide the free energy source to excite whistler mode waves and also the sub-relativistic electrons are the seed population of MeV electrons. Continuous hot electron injections as well as the shrink of the plasmapause are enhanced during a prolonged period of intense convection and/or substorms, which are driven by the southward IMF in high speed streams. Based on the superposed epoch analysis using the whole data base during solar cycle 23, we statistically show the significant differences in the time evolution of these particles, wave activities, and convection/substorms between the southward and northward dominant IMF in high speed streams. Considering these results, we propose a model of solar wind-radiation belt coupling in which wave-particle interactions driven by continuous hot electron injections play an important role for the flux enhancements.

Multiscale Studies of the 3-D Dayside X line

T E Moore[1], J L Burch[2], S A Fuselier[3], H Hasegawa[4], S Petrinec[3], Z Pu[5], D J Sibeck[1]

[1] *NASA Goddard SFC, Heliophysics Science Div. Greenbelt MD 20771, t.e.moore@nasa.gov*
[2] *Southwest Research Institute, San Antonio, TX 78238*
[3] *Lockheed Martin ATC, Palo Alto, CA 94304*
[4] *Inst. Space Astro. Science, Sagamihara Kanagawa 229-8510 Japan*
[5] *Dept. of Geophysics, Univ. of Beijing, 100871 China*

We examine experience from the Cluster, Double Star, and THEMIS missions for lessons that apply to the upcoming Magnetospheric Multiscale mission (MMS) being developed for launch in 2014. On global scales, statistical studies lead to a mean configuration of dayside reconnection [1], implying specific relative alignments of the inflow magnetic fields and X line, with implications for MMS operations designed to maximize the number of close encounters with the diffusion region. At intermediate MHD scales, Grad-Shafranov reconstruction [2] of features created by one or two X lines have developed to the point where data from a tetrahedral cluster of spacecraft can determine the approximate three-dimensional X line structure. High time resolution measurements from MMS will determine the detailed electron scale kinetics embedded within the global and MHD contexts [3]. This should allow a full three-dimensional multiscale picture of reconnection to emerge, leading to improved understanding of the global, MHD, and local factors controlling the onset or quenching, variability, and mean rate of reconnection, and improved predictability of the structural features created by transient reconnection, and their space weather consequences.

References

[1] J. Wang, Z.Y. Pu, et al., (2009), Statistic study on global shape of dayside magnetopause reconnection X line: based on Cluster & TC1 observations, AOGS 2009 - ST18-D2-PM2-P-020.
[2] Hasegawa, H., et al. (2010), Recovery of time evolution of Grad Shafranov equilibria from single spacecraft data: Benchmarking and application to a flux transfer event, J. Geophys. Res., 115, A11219, doi:10.1029/2010JA015679.
[3] Burch, J. L., and J. F. Drake, (2009), Reconnecting Magnetic Fields, American Scientist, Volume 97, p.392.

Generalized Jeans' Escape of Pick-Up Ions in Quasi-Linear Relaxation

T E Moore[1], G V Khazanov[1]

[1] *NASA Goddard SFC, Heliophysics Science Div. Greenbelt MD 20771, t.e.moore@nasa.gov*

Jeans' escape is a well-validated formulation of upper atmospheric escape that we have generalized to estimate plasma escape from ionospheres. It involves the computation of the parts of particle velocity space that are unbound by the gravitational potential at the exobase, followed by a calculation of the flux carried by such unbound particles as they escape from the potential well. To generalize this approach for ions, we superposed an electrostatic ambipolar potential and a centrifugal potential, for motions across and along a divergent magnetic field. We then considered how the presence of superthermal electrons, produced by precipitating auroral primary electrons, controls the ambipolar potential. We also showed that the centrifugal potential plays a small role in controlling the mass escape flux from the terrestrial ionosphere. We then applied the transverse ion velocity distribution produced when ions, picked up by supersonic (i.e., auroral) ionospheric convection, relax via quasi-linear diffusion, as estimated for cometary comas [1]. The results provide a theoretical basis for observed ion escape response to electromagnetic and kinetic energy sources. They also suggest that super-sonic but sub-Alfvénic flow, with ion pick-up, is a unique and important regime of ion-neutral coupling, in which plasma wave-particle interactions are *driven by ion-neutral collisions* at densities for which the collision frequency falls near or below the gyro-frequency. As another possible illustration of this process, the heliopause ribbon discovered by the IBEX mission involves interactions between the solar wind ions and the interstellar neutral gas, in a regime that may be analogous [2].

References

[1] Puhl, P., T. E. Cravens, and J. Lindgren (1993), Ion thermalization in the inner coma of a comet, Astrophys. J., 418, 899–911.

[2] Heerikhuisen, J., *et al.* 2010 *ApJ* **708** L126 doi: 10.1088/2041-8205/708/2/L126

A Catalogue of Solar and Environmental Data

P. Nedialkov[1], L. Tsankov[1], E. Donev[1]

[1] *Department of Physics, J. Bourchier blvd, Sofia, 1164, Bulgaria, japet@phys.uni-sofia.bg*

The catalog of Solar and environmental data was constructed as an output of the observing program of the project "Observatory for monitoring of the solar activity and environmental parameters" supported by the grant No. VU-NZ-01/2006 with the Bulgarian NSF. This has resulted in a catalogue of data including up-to-date information on solar radio flux, solar radiance (1071 points), ozone concentration (1071) and dose rate (443 and 243 points) for two observational points, one located at Astronomical observatory of Sofia University and another - at Plana mountain near Sofia.

Since observations with the Small Radio Telescope (SRT) were rather sparse (only 10 points) most of the daily solar flux values (834 points) are taken from Sagamore Hill Solar Radio Observatory where operating solar patrols at 1415 MHz are regularly carried out. Flux calibrations in units of 10-22 Wm-2 Hz-1 are made near the meridian transit each day but the values were interpolated on timing, corresponding to UT=12 a.m. All flux data, including solar radiance, are corrected to Sun-Earth distance of 1 AU.

Joule Heating in the Lower Thermosphere Caused by Large-Scale Field-Aligned Currents

P. Nenovski [1], D. Danov [2]

[1] *National Institute for Geophysics, Geodesy and Geography, Bulgarian Academy of Sciences, 1113 Sofia, Bulgaria*
[2] *Space and Solar-Terrestrial Research Institute, Bulg.Ac. of Sc.,1113 Sofia, Bulgaria, ddanov@stil.bas.bg*

Magnetosphere-ionosphere-thermosphere (M-I-T) coupling represents a nonlinear dynamical system having very complex properties. Recent studies on processes of (M-I-T) coupling have revealed that the global electromagnetic energy input exceeds the particle energy input by about 4 times (e.g. Lu et al., 1995). The electromagnetic energy flux between the magnetosphere and ionosphere consists mainly of field-aligned currents (FAC) and wave processes. In its turn, the neutral atmosphere (the thermosphere) can have significant influence on the ionospheric electrodynamics.

The thermospheric and ionospheric effects of the FAC variations at high latitudes have been modeled by the use of large-scale (LS) FAC models (Nenovski, 2008, Weimer, 2005). These FAC models yields quantitatively the FAC structures and FAC intensity distribution at higher latitudes (>60 degrees) depending on the solar wind (SW) and interplanetary magnetic field (IMF) variations.

While the electron concentration and electron temperature disturbances are caused mainly by ionization and heating processes due to the particle precipitation, the ion temperature disturbances are influenced strongly by Joule heating of the ions due to the electric field/FAC disturbances in the polar ionosphere.

The thermospheric disturbances are generated mainly by the Joule heating (ion drag) and propagate to lower latitudes as traveling ionospheric disturbances (TID) and/or LS atmospheric gravity waves. Modeling and examination of large-scale FAC structure dynamics and ionospheric parameters variations over wide range of SW and IMF parameters allows a thorough understanding of the physics of Joule heating processes at high latitudes under various geomagnetic conditions.

References

[1] Nenovski, P., *Ann Geophysicae* **26**, 281 (2008).
[2] Weimer, D.R., *J. Geophys. Res.* **110**, 110 (2005).

Auroral Asymmetries in the Conjugate Hemispheres

N. Østgaard[1]

[1] *Department of Physics and Technology, University of Bergen, Allegt. 55, N-5007, Norway, Nikolai.Ostgaard@ift.uib.no*

Using simultaneous global imaging in the ultraviolet wavelengths by the IMAGE and Polar satellites we will show that the auroral intensities in the two hemispheres can be completely asymmetric. These observations are interpreted as a signature of inter-hemispheric currents.

Earlier studies have demonstrated that the asymmetries of substorm onset locations in the two hemispheres are controlled by the IMF clock angle. Using more than 6600 substorms identified by IMAGE-FUV and Polar UVI we will show how both the IMF clock angle and IMF By can be used to organize the substorm location, and how they give slightly different information.

Finally we will show results obtained from following similar features in the two hemispheres during expansion phase of two substorms. We find that the asymmetry induced by the IMF clock angle at substorm onset disappears during the expansion phase implying that magnetic field lines with asymmetric footpoints are rectified during expansion phase. Various mechanisms that can re-establish the symmetric aurora are discussed.

Acknowledgement to B. K. Humberset, H.U. Frey, J. Sigwarth, K. Liou, J. Weygand, A. Aasnes, L. Juusola, S. Haaland

Study of the Ionospheric Variations Using Two-Dimensional Maps of Total Electron Content Obtained from GPS Receiver Networks

Y. Otsuka[1], M. Nishioka[2], T. Tsugawa[3], and A. Saito[4]

[1] *STEL, Nagoya University, Nagoya, 464-8601, Japan, otuska@stelab.nagoya-u.ac.jp*
[2] *STEL, Nagoya University, Nagoya, 464-8601, Japan*
[3] *NICT, Tokyo, 184-8795, Japan*
[4] *Graduate School of Science, Kyoto University, Kyoto, 606-8502, Japan*

At mid-latitude ionosphere, traveling ionospheric disturbances (TIDs), which are wavy structures of the plasma density, have been observed by using various techniques such as ionosondes, HF Doppler sounders, satellite beacons, and incoherent scatter radars [*e.g., Hocke and Schlegel*, 1996]. Since *Hines* [1960], TIDs have been believed to be an ionospheric manifestation of atmospheric gravity waves probably caused by geomagnetic activity at high latitude and/or propagated from lower atmosphere. TIDs with horizontal wavelengths of 100-250 km are classified into Medium-Scale TIDs (MSTIDs) [*Hunsucker*, 1982].

Using densely spaced GPS receivers in Japan, Southern California, and Europe, we have investigated two-dimensional maps of total electron content (TEC) perturbations with high spatial and temporal resolutions to reveal the statistical characteristics of MSTIDs [*Kotake et al.*, 2007; *Otsuka et al.*, 2011]. We have found that MSTIDs can be categorized mainly into two groups: daytime and nighttime MSTIDs. Daytime MSTIDs frequently occur in winter and tend to propagate southward and southeastward. We speculate that daytime MSTIDs are caused by atmospheric gravity waves in the thermosphere. Occurrence rate of the nighttime MSTIDs depends on longitude. The nighttime MSTIDs frequently occur around June solstice in Japan and Southern California, and around December solstice in Europe. They propagate southwestward. This propagation direction supports the notion that polarization electric fields could play an important role in generating nighttime MSTIDs.

GPS-TEC data have also detected the ionospheric disturbances after the earthquakes. Especially, two-dimensional structures of the ionospheric disturbances following the 2011 off the Pacific coast of Tohoku Earthquake that occur at 05:46 UT on 11 March 2011 with a moment magnitude of 9.0 have been investigated by using the dense GPS network in Japan [e.g., *Tsugawa et al.*, 2011]. Approximately seven minutes after the earthquake onset, an initial ionospheric disturbance appeared as sudden depletions by 6 TECU following small impulsive TEC enhancements near the epicenter. Concentric waves were also observed to propagate at the velocity of 138–423m/s. In the vicinity of the epicenter, short-period oscillations with period of 4 minutes were observed after 06:00 UT for 3 hours or more.

References

[1] Hines, C. O., *Can. J. Phys.*, **38**, 1441 (1960).
[2] Hocke, K. and K. Schlegel, *Ann. Geophysicae*, **14**, 14,917 (1996).
[3] Hunsucker, R., *Rev. Geophys. Space Phys.*,**20**, 293 (1982).
[4] Kotake, N., Y. Otsuka, T. Tsugawa, T. Ogawa, and A. Saito, *Earth Planet Space*, **59**, 95 (2007).
[5] Otsuka, Y., N. Kotake, K. Shiokawa, T. Ogawa, T. Tsugawa, and A. Saito, *Aeronomy of the Earth's Atmosphere and Ionosphere, IAGA Special Sopron Book Series*, **2**, 3 (2011).
[6] Tsugawa, T., A. Saito, Y. Otsuka, M. Nishioka, and T. Maruyama, *Earth Planet Space*, submitted.

Global Simulations of Solar Wind – Magnetosphere Coupling

M. Palmroth[1], I. Honkonen[1,2], C. R. Anekallu[1,2], A. Sandroos[1], S. von Alfthan[1], H. E. J Koskinen[1,2], T. V. Laitinen[1], T. I. Pulkkinen[3]

[1] *Finnish Meteorological Institute, PO Box 503, Helsinki, FI-00101, Finland, minna.palmroth@fmi.fi*
[2] *University of Helsinki, Department of Physics, PO Box 64, 00014 University of Helsinki, Finland*
[3] *Aalto University, School of Electrical Engineering, POBox 13000, 00076 AALTO, Finland*

Space missions provide *in-situ* measurements from spatially limited volume, making plasma modelling a key component of modern space research. Our simulations have earlier provided new results that need to be verified using observations. On the other hand, present simulations have strong limitations, calling for new model development as well as intensive testing against observations. In this light, the simulations 1) inspire new observational analyses, and 2) the observations are used to test and verify the simulations, and 3) the improved simulations are used to learn new physics about the processes in the terrestrial space environment. These topics form the backbone of the modelling work at the Finnish Meteorological Institute (FMI), and here we review recent advances highlighting all three aspects.

The FMI's GUMICS-4 MHD simulation has been used to quantify energy transfer within the near-Earth space. We briefly review the corresponding methodology, and present results that both agree with earlier observational studies, but also suggest new phenomena that have not been reported before. GUMICS-4 results suggest a good general agreement with the epsilon parameter, but also a "hysteresis" effect, where energy transfer remains large even if the clock angle is turning away from the southward orientation. Such a hysteresis effect introduces discrepancies between the energy input proxies and the energy input measured from GUMICS-4 especially after strong driving, although otherwise the simulation energy input captures the system dynamics. For the cause of the effect, we propose a simple feedback mechanism based on magnetic flux accumulation in the tail lobes. Furthermore, we review recent validation work on the spatial variation of energy transfer at the magnetopause surface using Cluster measurements.

Global MHD simulations have been successful in describing systems where the important spatial scales are larger than ion gyro radii and the plasma has a well-defined temperature. The weakness of global MHD simulations is their inability to model the multi-temperature, multi-component plasmas in the inner magnetosphere, where most of space-borne technology, including communication and navigation systems reside. Two possibilities exist to overcome the problem: 1) To couple the MHD simulation to a code modelling the inner magnetosphere, or 2) to develop a self-consistent global simulation based on another plasma description. We are developing a global Vlasov-hybrid simulation, where electrons are MHD fluid, but protons are modelled as distribution functions evolved in time using the Vlasov equation. This approach does not include the noise present in kinetic-hybrid simulations, but is computationally extremely challenging requiring petascale computations with thousands of cores. For instance, instead of the normal 3-dimensional approach, the hybrid-Vlasov simulation is 6-dimensional including a velocity space inside every cell of ordinary space. Here, we review our new simulation, which is using a massively parallel grid infrastructure and is solving the coupled proton-electron plasma in six dimensions. We compare the Vlasov simulation results with those from the GUMICS-4 global MHD simulation.

Magnetospheric Feedback in Solar Wind Energy Transfer

M. Palmroth[1], H. E. J Koskinen[1,2], T. I. Pulkkinen[3]

[1] *Finnish Meteorological Institute, PO Box 503, Helsinki, FI-00101, Finland, minna.palmroth@fmi.fi*
[2] *University of Helsinki, Department of Physics, PO Box 64, 00014 University of Helsinki, Finland*
[3] *Aalto University, School of Electrical Engineering, POBox 13000, 00076 AALTO, Finland*

The solar wind kinetic energy fueling all dynamical processes within the near-Earth space is extracted in a dynamo process at the magnetopause. This direct energy transfer from the solar wind into the magnetosphere depends on the orientation of the interplanetary magnetic field (IMF) as well as other solar wind parameters, such as the IMF magnitude and solar wind velocity. Using the GUMICS-4 magnetohydrodynamic (MHD) simulation, we find that the energy input from the solar wind into the magnetosphere depends on this direct driving as well as the magnetopause magnetic properties and their time history in such a way that the energy transfer can continue even after the direct driving conditions turned unfavorable. Such a hysteresis effect introduces discrepancies between the energy input proxies and the energy input measured from GUMICS-4 especially after strong driving, although otherwise the simulation energy input captures the system dynamics. For the cause of the effect, we propose a simple feedback mechanism based on magnetic flux accumulation in the tail lobes: By ideal MHD theory, the energy conversion at the magnetopause is proportional to the product of normal and tangential magnetic fields, the magnetic stress. During large magnetic flux accumulation, the tangential field at the magnetopause strengthens, enhancing the local instantaneous energy conversion and transfer. Our simulations show that this mechanism supports the energy transfer even under weak driving followed by favorable solar wind conditions, and transfer up to 50% more power than without the feedback.

Spatial Dependence of Magnetopause Energy Transfer: Cluster Measurements Verifying Global Simulations

M. Palmroth[1], T. V. Laitinen[1], C. R. Anekallu[1], T. I. Pulkkinen[2], M. Dunlop[3], E. A. Lucek[4], and I. Dandouras[5]

[1] *Finnish Meteorological Institute, PO Box 503, Helsinki, FI-00101, Finland, minna.palmroth@fmi.fi*
[2] *Aalto University, School of Electrical Engineering, POBox 13000, 00076 AALTO, Finland*
[3] *Rutherford Appleton Laboratory, Chilton, Didcot, UK*
[4] *Imperial College, London, UK*
[5] *IRAP, CNRS, Université de Toulouse, Toulouse, France*

We investigate the spatial variation of magnetopause energy conversion and transfer using Cluster spacecraft observations of two magnetopause crossing events as well as using a global magnetohydrodynamic (MHD) simulation GUMICS-4. These two events, (Jan 16, 2001, and Jan 26, 2001) are similar in all other aspects except for the sign of the interplanetary magnetic field (IMF) y component that has earlier been found to control the spatial dependence of energy transfer. In simulations of the two events using observed solar wind parameters as input, we find that the GUMICS-4 energy transfer agrees with the Cluster observations spatially and is about 30% lower in magnitude. According to the simulation, most of the energy transfer takes place in the plane of the IMF (as previous modelling results have suggested), and the locations of the load and generator regions on the magnetopause are controlled by the IMF orientation. Assuming that the model results are as well in accordance with the *in situ* observations also on other parts of the magnetopause, we are able to pin down the total energy transfer during the two Cluster magnetopause crossings. Here, we estimate that the instantaneous total power transferring through the magnetopause during the two events is at least 1500-2000 GW, agreeing with epsilon scaled using the mean magnetopause area in the simulation. Hence the combination of the simulation results and the Cluster observations indicate that the epsilon parameter is probably underestimated by a factor of 2-3.

A Comparison of the Response of the Near-Earth Magnetosphere to CME-and CIR-driven Storms

V. Peroomian[1], M. El-Alaoui[1]

[1] *UCLA-IGPP, Box 951567, Los Angeles, CA 90095-1567, USA, vahe@igpp.ucla.edu*

The acceleration of ions of ionospheric and solar wind origin in the near-Earth magnetotail during geomagnetic storms is investigated. We examine storms caused by the impact of a coronal mass ejections (CME) and by corotating interaction regions (CIRs) and high-speed streams (HSS). For each of the storms studied, we run a global magnetohydrodynamic (MHD) simulation of the event using upstream solar wind and IMF data. We then launch ions originating from the solar wind and from the ionosphere in the global, time-dependent electric and magnetic fields obtained from the MHD simulation of the event. We have investigated three CME-driven storms, occurring on 24 September 1998, 17 April 2002, and 28 October 2001, and one CIR/HSS event, the 8 – 9 March 2008 storm.

The acceleration of ions in the near-Earth plasma sheet and ring current during the sudden storm commencement (SSC) during CME-driven storms to the acceleration of ions during the more slowly evolving CIR-driven storms is then examined in detail, including the effect of various solar wind drivers on ion velocity distribution functions computed throughout the near-Earth tail during each event. The trapping of ions during storm commencement is also investigated for both ionospheric oxygen ions and solar wind protons. Where possible, our simulation results are compared with observations.

Variations of the Relativistic Electron Fluxes at L = 3.0-6.6 as Observed by CORONAS-F Satellite

N. V. Romanova[1], I. N. Myagkova [2], V. A. Pilipenko [3]

[1]*Institute of the Physics of the Earth RAS (IPE RAS), 10 B. Gruzinskaya Str., Moscow, 123995, Russian Federation, runatka@mail.ru*

[2] *Lomonosov Moscow State University Skobeltsyn Institute of Nuclear Physics (MSU SINP), 1(2) Leninskie gory, GSP-1, Moscow, 119991, Russian Federation*

[3] *Space Research Institute (IKI), , 84/32 Profsoyuznaya Str., Moscow, 117997, Russian Federation*

We consider the events in 2002 with the relativistic electron flux increases at different L-shells for various space weather conditions. We use the 1.5-3 MeV electron detector data from the low-orbiting CORONAS-F satellite and 1.1-1.5 MeV electron data from the geosynchronous LANL monitor. We have compared a relativistic electron response to the high-speed solar wind streams (HSS) from coronal holes and to the coronal mass ejections (CME). The electron behavior has turned out to be essentially different at L = 3-4 and at L > 4; an increase of electron fluxes at low L-shells is not synchronous with the increase at higher L. During CME-related storms the electron fluxes increase simultaneously at all L up to L = 4, whereas during the HSS-related storms the flux increases proceed from higher L to lower L. We have estimated statistically the electron response to the magnetospheric ULF activity as characterized by ULF-index. For HSS events the ULF activity contribution in the electron energization at L > 4 is higher than for CME events. The ULF driven electron energization at L = 4-5.5 for HSS events is slower than for CME events. At L = 5.5-6.6 the growth rate is about the same, ~2 days, for both types of events. We suppose that for HSS events the ULF driven radial diffusion and energization dominate at L > 4. For CME events the local acceleration mechanisms become more significant.

Knotty Magnetic Fields - MHD Invariants and their Violation

I. Roth

Space Sciences Laboratory, University of California, Berkeley, CA 94720 , ilan@ssl.berkeley.edu

Magnetized plasma exhibit a variety of characteristic features: over most of the large scale domain its evolution may be described satisfactorily by the MHD approximation, allowing bending and stretching, but not cutting of the magnetic field lines, while over smaller dimensions energy may cascade between adjacent scales or transferred to plasma via resonant processes or reconnection. Magnetic flux ropes which occur in various heliospheric locations, like solar prominences, coronal mass ejections and potentially in any magnetized configuration exhibit various topological structures, classified with the help of invariants which are preserved through the dynamical evolution of the magnetized plasma. Hence, general question of MHD classification via its invariants and the possible deviation from MHD description extending to the smaller ion or electron skin-depth scale in the reconnection configuration is of major importance. New method of classification of magnetized plasma is offered through the similarity between the MHD description and the various invariants encountered in the knot theory. Since the essence of knot theory analysis is based on the topological structure of continuous string penetrating a three dimensional domain (manifold), a closed loop of a non-self-intersecting curve, the classification of a knot is based on the crossing between two adjacent string segments as observed on planar projection. Each crossing can then be assigned an arithmetic value while the consistency for the whole knot results in one-to-one correspondence between each knot (topological entity) and its characteristic polynomial (mathematical entity). These polynomials (Alexander, Jones, bracket etc) constitute the knot invariants. Two knots with different polynomial signify different topological structures without a possibility to transform from one to another through the three basic topology-preserving knot (Reidemeister) moves. Figure 1 shows an example of two knots with identical structure: an un-knot and trefoil, differing only in crossing topology, resulting in different invariants. MHD turbulence forms then a collection of non-intersecting, entangled field lines whose evolution is determined via continuous deformation in R^3, following laws of MHD and/or knot topology – smooth changes in the surrounding viscous fluid, allowing only stretching or bending. The MHD invariants are embedded into the knot moves which preserve and characterize the topology of the magnetic field. For instance, magnetic helicity satisfies the knot moves. The similarity between MHD and knot theories allows one to distinguish between various magnetic configurations on topological grounds. Extension of knot theory through the connected sum of oriented knots forms a non-commutative semi-group which reconnects two separate knots and allows us to analyze over a small, electron skin-depth scale the violation of the frozen-in condition for electrons by replacing the magnetic field (electron gyro-frequency) into a generalized electron vorticity.

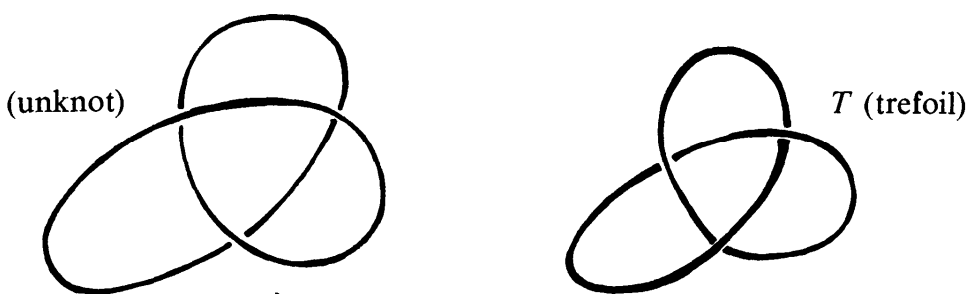

Figure1. Diagram of planar projection of an Unknot (equivalent to a circle) and Trefoil knot. Line segment with a small gap indicates that it threads behind the continuous line (underpass). Simple stretching and bending deforms the Unknot into a circle (loop), while it cannot be done for the Trefoil.

Quantitative Multi-Spacecraft Observation of Magnetic Cloud Erosion by Magnetic Reconnection during Propagation

A. Ruffenach[1], B. Lavraud[1], M. J. Owens[2], J.-A. Sauvaud[1], N. Savani[3], A. P. Rouillard[4], A.Opitz[1], A. Fedorov[1], J. G. Luhmann[5], C. T. Russell[6], and A.B. Galvin[7]

[1] *IRAP/CNRS/Université de Toulouse, France*
[2] *University of Reading, UK*
[3] *STELAB, Nagoya, Japan*
[4] *NRL, Maryland, USA*
[5] *SSL, Berkeley, USA*
[6] *UCLA, Los Anageles, USA*
[7] *UNH, Durham, USA*

Magnetic clouds, a subset of interplanetary coronal mass ejections, are characterized by a twisted magnetic flux rope topology. During propagation, the structure interacts with its environment and may thus at least partially reconnect, potentially eroding away part of the original magnetic cloud flux impinging on Earth. In the present study, we quantitatively analyze the complex interaction that occurred between a magnetic cloud (MC), the solar wind ahead of it, and a trailing high-speed stream observed by STEREO A, B and ACE. We first determine the orientation of the flux rope using different methods at the different spacecraft. We then estimate the amount of eroded magnetic flux, and associated errors, based on the observation of azimuthal flux imbalance during the spacecraft sampling of the flux rope. We show that small deviations in cloud axis determinations have an appreciable impact on the estimated eroded flux. However, the use of various methods for errors analyses, combined with other signatures observed in the data (e.g., at the front and rear of the magnetic cloud) permit to demonstrate the occurrence of erosion with confidence. Interestingly, significant erosion occurs despite the CME being slow. By removing substantial amounts of the MC magnetic flux, such erosion has direct and important consequences for CME geoeffectiveness.

Lunar Plasma Observation by MAP-PACE on Kaguya

Y. Saito[1], S. Yokota[2], M. N. Nishino[2], T. Yamamoto[2], K. Uemura[2], H. Tsunakawa[3] and Kaguya MAP-PACE Team

[1] *Institute of Space and Astronautical Science / Japan Aerospace Exploration Agency, 3-1-1 Yoshinodai, Chuo, Sagamihara, Kanagawa 252-5210, Japan, saito@stp.isas.jaxa.jp*
[2] *ISAS/JAXA, 3-1-1 Yoshinodai, Chuo, Sagamihara, Kanagawa 252-5210, Japan*
[3] *Tokyo Institute of Technology, 2-12-1 Ookayama, Meguro-ku, Tokyo, 152-8551, Japan*

Interaction between the solar wind and a solar system object varies largely according to the object's properties, such as the existence of a global intrinsic magnetic field and / or thick atmosphere. The Moon's case is characterized by the absence of both of them. Different from the Earth's case where the intrinsic global magnetic field prevents the solar wind from penetrating into the magnetosphere, solar wind directly impacts the lunar surface. On the other hand, plasmas originating from the Moon surface / exosphere can reach the Moon orbiting spacecraft. The hot plasma-sheet plasmas in the Earth's magnetosphere can also directly impact the lunar surface when the Moon stays in the Earth's magnetosphere for 3 - 4 days every month. Magnetic field and Plasma experiment - Plasma energy Angle and Composition Experiment (MAP-PACE) on Kaguya (SELENE) measured lunar plasmas in a polar orbit with altitude of 100km, 50km, and in an elliptical orbit with perilune altitude as low as 10km for nearly 1.5 years [1].

In the solar wind, one of the four MAP-PACE sensors IMA (anti-moon looking ion energy mass spectrometer) found four clearly distinguishable ion populations on the dayside of the Moon. 1) Solar wind protons backscattered at the lunar surface, 2) solar wind protons reflected by magnetic anomalies on the lunar surface, 3) reflected / backscattered protons picked-up by the solar wind, and 4) ions originating from the lunar surface / lunar exosphere. Using low altitude data, MAP-PACE also revealed the plasma structure over lunar magnetic anomalies on the dayside of the Moon.

Although the plasma density in the Earth's magnetosphere around the Moon orbit (at about 60Re) was quite tenuous, MAP-PACE sensors succeeded in measuring characteristic ion / electron distributions in the Earth's magnetosphere including lobe cold ions, fast flowing ions associated with plasmoids, and cold ion acceleration in the plasma sheet / lobe boundaries. According to MAP-PACE observations, several characteristic phenomena caused by the interaction between Earth's magnetosphere and the lunar surface were so far found: 1) Ions originating from the Moon surface / exosphere [2], 2) Gyro-loss effect of electrons in the lobe / plasma sheet [3], and 3) Plasmoid / plasma sheet signature that is different on the day-side and night-side of the Moon. The ions originating from the Moon surface / exosphere were observed both in the solar wind and in the Earth's magnetosphere. The mass profile of these ions shows heavy-ion peaks including C^+, O^+, Na^+, K^+, and Ar^+ that indicates that these ions are the Moon origin. In the Earth's magnetosphere, these ions were clearly observed on the dayside of the Moon in the lobe especially when the solar zenith angle was below 40deg. Since the convection electric field in the lobe region is much weaker than in the solar wind, the ions originating from the Moon surface / exosphere are possibly accelerated by the potential difference between the lunar surface and Kaguya. These ions often show characteristic variation of the flux and energy that presumably correlates with the lunar surface structure or composition. If these ions are accelerated by the potential difference between the lunar surface and Kaguya, the energy variation reflects the surface potential distribution on the lunar surface. In the Earth's magnetotail, Kaguya encountered the plasmoid / plasma sheet many times. The encounter was characterized by the transition between the lobe cold ions, cold ion acceleration in the plasma sheet / lobe boundaries, and hot plasma sheet ions or fast flowing ions associated with plasmoids. Different from the previous measurements made in the magnetotail, the ions were affected by the existence of the Moon. On the dayside of the Moon, tailward flowing cold ions and their acceleration were observed (as usual in the magnetotail). However, on the night side, tailward flowing cold ions could not be observed since the Moon blocked them. In stead, ion acceleration by the spacecraft potential and the electron beam accelerated by the potential difference between lunar surface and spacecraft were simultaneously observed. These data enabled us to determine the night side lunar surface potential and spacecraft potential from the observed data for the first time.

The plasmas around the Moon are gradually unveiling their characteristics. The newly obtained knowledge about the lunar plasma environment by Kaguya must contribute to the understanding of the plasma environment around non-magnetized solar system objects.

References

[1] Y. Saito, S. Yokota, K. Asamura, T. Tanaka, M. N. Nishino, T. Yamamoto, Y. Terakawa, M. Fujimoto, H. Hasegawa, H. Hayakawa, M. Hirahara, M. Hoshino, S. Machida, T. Mukai, T. Nagai, T. Nagatsuma, T. Nakagawa, M. Nakamura, K. Oyama, E. Sagawa, S. Sasaki, K. Seki, I. Shinohara, T. Terasawa, H. Tsunakawa, H. Shibuya, M. Matsushima, H. Shimizu, F. Takahashi, *Space Sci. Rev.*, 154, 1-4, 265-303 (2010)

[2] T. Tanaka, Y. Saito, S. Yokota, K. Asamura, M. N. Nishino, H. Tsunakawa, H. Shibuya, M. Matsushima, H. Shimizu, F. Takahashi, M. Fujimoto, T. Mukai, T. Terasawa, *Geophys. Res. Lett.*, *36*, L22106 (2009).

[3] Y. Harada, S. Machida, Y. Saito, S. Yokota, K. Asamura, M. N. Nishino, T. Tanaka, H. Tsunakawa, H. Shibuya, F. Takahashi, M. Matsushima, H. Shimizu, *Geophys. Res. Lett.,* 37, L19202 (2010).

Plasma-Wave Analysis Methods for Future Space Missions

O. Santolik[1,2]

[1] *Institute of Atmospheric Physics, Academy of Sciences of the Czech Republic, Bocni II/1401, 14131 Praha 4, Czech Republic, Phone: +420267103081, E-mail: os@ufa.cas.cz*

[2] *Charles University, Faculty of Mathematics and Physics, V Holesovickach 2, 18000 Praha 8, Czech Republic*

Future spacecraft missions (for example RBSP, Resonance, Solar Orbiter and Laplace) will carry comprehensive instrumentation to measure fluctuations electric and magnetic fields and waves in space plasmas. Whistler-mode chorus is a relevant example of the target of these measurements. Chorus has been shown to play a significant role in acceleration of relativistic electron in the outer Van Allen belt. It can also propagate from its source region and influence large regions of the inner magnetosphere. Distribution of the wave energy density in the space of the wave vector directions is a crucial parameter for modeling of both the wave-particle interactions and wave propagation in the inner magnetosphere. We present examples of observations of whistler-mode chorus emissions by the Plasma Wave Instrument on the Polar spacecraft in 1996 and 1997 together with a large data set obtained by the STAFF-SA instruments onboard the CLUSTER spacecraft. We show how these data can be used to design onboard analysis methods for future space missions.

Step by Step Model of Magnetospheric VLF Response to Atmospheric Infrasonic Waves

O. N. Savina [1], P. A. Bespalov[2]

[1] *State Technical University, 24 Minina St, Nizhny Novgorod, 603600, Russia, ONSavina@mail.ru*
[2] *Institute of Applied Physics, Russian Academy of Sciences, 46 Ulyanov St, Nizhny Novgorod, 603950, Russia, PBespalov@mail.ru*

In this paper we consider a model of the influence of atmospheric infrasonic waves on VLF whistler waves excitation in the magnetosthere. This influence occurs as a result of a succession of processes: a modulation of the plasma density in the ionosphere by acoustic-gravity waves, a variation of whistlers reflection from the ionosphere modulation, and a modification of whistler waves excitation conditions in the magnetospheric resonator. Variation of a magnetospheric resonator Q-factor has an influence on the operation of the plasma magnetospheric maser, where the active substances are radiation belts particles and the working modes are electromagnetic whistler waves. The magnetospheric resonator, which is an oscillatory system, can be responsible for an excitation of self-oscillations. These self-oscillations are frequently characterized by alternating stages of accumulation and precipitation of energetic particles into the radiation belts during a pulse of whistler emissions. Numerical and analytical investigations of the response of self-oscillations to harmonic oscillations of the whistler reflection coefficient shows that even a small modulation can significantly changes the magnetospheric VLF emissions. Our results can explain the reason of energetic electron fluxes and whistler wave intensity modulation with a time scale from 10 to 150 sec in the day-side magnetosphere. Such quasi-periodic VLF emissions are often observed in the sub-auroral and auroral magnetosphere and they have a noticeable effect on the space weather phenomena.

References

[1] P.A Bespalov, V.G. Mizonova and O.N. Savina, *Advances in Space Res.*, **31**, 1235–1240 (2003).
[2] P.A Bespalov and O.N. Savina, *Earth Planets Space*, **62**, (2011, *in press*).

Historical and Conceptual Foundations of Magnetospheric Physics

M. Schulz[1]

[1]*Lockheed Martin Retiree, 1037 Twin Oaks Court, Redwood City, CA 94061 (U.S.A.)*

This talk offers a historical overview of magnetospheric physics from its inception to the present time, with emphasis on underlying dynamical principles. Topics covered include the anticipation and discovery of the magnetosphere, geomagnetic storms and the aurora, Earth's plasma sheet and ring current, Earth's radiation belts, early misconceptions and their resolution, adiabatic invariants of charged-particle motion and their relationship to action-angle variables in classical mechanics, magnetic drift shells, source populations for ring-current and radiation-belt particles, magnetospheric electric fields, loss processes (e.g., atmospheric drag, atmospheric scattering, synchrotron emission, and wave-particle interactions), weak and strong pitch-angle diffusion, consequent limits on stably trapped particle fluxes and their energy spectra, mechanisms for diffusive radial transport and consequent particle energization in the magnetosphere, canonical and practical coordinates for transport theory, *in situ* particle energization, discovery of the plasmasphere and its evolution, and recent developments in the understanding of various magnetospheric processes.

Magnetosheath Coordinates

M. Schulz[1] and M. W. Chen[2]

[1]*Lockheed Martin Retiree, 1037 Twin Oaks Court, Redwood City, CA 94061 (U.S.A.)*
[2]*Space Science Applications Laboratory, The Aerospace Corporation, Los Angeles, CA 90009 (U.S.A.)*

The eventual goal of this work is to develop an approximate analytical representation of solar-wind streamlines in the magnetosheath surrounding a magnetosphere of rather general shape. Previous analytical representations of magnetosheath streamlines and magnetic fields have invoked magnetopause shapes that conform to standard coordinate systems (e.g., spherical, cylindrical, paraboloidal, ellipsoidal), but it seems now that such a restriction on magnetopause shape is unnecessary. In the present work it is assumed only that the magnetopause is a continuously differentiable convex surface axisymmetric about the Sun-Earth line. This geometry permits the construction of an orthogonal coordinate system ((μ, η, χ) such that η is the cosine of the cone angle between the Sun-Earth line and any conical surface extending normally outward from the magnetopause, μ is a measure of the perpendicular distance of any magnetosheath point from the magnetopause, and χ is an azimuthal coordinate measured around the Sun-Earth line. It is convenient here to assign a label $\mu = \mu^*$ to the magnetopause itself, so that $\mu - \mu^*$ denotes perpendicular distance from the magnetopause and μ^* is an adjustable parameter roughly comparable to the radius of the magnetotail. This choice provides for a rough correspondence between the (μ, η, χ) coordinates introduced here and the ellipsoidal coordinates used in our previous efforts at magnetosheath modeling.

Radiation Environment in Low-Earth Orbit According the Data from Experimental Measurements on ISS

J. Semkova[1], R. Koleva[1], St. Maltchev[1], N. Bankov[1], V. Benghin[2], I. Chernykh[2], V. Shurshakov[2], V. Petrov[2], S. Drobyshev[2]

[1] *Space and Solar-Terrestrial Research Institute, Bulgarian Academy of Sciences, Block 3, Acad. G. Bonchev str., 1113 Sofia, Bulgaria, jsemkova@stil.bas.bg*

[2] *Institute of Biomedical Problems, Russian Academy of Sciences, Moscow, Russia, benghin@pike.net.ru*

The radiation environment in a low-Earth orbiting (LEO) spacecraft like the International Space Station (ISS) is complex, composed by galactic cosmic rays, trapped radiation of the Earth radiation belts, albedo particles from Earth's atmosphere and the secondary radiation produced in the shielding materials of the spacecraft and in human body. Solar Particle Events also contribute transient increases to the radiation environment.

The Liulin-5 charged particle telescope has directly observed the radiation environment in the human phantom of MATROSHKA-R international project on ISS during the period June 2007-June 2010. The objectives of Liulin-5 experiment are studying the dynamics of dose distribution in a human phantom and mapping the radiation environment and its variations with time and orbital parameters (such as solar cycle, solar flare events, attitude and altitude). The particle telescope Liulin-5 measures time resolved linear energy transfer spectrum, flux and absorbed dose rates for electrons, protons and the biologically relevant heavy ion components of the cosmic radiation.

In this report we present results of Liulin-5 experiment for radiation quantities obtained from the different components of the radiation field in low-Earth orbit at the minimum of the 23-th solar cycle and comparison with data from other radiation detectors on ISS.

The Liulin-5 experiment will be continued in 2012-2015 to provide data for the radiation environment onboard ISS during solar activity maximum.

Magnetosphere-Ionosphere Coupling during Substorm Plasma Injections into the Inner Magnetosphere

V. A. Sergeev

[1] *St.Petersburg State University, Ulyanovskaya 1, St.Petersburg 198504, Russia, victor@geo.phys.spbu.ru*

We summarize some recent results pertaining to substorm-related plasma injections into the inner magnetosphere, and discuss three aspects which are essential to understand the injection process as well as the MI-coupling involved.

1/. Recent studies confirmed important role of depleted plasma tube entropy in the Earthward transport of the fast flow bursts (plasma bubbles). Particularly, the plasma tube entropy seem to control the penetration depth of individual BBF and its ability to reach the geosynchronous region. This also implies an important role of MI coupling in the bubble evolution.

2/. Testing a new quantitative model to describe both ionospheric and magnetospheric effects of the Substorm Current Wedge indicates its overall agreement with observations, but also shows substantial and systematic deviations of magnetospheric spacecraft observations from predictions of simple SCW contour, which particularly depend on the amount of magnetotail stretching and on the substorm time.

3/. Inspite of >40 years of auroral substorm research, the auroral manifestations of plasma injection process have been overlooked in past studies, and this now presents an attractive source of information about the penetration depth of injections and on the nature of turbulent structure in the injection body.

Photocurrent Influences on the Onboard Plasma Measurements

R. Shkevov, S. Chapkunov

Space and Solar-Terrestrial Research Institute - Bulgarian Academy of Sciences,
6 Moskovska Str., Sofia 1000, Bulgaria, e-mail: shkevov@space.bas.bg

Data received from space instruments onboard "Intercosmos Bulgaria - 1300" was processed. The main aim was to find a phenomenon like changes in measured space plasma parameters generated from the photocurrent effect. The data from the cylindrical Langmuir probe (CLP) was analyzed. The estimation of the current generated from electron photoemission from the surface of the cylindrical Langmuir probe and the booms, talking in account materials electron work function was done. The influence of the photocurrent in the registered data of the electron and ion densities and body potential in case of the obvious absence of the photoemission from the surface of the probe was discussed. Conclusion about photocurrent contribution to the measurement of the electron and ion densities and satellite body potential onboard "IKB-1300" was done.

Work plot from the future paper:

The part of data discovered on the routine processing of the CLP data, received from "Intercosmos Bulgaria - 1300" allows to made an estimation of the photocurrent influence on the onboard plasma measurements. Fig.1 shows the changes in electron density measurement in absence of photocurrent.

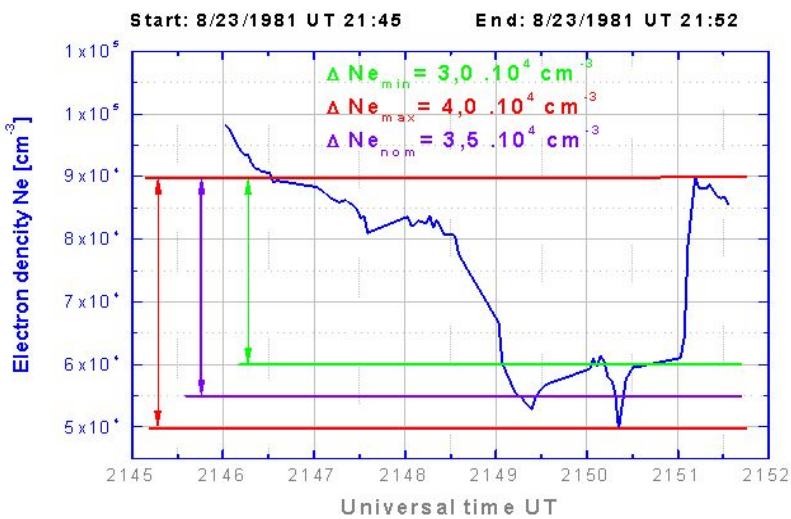

Fig.1. Changes in n_e when CLP goes in shadow.

References

[1] http://solarscience.msfc.nasa.gov/
[2] http://www.ngdc.noaa.gov/stp/solar/
[3] http://rredc.nrel.gov/solar/spectra/am0
[4] http://www.acrim.com/
[5] http://lasp.colorado.edu/sorce/data/tsi_coverage.html
[6] Gdalevich G. L., N. Bankov, St. Chapkunov, L. Todorieva, R. Shkevov, Volt-ampere characteristics of a cylindrical probe in the ionosphere plasma irregularities regions. Aerospace Research in Bulgaria, V. 20, pp. 32-37.
[7] Chapkunov S., Bankov N., Shkevov R., "Photocurrent effect influence investigation onboard "IKB-1300" satellite" - 10th Management Committee Meeting and Scientific Event COST 724 Action - Developing the basis for monitoring, modelling and predicting Space Weather, Sofia, 21- 25 May 2007. Link: http://www.stil.bas.bg/COST_BG/
[8] T.N. Ivanova, T.D. Samardjiev, S.M. Halova, P.T. Kostov, G.S. Karamishev, I.S. Kutiev, G.L. Gdalevich. Spherical Ion Trap for "Intercosmos-Bulgaria-1300" Adv. Space Res. V.2, 7, 21. (1983)
[9] V. De Renzi, R. Rousseau, D. Marchetto, R. Biagi, S. Scandolo, and U. del Pennino, Pysical Review Letters, PRL 95, 046804, (2005)

Cycles of the Solar Wind Flux at the Front of the Earth's Magnetosphere

Y. Shopov, D. Stoykova

University Center for Space Research and Technologies,
Faculty of Physics, University of Sofia, J. Bourchier 5, Sofia 1164, Bulgaria, YYSopov@phys.uni-sofia.bg

We studied various long solar wind proxy records in order to reveal prolonged solar wind cycles. Inverted rate of atmospheric ^{14}C production as derived from the standard radiocarbon calibration curve represents good proxy record of the past variations of the solar wind flux at the upper atmosphere because it modulates the galactic cosmic rays flux, which produces the radiocarbon there. We made periodogramme time series analysis of the inverted rate of atmospheric ^{14}C production record in order to obtain the solar wind cycles. This way we found cycles of 11 500, 1670, 1280, 835, 750 and 610 yrs in this solar wind proxy record.

Records of the intensity of the geomagnetic dipole are also proxy records of variations of the solar wind flux, because it modulates the geomagnetic field. We made periodogramme time series analysis of the one long record of the intensity of the geomagnetic dipole in order to obtain the solar wind cycles. This way we found cycles of 11 500, 4400, 3950, 2770, 2500, 2090, 1960, 1670, 1460, 1280, 1195, 1145, 1034, 935 and 835 yrs in this solar wind proxy record. We have confirmed the solar origin of all this cycles by their detection in an independent solar luminosity proxy record.

The 11 500-yr cycle was found previously to be the most intensive cycle in the ^{14}C calibration record and was interpreted to be of geomagnetic origin. Our recent studies suggest that this is a solar cycle modulating the geomagnetic field. We determined the solar origin of cycles with durations of 11 500, 4400, 3950, 2770, 2500, 2090, 1960, 1670, 1460, 1280, 1195, 1145, 1034, 935, 835, 750 and 610 yrs. This was achieved by their detection in proxy records of solar luminosity, atmospheric ^{14}C production and the intensity of the geomagnetic dipole. The main variations in the last two records are known to be produced by the solar wind while the first record is absolutely independent on the geomagnetic field, so non of this cycles can be of terrestrial origin.

The main variations in the ^{14}C and geomagnetic field records are produced by the solar wind. Known decadal and even centennial solar cycles have negligible intensity (100 times less intensive) relative to these cycles. These millennial solar luminosity cycles can produce climatic variations with intensity comparable to that of the orbital variations known to produce the glacial periods on Earth.

We discovered a sub-annual cycle of 27 days in very high-resolution soil surface temperature proxy records, attributed to solar rotation, which causes the periodic appearance of active zones on the visible solar surface, which are the major emitters of solar wind. Solar wind modulates cosmic ray flux at the Earth, while cosmic rays influence the atmospheric transparency, thus producing a multiplication of solar variations in insolation. These way small variations of the solar activity can produce a measurable influence on insolation.

Modeling Dynamical Evolution of the Earth's Radiation Belts

Y. Y. Shprits[1,2], D. Subbotin[2], K.C Kim[1], B. Ni[2]

[1] *IGPP, UCLA, 3845 Slichter Hall, Los Angeles, CA, USA, 90095 yshprits@atmos.ucla.edu*

[2] *DAOS, UCLA, MS7121, Los Angeles, CA, USA, 90095*

We present simulations of the inner and outer radiation belts using the Versatile Electron Radiation Belt (VERB) accounting for radial, pitch-angle, energy, and mixed diffusion. Qusi-linear diffusion coefficients are computed using the Full Diffusion Code (FDC) due to day-side and night-side chorus waves, magneto-sonic waves, phasmaspheric hiss waves, EMIC and hiss waves in the regions of plumes, lightning generated whistlers, and anthropogenic whistlers. Sensitivity simulations show that the knowledge of wave spectral properties and spatial distribution of waves is crucially important for reproducing long term observations. The 3D VERB code simulations are compared to 3D reanalysis of the radiation belt fluxes that are obtained by blending the predictive model with observations from GEO, CRRES, Akebono, GPS and LANL. Simulations of extreme superstorms indicate that very strong storms may result in the increase of electron fluxes in the inner belt which may be truly devastating for the Earth orbiting spacecraft.

Observations of Energetic Protons and Neutral Atoms (ENA) at Low Altitudes during Geomagnetic Storms

F. Søraas[1] and M. Sørbø[1,2]

[1] *Department of physics and technology,University of Bergen, Allegaten 55, Bergen, 5007, Norway, finn.soraas@ift.uib.no*

[2]*Bergen Oilfield Services, Norway*

Satellite observations of Energetic Neutral Atoms (ENA), with an instrument not dedicated to ENA observations, are possible in the polar cap where the magnetic field lines normally are not populated with energetic particles and in the equatorial regions by a satellite below the intense trapped radiation

ENA in the Earth's magnetosphere are produced via charge exchange mechanism between singly charged ions and neutral atoms in the exosphere. The produced neutrals leave the interaction region with essentially the same energy and velocity as the originally ions, and are unaffected by ambient electric and magnetic fields.

ENA emission is markedly brightest at the lowest altitudes, in the auroral zone, because the density of the ambient neutrals strongly increases with decreasing height. These ENAs produced by the proton aurora are spread in all directions and some move away from the Earth and are lost into space.

During geomagnetic storms a Storm Time Equatorial Belt (STEB) of Energetic Neutral Atoms (ENA) and ions is found to exist at low altitudes around the geomagnetic equator. Their source is the ring current protons existing at larger L-values. . Ring Current asymmetry and symmetry inferred from the STEB are largely in accordance with results from ground based magnetic observations. The STEB appears first in the midnight/evening sector and then later in the morning sector largely consistent with the drift of the RC ions. Maximum particle injection into the ring current is associated with the rapid fall in Dst and the maximum production of ENA is associated with minimum Dst.

Low altitude observations of proton precipitation and ENA in the equatorial and polar regions will be presented.

Multivariate Probability Model for Ground Detection of Cosmic Rays

A. G. Tchorbadjieff[1]

[1] *Institute for Nuclear Research and Nuclear Energy 72 Tzarigradsko chaussee, blvd, Sofia, 1784, Bulgaria, assen@inrne.bas.bg*

Basic Environmental Observatory in Moussala is complex research complex. It proceeds a complex aero-terrestrial monitoring. The uninterrupted observation of secondary cosmic rays and atmosphere particle physics produces large volumes of raw data. For analysis, it was modeled a basic probabilistic multivariate model for data calibration of SEVAN space weather detector. The model tries to estimate atmosphere process influences on barometric and temperature calibration coefficients. The results must enable automatic smoothing of real time ground detected space weather data.

References

[1] A.Chilingarian, …, New Particle Detector Network for Solar Physics and Space Weather Research *31st ICRC, LODZ 2009*

[2] Peter J. Brockwell, Richard A. Davis, Introduction to Time Series and Forecasting, Springer-Verlag, 2002

[3] John.H.Seinfeld, Spiros N.Pandis, Atmosphere Chemistry and Physics – 2nd ed., John Wiley&Sons, Inc 2006

Thermosphere Response to CIR/HSS Events

J. P. Thayer, J. Lei, X. Lui

University of Colorado, Aerospace Engineering Sciences Department, UCB 429, Boulder, CO, 80309, USA, jeffrey.thayer@colorado.edu , jiuhou.lei@colorado.edu, xianjing.lui@colorado.edu

That the smallest of interactions in the form of ion-neutral collisions in the polar thermosphere can impact the largest of scales in upper atmosphere response is a testament to the primary importance of the Joule heating rate as an energy source for the upper atmosphere. Yet, our understanding/quantification of this primary energy source is woefully represented by numerical models and poorly sampled by measurement. For numerical models, the Joule heating rate requires parameterizations to account for the presumed "missing" energy in the simulations while, for measurements, numerous approximations abound. The thermospheric gas responds to the Joule heating globally but this response is dependent upon the altitude distribution of heating and cooling processes and on the preconditioned state of the thermosphere, as will be demonstrated in this talk.

In addition to being a primary energy source for the upper atmosphere, the Joule heating rate is dependent on processes originating in the Sun's corona and exchange processes among the solar wind, magnetosphere, ionosphere, and thermosphere. The coupling of the ionosphere and thermosphere challenges how this electromagnetic energy input from the solar wind / magnetosphere is transformed into heat through the upper atmosphere. The recent solar minimum provides a unique opportunity to evaluate these processes owing to the regular forcing of geospace by recurrent corotating interaction regions and high speed streams, and the extremely low and steady solar fluxes establishing a base state of the thermosphere. A superposed epoch analysis of the thermosphere density response to CIR/HSS events during 2008 illustrates global changes in density with a maximum percent change at 400 km of 75%, although this change is greater during the night[1].

The contracted thermosphere during this recent solar minimum also presented an altered compositional state of the thermosphere to low-earth orbiting spacecraft. The presence of helium is apparent by analyzing the relative response of density change from two altitudes during a period in 2008 when CHAMP and GRACE satellites were coplanar and orbiting at an average altitude of 340 km and 480km, respectively. Analysis of the coplanar measurements illustrates the altitude response of the thermosphere to CIR/HSS storm activity under a mixed composition of thermospheric gas.

References

[1] J. Lei, J. P. Thayer, W. Wang, and R. L. McPherron, Impact of CIR Storms on Thermosphere Density Variability during the Solar Minimum of 2008, *Solar Physics*, DOI 10.1007/s11207-010-9563-y (2010).

Electric Currents and Fields in Polar Lower Ionosphere and Strato/Mesosphere Caused by 'Solar Wind – Magnetosphere' Interaction and their Possible Effects – a Model Study

P.T. Tonev, P.I.Y. Velinov

Space and Solar-Terr. Research Institute, BAS, Moskovska str.6, Sofia 1000, Bulgaria, e-mail: ptonev@bas.bg

Generation of electric currents and fields in the lower ionosphere, mesosphere and stratosphere at polar and high latitudes as a result of the solar wind (SW) interaction with the magnetosphere is studied theoretically. This interaction leads to creation of field-aligned currents and of a large-scale (~3000 km) trans-polar dawn-to-dusk potential difference V_{PC} in the polar ionosphere. V_{PC} varies with the IMF and SW parameters between ~30 and 140 kV. The horizontal electric fields formed in both polar caps are transmitted below and are transformed to vertical electric fields at the earth's surface [1] of intensity smaller by about six orders. This is a significant part of the total fair-weather electric fields in the global atmospheric electrical circuit (GEC) generated by thunderstorms and electrified clouds [2]. Estimations are given by us below of the variations of the total fair-weather electric current j by those (j_{SW}) caused by SW-magnetosphere interaction in four sample cases. They are comparable to the basic air-earth current of few pA/m^2.

Table. AIR-EARTH CURRENT DENSITY GENERATED BY TRANS-POLAR IONOSPHERE POTENTIAL DIFFERENCE (BELOW DAWN AND DUSK MAXIMUMS)

IMF components *By, Bz* [nT]	-1.0, -0.5	-2.0, -2.0	0.0, -5.0	-4.0, -7.0
j_{SW} (dawn / dusk) [pA.m^{-2}]	0.17 / -0.21	0.32 / -0.32	0.52 / -0.56	0.70 / -0.74

Relation of variations of air-earth current to the ionospheric potential distribution in polar caps is demonstrated experimentally in [3]. By downward transmission the electric field attenuate mainly in the dynamo region where an effective closure of the field-aligned currents takes place. Closure currents are created in the lower ionosphere, as well, although much smaller than those in the dynamo region, and degrade to lower altitudes. Therefore, the downward decrease of the field-aligned currents is gradual, and their corresponding electric fields are possibly relatively large in the lower ionosphere, and in the strato/mesosphere. Unexpectedly large electrostatic fields in the D-region and below (from ~1 V/m up to several V/m) have been experimentally measured at polar and high latitudes [4] as influenced by factors outer to GEC. Such large electrostatic fields can cause in the lower ionosphere electron heating, changes in the chemical balance, and thus significant variations of the electron density [5].

Our goal is to estimate theoretically the electric currents and fields considered. For our goals we propose a theoretical 3D model which is based on the continuity equation for the conduction electric current of density $\mathbf{j}_{SW}$:

$$\text{div}\, \mathbf{j}_{SW} = 0, \qquad \text{where} \qquad \mathbf{j}_{SW} = [\sigma]\mathbf{E}_{SW} = -[\sigma]\, \text{grad}\, U_{SW} \qquad (1)$$

Here $\mathbf{E}_{SW}$ is the electric field with a potential U_{SW}, $[\sigma]$ is the conductivity tensor. Eq.(1) is solved in geocentric modified spherical coordinates (θ,φ,z) adapted to the geomagnetic field: θ and φ are gm latitude and longitude; z is the altitude from sea level up to 80 km, and the distance along a magnetic field line above 80 km. The 3D domain of Eq.(1) comprises altitudes from the surface up to Z_B=160 km and a part of a hemisphere for gm latitudes $|\theta| > \theta_B = 30^0$. The boundary conditions are formulated at: (***i***) boundary altitudes z= 0 where U_{SW} = 0, and z= Z_B where U_{SW} is obtained from model of Weimer [6]; (***ii***) boundary gm latitude θ_B where the normal component of the current density is zero.

Data for the anisotropic atmospheric conductivity in the region 80-160 km are taken from the ionospheric conductivity model IRI2007. The scalar conductivity below 80 km is represented by piece-wise exponential functions by all three components so that to fit the total columnar resistance, the typical conductivity at the surface, and the typical profile parameters in the troposphere. The model can also represent more complex details required, such as the possible reduction of the stratospheric conductivity due to enhancements of fine aerosol density at polar latitudes. The orography is represented by specific modification of the conductivity profiles in the troposphere. Eq.(1) is solved numerically by a modification of the finite volume method.

Our results for $\mathbf{j}_{SW}$ and $\mathbf{E}_{SW}$ in the lower ionosphere and strato/mesosphere strongly depend on the input parameters. The vertical electric field E_{SWz} is enhanced in layers with sharp field-aligned conductivity decrease. Under specific conditions E_{SWz} at altitudes 70-85 km is comparable to the quasi-electrostatic fields generated above thunderclouds [7-10]. Therefore it can be large enough to change significantly the coefficients of the attachment, detachment and dissociative recombination and variations of the electron density [5].

References

[1] C. Park, *J. Geophys. Res*., **81**, 168 (1976).
[2] P.I.Y. Velinov and P.T. Tonev, *Adv. Space Res*., **42**, 1569 (2008).
[3] A. Frank-Kamenetsky, G. Burns, et al., *J. Atmos. Solar-Terr. Phys*., **61**, 1347 (1999).
[4] A. Zadorozhni and A.Tyutin, *Adv.Space Res*, **20**, 2177 (1997).
[5] V. Pasko, *J. Atmos. Solar-Terr. Phys*., **60**, 863 (1998).
[6] D. Weimer, *J. Geoph. Res*., **100**, 19595 (1995).
[7] P. Tonev and P.I.Y. Velinov, *Adv. Space Res.,* **30**, 2625 (2002).
[8] P. Tonev and P.I.Y. Velinov, *Adv. Space Res.,* .**31**, 1443 (2003).
[9] P. Tonev and P.I.Y. Velinov, *Adv. Space Res.,*.**35,** 1461 (2005).
[10] P. Tonev and P. Velinov, *J. Atmos. Solar-Terr. Phys*., **69**, 2510 (2007).

Propagation of Plasmoids Generated by Fast Reconnection in the Geomagnetic Tail

M. Ugai

Research Center for Space and Cosmic Evolution, Ehime University, ugai@cosmos.ehime-u.ac.jp

In order to study the Sun-Earth system, it is fundamental to understand large dissipative events, such as solar flares and geomagnetic substorms, and it is widely believed that magnetic reconnection is essential for flares and substorms. In particular, the so-called fast reconnection mechanism, involving slow shocks and Alfvenic jets, is most responsible for these flare phenomena. In this respect, we have proposed the spontaneous fast reconnection model, where the fast reconnection mechanism grows as a nonlinear instability due to positive feedback between reconnection flows and current-driven anomalous resistivities [1]. On the basis of the fast reconnection model, we have demonstrated that many distinct plasma processes associated with flares and substorms can well be explained by the fast reconnection evolution in space (collisionless) plasmas [2]. In particular, so-called plasmoids are known to be generated and propagate in the geomagnetic tail in accordance with substorm onset, and precise measurements of magnetic fields inside plasmoids have been done by in situ satellite observations. Recently, we clarified the detailed structure and dynamics of plasmoids generated by fast reconnection in the geomagnetic tail [3]. Hence, the main theme of the present paper is to examine fundamental features of plasmoid propagation by virtual satellite observations in the simulation box. It is clearly shown that the magnetic field profiles observed by the virtual satellites are, both qualitatively and quantitatively, in good agreement with actual satellite observations. Unlike the traditional flux rope model due to multiple reconnections, it is argued that the standard magnetic field profile, observed for plasmoids propagating in the geomagnetic tail, is the direct outcome of the single fast reconnection evolution.

References

[1] M. Ugai, Phys. Plasmas **15**, 082306 (2008); Phys. Fluids B **4**, 2953 (1992); Phys. Fluids **29**, 3659 (1986).
[2] M. Ugai, Phys. Plasmas **18**, 032304 (2011); Phys. Plasmas **16**, 012901 (2009).
[3] M. Ugai, Ann. Geophys. **29**, 147 (2011); Ann. Geophys. **28**, 1511 (2010).

THEMIS Observations of EMIC Pc1 Waves in the Inner Magnetosphere: A Statistical Study

M. E. Usanova[1], I. R. Mann[1], L. Shao[1], V. Angelopoulos[2], J. Bortnik[2]

1 University of Alberta, Department of Physics, 3-102 CCIS 11455 Saskatchewan Drive, Edmonton, Alberta, T6G 2E9, Canada, musanova@ualberta.ca

2 Department of Atmospheric and Oceanic Sciences, University of California, Los Angeles, California, USA

Electromagnetic ion cyclotron (EMIC) waves are transverse plasma waves generated by anisotropic proton distributions with Tperp>Tpara. EMIC waves are believed to play an important role in the dynamics of the ring current and radiation belts, therefore, it is important to know their localization in the magnetosphere. Using observations from multiple satellites traversing the same region of space in a "string-of-pearls" configuration, it is possible to resolve spatial-temporal ambiguity and define regions of enhanced EMIC wave activity. Utilizing magnetic field data from three THEMIS probes, Usanova et al., 2008 observed radially confined EMIC waves in the inner dayside magnetosphere, just inside the plasmapause. We applied an automatic Pc 1 detection algorithm (see Bortnik et al., 2007) to THEMIS FGM data to identify EMIC Pc1 waves. We will present a statistical study of EMIC wave radial extent in the inner magnetosphere, typical location with respect to the plasmapause, and wave power. These observations can be further used for calculation of pitch-angle diffusion rates of energetic particles scattered by EMIC waves.

References

[1] M. E. Usanova et al., *Geophys. Res. Lett.,* **35**, *L17S25, doi:10.1029/2008GL034458* (2008).

[2] Bortnik, J. W. Cutler, C. Dunson, and T. E. Bleier, *J. Geophys. Res.,* **112**, *A04204, doi:10.1029/2006JA011900* (2007).

Dipolarization Front Formation at Magnetic Reconnection in a 3D Particle-In-Cell Simulation

A. E. Vapirev[1], G. Lapenta[1], S. Markidis[1], A. Beck[1], D. Vucinic[2]

[1]*KU Leuven, Afdeling Plasma-astrofysica,Celestijnenlaan 200b, 3001 Heverlee, Belgium, email: alexander.vapirev@wis.kuleuven.be*

[2] *Vrije Universiteit Brussel, Faculty of Applied Science, Triomflaan 43, Brussels, Belgium*

We use a semi-implicit Particle-In-Cell method to simulate and study the development of the dipolarization front related to collisionless magnetic reconnection. We study the propagation of structures which are characterized by a rapid increase of the magnetic Bz-field, normal to the neutral plane. A small decrease in Bz is observed in the region of the precursor of the dipolarization front. Earthward propagating fluctuations in the Bx and By components are also observed shortly after the passing of the dipolarization front. We also study the pressure imbalance and the density profile around and inside the region of the dipolariztion front. An instability forms due to fact that the density gradient is opposite to the direction of the acceleration field.

References

[1] S. Markidis, G. Lapenta, and R. Uddin, *Mathematics and Computers in Simulation.* **80, 7**, (2010).

Elaboration of New Cosmic Ray Ionization Model for the Atmosphere - CRIMA for the Planetary Environments

P.I.Y. Velinov [1], S. Asenovski [1], L. Mateev [1], A. Mishev [2]

[1] *Institute for Space and Solar-Terrestrial Research, Bulgarian Academy of Sciences,6 Moskovska Str., Sofia 1000, Bulgaria*

[2] *Institute for Nuclear Research and Nuclear Energy , Bulgarian Academy of Sciences,Sofia 1784, Bulgaria*

The effects of galactic and solar cosmic rays (CR) in the atmosphere with account of the CR modulation by solar wind and the anomalous CR component can be computed with our new model. In fact, CR determine the electric conductivity in the atmosphere and influence the electric processes in the global electric circuit in the system Earth - ionosphere. CR introduce the solar variability in the terrestrial atmosphere and ozonosphere and they control on this way the solar constant. A new analytical approach for CR ionization by protons and nuclei with charge Z in the lower ionosphere and the atmosphere is developed. For this purpose, the ionization losses *(dE/dh)* for the energetic charged particles according to the Bohr-Bethe-Bloch formula are approximated in different energy intervals (three ionization losses intervals, one charge Z decrease interval and intermediate coupling interval). Electron production rate profiles *q(h)* are determined by the numerical evaluation of a 3D integral with account of cut-off rigidities.

The integrand in *q(h)* gives the possibility for application of adequate numerical methods - in this case Wolfram Mathematica 7 and Maple 14 interactive procedures, for the solution of the mathematical problem. The contributions of the different approximation energy intervals can be presented in a graphical mode. In this way the process of interaction of CR particles with the upper and middle atmosphere are described much more realistically. The full CR composition is taken into account. The COSPAR International Reference Atmosphere CIRA'86 is applied in the computer program for the neutral air density and scale height values. The proposed improved cosmic ray ionization model for the atmosphere - CRIMA will contribute to the quantitative understanding of solar-atmosphere relationships.

These investigations are based on particle ionization theory developed by Bohr, Bethe and Bloch, on the base of quantum mechanics. Moreover, for the altitude above 50 km, one can further neglect energy changes of the high energetic particles, thus reducing the computation of the cosmic ray induced ionization to an analytical thin target model. In the altitude range from 25-30 to 50 km, an intermediate target model needs to be used, that accounts also for the particle's deceleration due to ionization losses. The analytical and numerical full target model includes an analytical approximation of the direct ionization by CR primaries as well as CORSIKA/FLUKA programme system Monte-Carlo simulations with account of hadron interactions.

Our improved CRIMA is important for investigation of the different space weather effects. The cosmic rays and XUV radiations determine to a great extent the chemistry and electrical parameters in the middle and upper atmosphere, where are situated strato-mesosphere and thermosphere. They create ozonosphere and influence actively the stratosphere ozone processes. But the ozonosphere controls the meteorological solar constant and the thermal regime and dynamics of the lower atmosphere, i.e. the weather and climate processes. CR influence dominates during the night and sunrise-sunset periods, because galactic CR are always bombarding the Earth's atmosphere. The CR flux varies during the solar cycle in an opposite face to that of sunspots. This hypothesis of the solar-terrestrial relationships shows the way to a non-contradictory solution of the key problems of the solar-terrestrial physics.

The structure of the proposed model allows its decomposition in several submodels. In this case we take into account the physical meaning of the independent variables subintervals. The ionization losses function is calculated taking into account the energetic particles charge decrease interval. The energy intervals investigation takes place according to the goal of the user of the model with respect to accuracy and interval types.

Several recent results from the full target model important for production of ion pairs in the Earth atmosphere by primary cosmic ray nuclei are presented. The direct ionization by various primary CR nuclei is explicitly obtained. The longitudinal profile of atmospheric cascades is sensitive to the energy and mass (charge) of the primary particle. In this study different CR nuclei are considered as primaries, namely proton, Helium, Oxygen and Iron nuclei.

The main part of the full target model is the CR induced ionization, obtained on the basis of CORSIKA 6.52 code simulations using FLUKA 2006 and QGSJET II hadronic interaction models. The energy of the primary particles is normalized to GeV per nucleon. In addition, the ionization yield function Y is normalized as ion pair production per nucleon. The obtained ionization yield functions Y for various primaries are compared. The presented results and their application are discussed.

References

[1] A. Mishev and P.I.Y. Velinov, *Compt. rend. Acad. bulg. Sci.* **60**, 725 (2007).
[2] P.I.Y. Velinov and A. Mishev, *Compt. rend. Acad. bulg. Sci.* **60**, 947 (2007).
[3] P.I.Y. Velinov, A. Mishev and L. Mateev, *J. Adv. Space Res*. **44**, 1002 (2009).
[4] D. Heck, J. Knapp, J.N. Capdevielle et al. *CORSIKA: A Monte Carlo Code to Simulate Extensive Air Showers*. Forschungszentrum Karlsruhe Report FZKA 6019 (1998).
[5] P.I.Y. Velinov and L. Mateev, *J. Atmos. Solar-Terr. Phys.* **70**, 574 (2008).
[6] M. Buchvarova, P.I.Y. Velinov and I. Buchvarov, *Planet. Space Sci.* **59**, 355 (2011).
[7] G. Gronoff, C. Mertens, J. Lilensten, L. Desorgher, E. Flueckiger and P.I.Y. Velinov, *A & A*, **529**, A143 (2011).
[8] P.I.Y. Velinov and L. Mateev, *J. Adv. Space Res.* **42**, 1586 (2008).

Trend Analysis of the NO_2 Slant Column Abundance Obtained by DOAS Measurements at Stara Zagora

R. Werner[1], D. Valev[1], Atanas Atanasov[1], V. Guineva[1], I. Kostadinov[2], G. Giovanelli[2], A. Kirilov[3], M. Goranova[4]

1 Space and Solar-Terrestrial Research Institute (SSTRI), BAS, Stara Zagora Department, Stara Zagora 6000, P.O.B. 73, Bulgari , rolwer52@yahoo.co.uk

2 Institute of Atmospheric Science and Climate (ISAC), CNR, 101 Via Gobetti, Bologna 40129, Italy

3 Polar Geophysical Institute, RAS, 14, Fersman str., Apatity 184200 , Russia

4Technical University Sofia, Faculty of Computer Systems and Control, Boulevard Kliment Ohridski 8, Sofia 1000, Bulgaria

Since August 1999 daily ground-based spectrometric measurements are carried out during sunrise and sunset at the Stara Zagora (42°N, 25°E) department of SSTRI-BAS for the determination of the NO_2 slant column abundance by the help of the GASCOD-BG instrument. DOAS technique is applied to retrieve NO_2 amounts from the spectra obtained during sunrise and sunset. Increase or decrease of the stratospheric NO_2 density can change the ozone concentration, which act on the radiative balance in the stratosphere and troposphere. Therefore the NO_2 trend analysis is very important for the global climate change study. Daily time series of the NO_2 slant column amounts of different stations are analysed and extreme values, which can be a result of tropospheric pollutions or are connected with strong lightning processes, are removed and from the remaining values monthly averages are determined. By the help of regression based on the Ordinary Least Squares method between the station series, the NO_2 time series are homogenized. To determine the linear trend a linear regression model, including different impact factors, is applied and the significances are tested, taking into account the auto-correlation of the NO_2 data.

Interactive Model of Auroral Electron Precipitation: Statistical Treatment of DMSP F6 and F7 Spacecraft Observations

O.I. Yagodkina, V.G. Vorobjev, Yu.V. Katkalov

Polar Geophysical Institute, Apatity, Murmansk region, 184200, Russia, yagodkina@pgia.ru

Statistical treatment of DMSP F6 and F7 spacecraft observations during more than 35000 passes through the auroral zones of both hemispheres was used to create the interactive Auroral Precipitation Model (APM) which is placed now on http://pgia.ru/lang/ru/webapps/. The model at a level of magnetic activity (AL and Dst indexes) set by the user allows to receive: (1) global distribution of different types of auroral precipitation, (2) planetary picture of average electron energy in different precipitating zones, (3) the that of energy fluxes and (4) the pattern of auroral luminosity in visible and UVI spectral range. Global distribution of different precipitating zones can be presented both in corrected geomagnetic and geographic coordinates. Observatories or any points interested by the user can be mark off on the picture by the geographical coordinate dimensioning or a click by "the mouse" on Google maps. The model allows us to calculate the precipitation power in different zones and MLT sectors, total precipitation power, the polar cap area and so on depending on the magnetic activity level as well as relations between these parameters.
This study is supported by the RFBR grant 09-05-00818 and Program 4 of the RAS Presidium.

Sub-Oval Proton Auroras: Origin and Mapping into the Magnetosphere

A. G. Yahnin[1]

[1] *Polar Geophysical Institute, Apatity, Russia, E-mail: ayahnin@gmail.com*

Proton auroral oval maps into the magnetotail region where fluxes of energetic protons are isotropic. At sub-oval latitudes the particles are generally trapped. However, localized precipitation of energetic (E>10 keV) protons can be sometimes observed within the anisotropy zone. Such precipitation can produce proton aurora. Different forms of the sub-oval proton aurora were observed by the FUV instrument on the IMAGE spacecraft.

In this report recent results on interrelation of the sub-oval proton auroras with space-borne observations of EMIC waves and ground-based observations of geomagnetic pulsations in the Pc1 range are summarized. In particular, different forms of the sub-oval proton aurora (spots, arcs, and dayside flashes) are found to be correlated, respectively, with different types of pulsations in the Pc1 range (quasi-monochromatic Pc1, IPDP, and Pc1 bursts). These findings indicate that precipitation responsible for proton auroras is the result of interaction of ring current ions and cyclotron waves. The variety of the sub-oval proton aurora forms and their wave counterparts is explained by different regimes of the ion-cyclotron instability developing in different geophysical conditions (such as, respectively, recovery phase of geomagnetic storm, substorm, and magnetosphere compression). Thus, proton auroras visualize on the ionospheric screen the regions of the ion-cyclotron interaction.

By mapping of the proton aurora onto the equatorial plane and using the plasmapause location model developed by Viviane Pierrard and available at http://www.spaceweather.eu, we compare the projection of the sub-oval proton auroras with the position of the plasmapause. Origin of proton aurora spots is found in the vicinity of the modeled plasmapause. This agrees with the suggestion concerning the plasmapause as the source region for quasi-monochromatic Pc1 (pearls). Dayside proton aurora flashes typically originate outside the modeled plasmasphere. The Earthward boundary of the source region can be located at distance of a few R_E from the plasmapause, but it approaches the plasmapause when the background geomagnetic activity increases.

Plasmasphere from the Moon

I. Yoshikawa[1], G. Murakami[2], K. Yoshioka[3], K. Sakai[1], T. Homma[1], Y. Obana[4]

[1] *Department of Earth and Planetary Science, The University of Tokyo, 7-3-1 Hongo, Bunkyo, Tokyo, 113-0033, Japan,yoshikawa@eps.s.u-tokyo.ac.jpl*

[2] *Institute of Space and Astronautical Science, 3-1-1 Yoshinodai, Sagamihara, Kanagawa, 229-8510, Japan*

[3] *Department of Physics, Rikkyo University, 3-34 Nishiikebukuro, Toshima, Tokyo, 171-8501, Japan*

[4] *Department of Physics, Rikkyo University, 3-34 Nishiikebukuro, Toshima, Tokyo, 171-8501, Japan*

A small Extreme Ultraviolet (EUV) scanning instrument carried onboard Planet-B (Nozomi) spacecraft performed the first ever imaging of the plasmasphere from outside the terrestrial magnetosphere. This EUV scanner on Nozomi provided static pictures of the plasmasphere [1][2] and demonstrated its evolution during periods of fairly quiet [3] and stormy geomagnetic activity [4]. This first plasmaspheric EUV imaging has provided a more global perspective of the plasmasphere, and has led us to take more global images of the terrestrial plasma distribution, i.e., plasmasphere, polar wind, and plasma sheet [5][6]. A few years later, the Imager for Magnetopause-to-Aurora Global Exploration (IMAGE) mission produced consecutive images of the terrestrial plasmasphere from the high-latitude view [7][8]. The IMAGE mission identified not only the well-known morphology of the plasmasphere (plasmapause, tails, and duskside bulge), but also described novel structures, e.g., depleted regions that are called "notches" and a radially extended, narrow MLT enhanced-density feature called "finger" [9].

Furthermore, the understanding of plasmaspheric dynamics has advanced in many areas, for example determining how rapidly storm-time convective electric fields penetrate into the body of plasmasphere. Goldstein first studied the inward motion of the plasmapause as seen in the EUV images in response to the solar wind electric field which was measured by solar wind monitor (ACE satellite) [10]. Later, Murakami found 16 events in the period of May 2000-December 2001, showing that the inward motion of the plasmapause was driven by the southward turning of IMF.They showed that the plasmapause responds to the southward turning with a delay in the range 10-30 minutes, and average of 18 minutes [11].

The Upper atmosphere and Plasma Imager (UPI) on KAGUYA produces images of the Earth in the visible and EUV spectral ranges. There are two telescopes, the Telescope for VISible emission (UPI-TVIS) and the Telescope of EXtreme ultraviolet emission (UPI-TEX). UPI-TVIS images the Earth's airglow and aurora at 4 wavelengths [12][13]. UPI-TEX images the resonantly-scattered emissions of oxygen ions at 83.4 nm (O II) and helium ions at 30.4 nm (He II) [14][15]. KAGUYA was launched by the H-IIA rocket in 2007 and inserted into lunar orbit From lunar orbit, the KAGUYA project has carried out both scientific observations of the Moon and from a lunar perspective.

In this paper we report the analysis of the images of terrestrial He II (30.4 nm) radiation obtained by the UPI-TEX instrument. These first 2-dimensional images by KAGUYA provide a meridian perspective from outside the magnetosphere. The novel images taken by the other EUV channel (83.4 nm) will be published in a separate paper.

The Telescope of Extreme Ultraviolet (TEX) aboard Japan's lunar orbiter KAGUYA has succeeded in imaging of the plasmaspheric helium ions by detecting resonantly-scattered emission at 30.4 nm. The view afforded by the KAGUYA orbit encompasses the plasma (He ions) distribution in a single exposure, enabling us to examine for the first time the globally-averaged properties of the terrestrial plasmasphere from the "side" (meridian) perspective.

In this paper we report the inward motion of the nightside plasmapause on 2 May 2008 as seen from this remote meridian view of the Earth.The southward turning of the IMF initiated the inward motion of the plasmapause, and the nightside plasmasphere shrunk at the rate of 0.2 Re/hour. Simultaneous solar wind velocity measurements provide a possible explanation for the total radial displacement of the plasmasphere observed in the EUV images [16].

References

[1] M. Nakamura et al., *Earth Planets and Space* **51**, 61-70 (1999).
[2] M. Nakamura et al., *Geophys. Res. Lett.* **27**, 141-144 (2000).
[3] I. Yoshikawa et al., *J. Geophys. Res.* **108** (2003).
[4] I. Yoshikawa et al., *J. Geophys. Res.* **106**, 18911-18918 (2001).
[5] I. Yoshikawa et al., *J. Geophys. Res.* **105**, 27777-27789 (2000).
[6] I. Yoshikawa et al., *J. Geophys. Res.* **106**, 25745-25758 (2001).
[7] B. R. Sandel et al., *Space Science Reviews* **91**, 197-242 (2000).
[8] J. L. Burch et al., *Science* **291**, 5504 (2001).
[9] F. Darrouzet et al., *Space Science Reviews* **145**, 55-106 (2009).
[10] J. Goldstein et al., *Geophys. Res. Lett* **30** (2003).
[11] G. Murakami et al., *J. Geophys. Res.* **112** (2007).
[12] M. Taguchi et al., *Earth Planets and Space* **61**, XVII-XXIII (2009).
[13] M. Kagitani et al., *Earth Planets and Space* **61**, 1025-1029 (2009).
[14] I. Yoshikawa et al., *Earth Planets and Space* **60**, 407-416 (2008).
[15] G. Murakami et al., *Earth Planets and Space* **62**, E9-E12 (2010).
[16] I. Yoshikawa et al., *J. Geophys. Res.* **115** (2010).

Simulations of Near-Earth Magnetosphere Storm Dynamics with RAM-SCB: Effect of Plasma Sheet Conditions and Induced Electric Fields

S. G. Zaharia[1], V. K. Jordanova[1], D. T. Welling[1]

[1] *Los Alamos National Laboratory, Los Alamos, NM 87545 USA, szaharia@lanl.gov*

Plasma sheet conditions and the driving electric field are two main factors in the formation of the storm-time ring current. The plasma sheet is the reservoir supplying particles that are transported into the inner magnetosphere and energized during geomagnetic storms through the action of the electric field. In this study we examine the influence of these two factors on ring current dynamics through data-driven numerical simulations with our self-consistent model RAM-SCB. RAM-SCB couples the kinetic ring current-atmosphere interactions model (RAM) with an Euler potential-based three-dimensional plasma equilibrium code with anisotropic pressure. The model thus treats both the kinetic drift physics crucial in the inner magnetosphere and the self-consistent interaction between plasma and magnetic field. Recent improvements in RAM-SCB in support of this study are the expansion of the model boundary to 9 RE in the plasma sheet and the full inclusion of the induced electric fields. While the role of the convective (potential) electric fields in the energization of the ring current during storms has been studied extensively, the impact of the electric fields induced by the time change of the magnetic field is less well known. Based on RAM-SCB simulations of actual storms, the presentation discusses the effect on the ring current and region 2 field-aligned currents of: 1). plasma sheet conditions (density, temperature, local time variation), 2). self-consistent feedback between plasma and magnetic field, and 3). induced vs. convective electric fields. Model results are also compared with observations, including the observed Dst index, plasma and magnetic and electric field observations from available spacecraft (e.g. POLAR, CLUSTER and GOES), as well as Iridium-derived low-altitude field-aligned current densities.

Acceleration Process in the Earth's Magnetotail

L. M. Zelenyi[1], A. V. Artemyev[1,2], E. E. Grigorenko[1], H. V. Malova[1,2], D. Delcourt[3]

[1] *Space Research Institute RAS, 84/32 Profsoyuznaya Str, Moscow, 117997, Russia, lzelenyi@iki.rssi.ru*

[2] *Nuclear Physics Institute, Moscow State University, Moscow, Russia*

[3] *Laboratoire de Physique des Plasmas, CNRS, Saint-Maur-des-Foss´es, France*

This report is devoted to the problems of charged particle (ions and electrons) motion and energization in the inhomogeneous electromagnetic field of the Earth magnetotail. The geometry of the Earth magnetotail current sheet is considered. We demonstrate that taking into account the quasi-adiabatic invariants of motion allow to describe the dynamics and acceleration of unmagnetized ions in the vicinity of the neutral plane of the current sheet. The resonance mechanism of ion acceleration by the dawn-dusk electrostatic field in the current sheet and formation of monoenergetic beams of accelerated ions (beamlets) are described in a frame of Hamiltonian approach. We show that theoretical predictions are in very good agreement with experimental observations carried out in plasma sheet boundary layer and in the auroral zone. The same approach is applied for the description of charged particle dynamics and heating in the vicinity of X-line(s). The analytical model reproduces the features of observed spectra of high energy ions. The adiabatic theory of magnetized electron motion is applied for the description of the electron acceleration in course of the Earthward convection. We demonstrate that analytical model reproduces the observed profiles of the electron temperature with the reasonable accuracy. The comparison between theoretical model and observed data allows to estimate the important parameters of the magnetotail current sheet (the spatial scale of the magnetic field inhomogeneity along Earth-Sun direction).

PARTICIPANTS

Jay Albert, Air Force Research Lab, USA	jay.m.albert@gmail.com
Sebastian von Alfthan, Finnish Meteorological Institute, Finland	sebastian.von.alfthan@fmi.fi
Ivo Angelov,Institute for Nuclear Research and Nuclear Energy, Bulgaria	i_angeloff@mail.bg
Elizaveta Antonova, Moscow State University, Russia	antonova@orearm.msk.ru
Simeon Asenovski,Space & Solar-Terrestrial Research Institute,Bulgaria	asenovski@gmail.com
Peter Bespalov, Institute of Applied Physics, Russia	
Lilia Biktash, IZMIRAN, Russia	lsizova@izmiran.ru
Joseph Borovsky, Los Alamos National Laboratory, USA	jborovsky@lanl.gov
Marusya Buchvarova,Space&Solar-Terrestrial Research Institute,Bulgaria	marusjab@yahoo.com
Jim Burch, Southwest Research Institute, USA	jburch@swri.edu
Natalia Buzulukova, NASA GSFC/UMCP, USA	nbuzulukova@gmail.com
Christopher Chaston, University of California at Berkeley, USA	ccc@ssl.berkeley.edu
Seth Claudepierre, The Aerospace Corporation, USA	Seth.G.Claudepierre@aero.org
Tsvetan Dachev,Space&Solar-Terrestrial Research Institute,Bulgaria	tdachev59@gmail.com
Dimitar Danov, Space&Solar-Terrestrial Research Institute, Bulgaria	ddanov@stil.bas.bg
Fabien Darrouzet, Belgian Institute For Space Aeronomy, Belgium	Fabien.Darrouzet@oma.be
Michael Denton, Lancaster University, UK	m.denton@lancaster.ac.uk
Irina Despirak, Polar Geophysical Institute, Russia	despirak@gmail.com
Svetla Dimitrova,Space&Solar-Terrestrial Research Institute,Bulgaria	svetla_stil@abv.bg
Polya Dobreva, Institute of Mechanics, Bukgaria	polya2006@yahoo.com
Dimitar Draganov,Space&Solar-Terrestrial Research Institute,Bulgaria	dimitar@phys.uni-sofia.bg
Charles Farrugia, University of New Hampshire, USA	charlie.farrugia@unh.edu
Reiner Friedel, Los Alamos National Laboratory, USA	rfriedel@lanl.gov
Stephen Fuselier, Lockheed Martin Advanced Technology Center, USA	stephen.a.fuselier@lmco.com
Georgi Georgiev,Space & Solar-Terrestrial Research Institute,Bulgaria	rumik@abv.bg
Jerry Goldstein, Southwest Research Institute, USA	jgoldstein@swri.edu
Evgeniy Gordeev, St. Petersburg State University, Russia	evgeniy_gordeev@yahoo.com
Rod Heelis, University of Texas at Dallas, USA	heelis@utdallas.edu
Ilja Honkonen, Finnish Meteorological Institute, Finland	ilja.honkonen@fmi.fi
Mary Hudson, Dartmouth College, USA	mary.k.hudson@dartmouth.edu
Raluca Ilie, Los Alamos National Laboratory, USA	rilie@lanl.gov
Christian Jacquey, IRAP, CNRS/UPS, France	Christian.Jacquey@cesr.fr
Valentin Jordanov, Yantel, LLC, USA	jordanov@ieee.org
Vania Jordanova, Los Alamos National Laboratory, USA	vania@lanl.gov
Rumiana Kancheva,Space&Solar-Terrestrial Research Institute,Bulgaria	rumik@abv.bg
Monio Kartalev, Institute of Mechanics, Bulgaria	m_kartalev@yahoo.com
Natalya Kilifarska, National Institute of Geophysics, Geodesy & Geography, Bulgaria	nkilifarska@geophys.bas.bg
Craig Kletzing, University of Iowa, USA	craig-kletzing@uiowa.edu

Rositza Koleva,Space&Solar-Terrestrial Research Institute,Bulgaria rkoleva@stil.bas.bg
Ivana Kolmasova, IAP AS CZ, Czech Republic iko@ufa.cas.cz
Dmitri Kondrashov, University of California, USA dkondras@atmos.ucla.edu
Hideki Koshiishi, Japan Aerospace Exploration Agency, Japan koshiishi.hideki@jaxa.jp
Dora Krezhova, Space&Solar-Terrestrial Research Institute,Bulgaria dkrezhova@stil.bas.bg
Jan Kubancak, Nuclear Physics Institute, Czech Republic kubancak@ujf.cas.cz
Ivan Kutiev, National Institute for Geophysics, Geodesy & Geography, Bulgaria ivankutiev@yahoo.com
Tamara Kuznetsova, IZMIRAN, Russia tvkuz@izmiran.ru
Philippe Lamy, LAM, France philippe.lamy@oamp.fr
Benoit Lavraud, IRAP/CNRS, Université de Toulouse, France benoit.lavraud@cesr.fr
Colby Lemon, Aerospace Corporation, USA, colby.lemon@aero.org
Michael Liemohn, University of Michigan, USA liemohn@umich.edu
Ramon Lopez, University of Texas at Arlington, USA relopez@uta.edu
William Lotko, Dartmouth College, USA, william.lotko@dartmouth.edu
Gang Lu, National Center for Atmospheric Research, USA ganglu@ucar.edu
Noe Lugaz, University of Hawaii, USA nlugaz@IfA.Hawaii.Edu
Lachezar Mateev,Space&Solar-Terrestrial Research Institute,Bulgaria lnmateev@bas.bg
Robert McPherron, University of California Los Angeles, USA rmcpherron@igpp.ucla.edu
Bogdana Mendeva,Space&Solar-Terrestrial Research Institute,Bulgaria bmendeva@abv.bg
Yoshizumi Miyoshi, STEL, Nagoya University, Japan miyoshi@stelab.nagoya-u.ac.jp
Thomas Moore, NASA Goddard SFC, USA thomas.e.moore@nasa.gov
Petko Nedialkov, University of Sofia, Bulgaria japet@phys.uni-sofia.bg
Petko Nenovski, National Institute for Geophysics, Geodesy & Geography,Bulgaria nenovski@geophys.bas.bg
Nikolai Østgaard, University of Bergen, Norway Nikolai.Ostgaard@ift.uib.no
Yuichi Otsuka, STEL, Nagoya University, Japan otsuka@stelab.nagoya-u.ac.jp
Minna Palmroth, Finnish Meteorological Institute, Finland minna.palmroth@fmi.fi
Vahe Peroomian, University of California Los Angeles, USA vahe@igpp.ucla.edu
Ilan Roth, University of California at Berkeley, USA ilan@ssl.berkeley.edu
Ilia Roussev, University of Hawaii, USA iroussev@ifa.hawaii.edu
Ventzislav Rusanov, University of Sofia, Bulgaria rusanov@phys.uni-sofia.bg
Yoshifumi Saito, Institute of Space and Astronautical Science, Japan saito@stp.isas.jaxa.jp
Ondrej Santolik, IAP AS CR Prague, Czech Republic os@ufa.cas.cz
Olga Savina, State Technical Univesity, Russia onsavina@mail.ru
Michael Schulz, Lockheed Martin, USA mschulz43@gmail.com
Jordanka Semkova,Space&Solar-Terrestrial Research Institute,Bulgaria jsemkova@stil.bas.bg
Victor Sergeev, St.Petersburg State University, Russia victor@geo.phys.spbu.ru
Rumen Shkevov,Space&Solar-Terrestrial Research Institute,Bulgaria shkevov@space.bas.bg
Yavor Shopov, University of Sofia, Bulgaria yyshopov@phys.uni-sofia.bg
Yuri Shprits, University of California Los Angeles, USA yshprits@atmos.ucla.edu

Finn Søraas, University of Bergen, Norway Finn.Soraas@ift.uib.no
Ivanka Stateva, Institute of Astronomy with NAO, Bulgaria stateva@astro.bas.bg
Yordan Tassev,Space&Solar-Terrestrial Research Institute,Bulgaria yktassev@bas.bg
Assen Tchorbadjieff, Institute for Nuclear Research and Nuclear Energy, Bulgaria tchorbadjieff@hotmail.com
Jeffrey Thayer, University of Colorado, USA Jeffrey.Thayer@Colorado.EDU
P. Tonev, Space&Solar-Terrestrial Research Institute, Bulgaria ptonev@bas.bg
Masayuki Ugai, Ehime University, Japan ugai@cosmos.ehime-u.ac.jp
Maria Usanova, University of Alberta, Canada musanova@phys.ualberta.ca
Alexander Vapirev, KU Leuven, Belgium Alexander.Vapirev@wis.kuleuven.be
Peter Velinov, Space&Solar-Terrestrial Research Institute, Bulgaria pvelinov@bas.bg
Rolf Werner, Space&Solar-Terrestrial Research Institute, Bulgaria rolwer52@yahoo.co.uk
Alexander Yahnin, Polar Geophysical Institute, Russia yahnin@pgia.ru
Ginka Yankova, University of Sofia, Bulgaria gianyy@phys.uni-sofia.bg
Ichiro Yoshikawa, University of Tokyo, Japan yoshikawa@eps.s.u-tokyo.ac.jp
Sorin Zaharia, Los Alamos National Laboratory, USA szaharia@lanl.gov
Lev Zelenyi, Space Research Institute, Russia lzelenyi@iki.rssi.ru

AUTHOR INDEX

Albert, J.M., p.1, 41
von Alfthan, S., p.2, 71
Anderson, R.R., p.30
André, N., p.40
Anekallu, C.R., p.71, 73
Angelopoulos, V., p.93
Angelov, I.I., p.3, 19
Antonova, E.E., p.4
Artemyev, A.V., p.100
Asamura, K., p.12
Asenovski, S., p.95
Atanasov, A., p.96

Bailey, J., p.39
Bankov, N.G., p.14, 83
Base, J., p.47
Beck, A., p.94
Benghin, V., p.83
Bespalov, P.A., p.80
Besson, B., p.40
Biktash, L.Z., p.5, 6
Birn, J., p.7
Borodkova, N.L., p.20
Borovsky, J.E., p.7, 17
Bortnik, J., p.1, 93
Bouchemit, M., p.40
Brambles, O.J., p.59
Briand, C., p.40
Brito, T., p.38
Buchvarova, M., p.8, 21
Budnik, E., p.40
Burch, J.L., p.9, 65
Buzulukova, N., p.10

Cecconi, B., p.40
Chakarova, K., p.11
Chapkunov, St., p.85
Chappell, C.R., p.30
Chaston, C.C., p.12
Chen, M.W., p.56, 82
Chen, Y., p.41
Chernykh, I., p.83
Chu, X., p.62
Chum, J., p.47
Claudepierre, S.G., p.13

Dachev, Ts.P., p.14, 15, 51
Dandouras, I., p.73
Danov, D., p.68
Darrouzet, F., p.16
De Keyser, J., p.16
De Zeeuw, D.L., p.57
Delcourt, D., p.100
Denton, M.H., p.7, 17
Denton, R.E., p.13, 30
Despirak, I.V., p.18, 31, 33
Dimitrov, Pl.G., p.14
Dimitrova, S., p.19
Dobreva, P.S., p.20
Donev, E., p.67
Draganov, D., p.8, 21
Drobyshev, S., p.83
Dufourg, N., p.40
Dunlop, M., p.73

El-Alaoui, M., p.74
Elkington, S., p.38
Erokhin, N.S., p.22, 23

Farrugia, C.J., p.24
Fedorov, A., p.40, 77
Freeman, M.P., p.24

Friedel, R.H.W., p.25, 41
Funsten, H., p.39
Fuselier, S.A., p.26, 65

Galvin, A.B., p.77
Gangloff, M., p.40
Ganushkina, N.Yu., p.16, 27, 57
Génot, V., p.40
Georgiev, G.S., p.28, 42
Ghil, M., p.48
Giovanelli, G., p.96
Gogosheva, Ts.N., p.63
Goldstein, J., p.29, 30
Golovchanskaya, I.V., p.31
Goranova, M., p.96
Gordeev, E., p.32
Grigorenko, E.E., p.46, 100
Gruntman, M., p.39
Guild, T.B., p.56
Guineva, V.H., p.33, 34, 96

Häder, D.-P., p.14
Hasegawa, H., p.65
Heelis, R.A., p.35
Hirahara, M., p.12
Hitier, R., p.40
Homma, T., p.98
Honkonen, I., p.2, 36, 37, 71
Horne, R.B., p.41
Horneck, G., p.14
Hruska, F., p.47
Hsu, T-S., p.62
Hudson, M.K., p.13, 38

Ilie, R., p.39, 57

Jacquey C., p.40
Janhunen, P., p.37
Jefferey, C.A., p.25
Jordanova, V.K., p.1, 24, 41, 99

Kaguya MAP-PACE Team, p.78
Kancheva, R.H., p.28, 42
Kartalev, M.D., p.20, 43
Kasahara, Y., p.64
Kataoka, R., p.64
Khazanov, G.V., p.66
Kilifarska, N.A., p.44
Kim, K.C., p.87
Kirilov, A., p.34, 96
Kirpichev, I.P., p.4
Kissinger, J., p.62
Kletzing, C.A., p.45
Koleva, R., p.18, 46, 83
Kolmasova, I., p.47
Kondrashov, D., p.48
Koshiishi, H., p.49
Koskinen, H.E.J., p.71, 72
Kostadinov, I., p.96
Kozelov, B.V., p.31
Krastev, D.G., p.63
Kress, B., p.38
Krezhova, D., p.50
Kubancak, J., p.51
Kumamoto, A., p.64
Kutiev, I., p.52
Kuznetsova, T.V., p.53, 54

Laitinen, T.V., p.71, 73
Lapenta, G., p.94
Laptukhov, A.I., p.53, 54
Lavraud, B., p.40, 55, 77
Lei, J., p.90
Lemon, C.L., p.56

Li, W., p.1,
Li, Z., p.38
Liemohn, M.W., p.27, 39, 57
Lopez, R.E., p.58
Lotko, W., p.13, 59
Lu, G., p.60
Lubchich, A.A., p.18
Lucek, E.A., p.73
Lugaz, N., p.61
Luhmann, J.G., p.77
Lui, X., p.90
Lyon, J.G., p.13, 59

Malova, H.V., p.100
Maltchev, St., p.83
Mann, I.R., p.93
Markidis, S., p.94
Mateev, L., p.95
Matsui, H., p.16
Matviichuk, Yu.N., p.14
McComas, D.J., p.29
McPherron, R.L., p.62
Mendeva, B.D., p.63
Meredith, N., p.41
Mikhailovskaya, L.A., p.22, 23
Mishev, A., p.95
Miyoshi, Y., p.41, 64
Moore, T.E., p.64, 66
Mrázová, Z., p.51
Muehlbachler, S., p.24
Murakami, G., p.98
Myagkova , I.N., p.75

Nedialkov, P., p.67
Nenovski , P., p.68
Ni, B., p.87
Nishino, M.N., p.78
Nishioka, M., p.70

Obana, Y., p.98
Opitz, A., p.77
Orlova, K.G., p.4
Østgaard, N., p.69
Otsuka, Y., p.70
Ovchinnikov, I.I., p.4
Owens, M.J., p.77

Palin, L., p.40
Pallier, E., p.40
Palmrooth, M., p.2, 32, 36, 37, 71, 72, 73
Penou, E., p.40
Peroomian, V., p.74
Petrinec, S., p.26, 65
Petrov, V., p.83
Petrova, E., p.19
Pierrard, V., p.16
Pilipenko, V.A., p.75
Pitout, F., p.40
Ploc, O., p.51
Pu, Z., p.65
Pulinets, M.S., p.4
Pulkkinen, T.I., p.32, 71, 72, 73

Redfern, J., p.29
Reeves , G.D., p.25
Reitz, G., p.14
Riazantseva, M.O., p.4
Romanova, N.V., p.75
Roth, I., p.76
Rouillard, A.P., p.77
Roussev, I.I., p.61
Ruffenach, A., p.77
Rusanov, V., p.11
Russell, C.T., p.77

Saito, A., p.70
Saito, Y., p.78
Sakai, K., p.98
Sakanoi, T., p.12
Sandholt, P.E., p.24
Sandroos, A., p.2, 36, 71
Santolik, O., p.47, 80
Sauvaud, J.-A., p.46, 77
Savani, N., p.77
Savina, O.N., p.80
Schulz, M., p.81, 82
Seki, K., p.12
Semkova, J., p.83
Sergeev, V.A., p.32, 84
Shao, L., p.93
Shkevov, R., p.22, 23, 85
Shopov, Y., p.86
Shprits, Y.Y., p.48, 87
Shurshakov, V., p.83
Sibeck, D.J., p.65
Skoug, R., p.39
Søraas, F., p.88
Sørbø, M., p.88
Stepanova, M.V., p.4
Stoykova, D., p.86
Strangeway, R.J., p.59
Subbotin, D., p.48, 87

Tchorbadjieff, A.G., p.89
Thayer, J.P., p.90
Thorne, R.M., p.1
Tomov, B.T., p.14
Tonev, P.T., p.91
Torbert, R.B., p.24
Trattner, K.J., p.26
Trautwein, A.X., p.11
Trøndsen, E., p.33
Tsankov, L., p.67
Tsugawa, T., p.70
Tsunakawa, H., p.78

Uemura, K., p.78
Ugai, M., p.92
Uhlir, L., p.47
Usanova, M.E., p.93

Valek, P., p.29
Valev, D., p.96
Vapirev, A.E., p.94
Velinov, P.I.Y., p.91, 95
Vince, I., p.34
Vovchenko, V.V., p.4
Vucinic, D., p.94

Welling, D.T., p.7, 99
Werner, R.H., p.33, 34, 96
Wiltberger, M., p.38, 59

Yahnin, A.G., p.97
Yamamoto, T., p.78
Yokota, S., p.78
Yoshikawa, I., p.98
Yoshioka, K., p.98

Zaharia, S.G., p.99
Zastenker, G.N., p.20
Zelenyi, L.M., p.46, 100
Zhang, B., p.59
Znatkova, S.S., p.4
Zolnikova, N.N., p.22, 23